

GASEOUS TRACER DIFFUSION FROM A POINT SOURCE AS A SITE INVESTIGATION METHOD

THÈSE N° 2625 (2002)

PRÉSENTÉE À LA FACULTÉ ENVIRONNEMENT NATUREL, ARCHITECTURAL ET CONSTRUIT

ÉCOLE POLYTECHNIQUE FÉDÉRALE DE LAUSANNE

POUR L'OBTENTION DU GRADE DE DOCTEUR ÈS SCIENCES

DANS LE DOMAINE DES SCIENCES ET INGÉNIERIE DE L'ENVIRONNEMENT

PAR

David WERNER

**ingénieur en sciences de l'environnement diplômé EPF
de nationalité suisse et originaire de Merishausen (SH)**

acceptée sur proposition du jury:

**Dr P. Höhener, directeur de thèse
Prof. P. Grathwohl, rapporteur
Prof. A. Mermoud, rapporteur
Prof. R. Schwarzenbach, rapporteur**

**Lausanne, EPFL
2002**

“Sie ist wie ein kleines, oder grosses Kind, solch eine Uhr” dachte der Angestellte, “wie ein eigensinniges Kind, das der beständigen aufopfernden Pflege bedarf, und das nicht einmal dankt dafür. Gedeiht denn eigentlich dieses Unternehmen, wächst dieses Kind? Man merkt wenig davon. Ein Erfinder liebt seine Erfindungen. Diese kostspielige Uhr ist Tobler beinahe ans Herz gewachsen. Was aber denken andere Leute von dieser Idee? Eine Idee muss hinreissen, muss überwältigen, sonst ist es eine schwere Sache, sie zu praktizieren.”

Aus: Robert Walser, *Der Gehülfe*

Acknowledgment

I thank Dr. P. Höhener for supervising this thesis. Prof. R. Schwarzenbach, Prof. P. Grathwohl, Prof. A. Mermoud and Prof. H. Harms were members of the examination committee. Their scientific expertise was much appreciated. I gratefully acknowledge Prof. D. D. Genskes contribution to the initiation of this research.

This work profited from the collaboration with the other members of Patrick Höheners research group at the École Polytechnique Fédérale de Lausanne (EPFL), namely: Christian Balsiger, Gabriele Pasteris, Karin Kaufmann, Nathalie Dakhel and Céline Duwig. Peter Kjeldsen, Mette Christopherson, Mette Broholm, Lone E. Holtegaard and Trine M. Bjerre supported me during my stay at the Danish Technical University (DTU). Thank you!

Financial support came from the Board of the Swiss Federal Institute of Technology, the Swiss National Science Foundation and from the European project Groundwater Risk Assessment at Contaminated Sites (GRACOS).

Summary

Transport modelling, risk assessment, and the evaluation of remediation strategies at sites contaminated with volatile organic compounds (VOCs) require the knowledge of *gas-phase diffusion coefficients* in *unsaturated porous media*. This thesis presents a *new in situ method* for the simultaneous measurement of effective and sorption-affected diffusion coefficients. The method relies on the injection of a gaseous compound and a conservative gaseous tracer using a soil gas probe. Concentrations are monitored at the tip of the probe during 8 hours and evaluated with an analytical equation for reactive transport in a homogeneous medium. Results are reported for volatile organic pollutants in a sand-filled lysimeter and at a field site with a sandy unsaturated zone. The determination of the effective diffusion coefficients showed good reproducibility and robustness with respect to analytical error, with an estimated overall error of 13%. The determination of the sorption-affected diffusion coefficients also showed good reproducibility. However, batch experiments suggest a systematic overestimation by 15-20%, because the tracers were not truly conservative. The in situ method avoids considerable uncertainties associated with estimating apparent diffusion coefficients from empirical relationships and avoids problems with establishing representative soil conditions in laboratory experiments.

Another key issue for risk assessment at contaminated sites is the *localization* and *quantification* of *nonaqueous phase liquids (NAPLs)* such as gasoline, kerosene or heating oil in the subsurface. This thesis proposes the theory and practical application of a *new diffusive partitioning tracer test (DPTT)* for NAPL detection in the vadose zone. The general approach is the same as for the determination of apparent diffusion coefficients. A mixture of chlorofluorocarbons as gaseous tracers is injected into the vadose zone using a soil gas probe. While the tracers diffuse away, small volumes of gas are withdrawn from the injection point. The quantitative determination of the NAPL saturation is based on a comparison of the concentration decline of tracers with different air-NAPL partitioning coefficients. An alternative approach is the measurement of diffusive breakthrough curves in some dis-

tance from the injection point. The test has been evaluated in laboratory sand columns, at a field site with an artificial contamination embedded in a sandy unsaturated zone and in a sand-filled lysimeter, where the NAPL distribution was heterogeneous. NAPLs in saturations between 0 and 4 % of the total porosity have been reliably detected and quantified in a wide range of different water contents. NAPL saturations determined by DPTTs and by extraction from soil cores agree within a factor 2 or better. Results from the lysimeter study suggest that the NAPL saturation derived from the tracer concentrations at the injection point represent a small soil volume in the vicinity of the injection point, whereas the NAPL saturation determined from diffusive tracer breakthrough curves represent the soil between injection and monitoring point.

These innovative investigation methods for the vadose zone are *inexpensive*, require little technical equipment on site, and allow the *simultaneous determination of different parameters* at one location from a few single measurements: as demonstrated in situ for two sandy soils, the effective and the apparent diffusion coefficient or the NAPL saturation, the effective diffusion coefficient and the soil gas concentration of several VOCs can be determined simultaneously by the proposed methods. This new approach has been tested in sandy, unsaturated porous media. The performance of the methods in heterogeneous environments or in porous media other than sand needs to be further investigated.

Version abrégée

La modélisation, l'évaluation des risques et le choix d'une stratégie pour l'assainissement d'un site contaminé par des composés organiques volatiles (COVs) nécessite de connaître les *constantes apparentes de diffusion en phase gazeuse* de ces composés dans la *zone non-saturée*. Cette thèse présente *une nouvelle méthode* pour déterminer simultanément la constante de diffusion effective et la constante de diffusion apparente limitée par la sorption *in situ*. La méthode consiste à injecter le COV sous forme gazeuse en même temps qu'un traceur inerte (composé chlorofluoré) dans le sol. Les concentrations sont ensuite surveillées au point d'injection pendant 8 heures et sont interprétées à l'aide d'une équation qui décrit le transport réactif dans un sol homogène. Des résultats sont présentés pour des COVs dans un lysimètre rempli de sable et *in situ* dans un sol sableux. La détermination de la constante de diffusion effective était reproductible et robuste, avec une erreur totale estimée à 13%. La détermination de la constante de diffusion apparente limitée par la sorption était également reproductible. Cependant, des expériences menées en batch ont indiqué que la constante était surestimée de 15-20% parce que les traceurs n'étaient pas complètement inertes. Cette méthode *in situ* évite les incertitudes considérables associées à l'estimation des constantes apparentes de diffusion à l'aide de relations empiriques ainsi que le problème de reproduire des conditions représentatives d'un sol naturel en laboratoire.

Une autre question importante pour l'évaluation des risques provenant d'un site contaminé est la *localisation* et la *quantification* des *liquides organiques (NAPLs)* comme par exemple l'essence, le kérosène ou le mazout dans la zone non-saturée. L'approche générale est la même que pour la détermination des constantes apparentes de diffusion. Un mélange de composés chlorofluorés est injecté dans le sol. Pendant que les traceurs diffusent dans le sol, de petits volumes de gaz sont échantillonnés au point d'injection. La comparaison des concentrations de traceurs ayant une affinité différente pour la phase organique permet de quantifier le volume de la phase organique par rapport au volume total de la porosité, c'est-à-dire le taux de saturation

VIII

en NAPL. Une autre alternative consiste à suivre l'évolution des concentrations des traceurs à une certaine distance du point d'injection. Ces deux méthodes ont été testées au laboratoire avec des colonnes en verre remplies de sable, dans un lysimètre où la distribution spatiale de la phase organique était hétérogène et in situ dans un sol sableux contaminé artificiellement. Le liquide organique a été détecté de manière fiable pour un taux de saturation en NAPL compris entre 0 et 4% et pour des teneurs en eau variable. Le taux de saturation en NAPL déterminé ainsi différait au maximum d'un facteur 2 par rapport à la quantification effectuée après extraction du sol. Les résultats de l'étude en lysimètre ont montré que le degré de saturation en NAPL estimé à partir du suivi de la concentration des traceurs au point d'injection n'était valable que pour un petit volume de sol aux alentours du point d'injection. Par contre, le degré de saturation en NAPL estimé en analysant la concentration des traceurs à une certaine distance du point d'injection représente le sol compris entre le point d'injection et le point d'observation.

Ces nouvelles méthodes d'investigation de la zone non-saturée sont *peu coûteuses*, demandent peu d'équipement de terrain et permettent de déterminer *simultanément plusieurs paramètres* avec peu d'analyses. Comme il a été démontré in situ pour deux sols sableux, la constante de diffusion effective, la constante de diffusion apparente limitée par la sorption, la saturation en NAPL et les concentrations de plusieurs COVs peuvent être déterminées simultanément avec une des méthodes proposées. La performance de cette nouvelle approche dans un environnement hétérogène ou dans un autre milieu que les sols sableux reste à être déterminée.

Contents

Summary	V
Version abrégée	VII
1 General Introduction	1
2 Objectives, Innovation and Outline	3
3 Basic Theory	7
4 Batch Experiments	13
4.1 Introduction	13
4.2 Theory	16
4.3 Materials and Methods	17
4.4 Results	20
4.5 Discussion	23
5 Determination of Apparent Diffusion Coefficients	27
5.1 Introduction	27
5.2 Theory	30
5.3 Materials and Methods	32
5.4 Results	35
5.5 Discussion	39
6 Diffusive Partitioning Tracer Test: Column Experiments	45
6.1 Introduction.	45
6.2 Theory	46
6.3 Materials and Methods	48
6.4 Results	50
6.5 Discussion	53

7	Diffusive Partitioning Tracer Test: Field Experiments	57
7.1	Introduction	57
7.2	Theory	58
7.3	Materials and Methods	60
7.4	Results	62
7.5	Discussion	65
8	Diffusive Partitioning Tracer Test: Lysimeter Experiments	69
8.1	Introduction	69
8.2	Theory	70
8.3	Materials and Methods	72
8.4	Results	74
8.5	Discussion	79
9	Synopsis, Conclusions and Outlook	85
	Bibliography	93
A	Notation	99
B	Raw Data	101
	Curriculum Vitae	109

Chapter 1

General Introduction

A typical gasoline spill. Modern industrialized societies use huge amounts of petroleum hydrocarbons such as gasoline, kerosene, diesel and heating oil to cover their energy needs. It comes not as a big surprise that the number of sites contaminated with such organic liquids is legion. A typical scenario is the following: Due to corrosion of an underground storage tank gasoline is leaking into the surrounding soil. The force of gravity moves the liquid gasoline downwards through the vadose zone until it meets an impermeable barrier, for instance the upper boundary of the aquifer. Besides vertical migration, capillary forces in the soil pores or spatial heterogeneity of the subsurface can spread the gasoline laterally. Once the leak in the storage tank has been discovered and fixed, the flow of liquid gasoline through the soil will eventually come to a halt. Any soil, which has been in contact with the liquid gasoline, will retain some in its pore space, where capillary forces compensate the force of gravity [36]. This contaminated region is often referred to as source zone. Even if the organic liquid is immobilized in the soil pores of the source zone, gas-phase diffusion will continue to spread the gasoline vapors in the surrounding soil. Some of these vapors will dissolve into the soil water and may reach the aquifer through infiltration.

Natural attenuation. In many soils the indigenous microbial population will after a certain time period get adapted to the presence of gasoline constituents in the soil water and use them for their respiration cycle. Some microorganisms can transform potentially harmful chemicals into CO_2 . Under favorable conditions, this process can confine many harmful constituents of gasoline to a limited area around the source zone. The reduction in contaminant concentration with increasing distance from the source zone is often referred to as natural attenuation [57]. This favorable process, which includes dilution, sorptive uptake and degradation, may help to contain the contam-

Table 1.1: Typical site investigation methods for the vadose zone.

Method	Characterization
Soil core sampling	Local investigation of the soil profile [2].
Soil gas sampling	Soil gas concentrations of contaminants, O ₂ , CO ₂ [2].
Flux chambers	Diffusive contaminant flux to the atmosphere [48].
Partitioning Inter-well Tracer Test	Average NAPL saturation between 2 profilers [47].
²²² Rn activities	NAPL localization, through analysis of naturally occurring ²²² Rn [23].
Fluorescence probes	NAPL localization with special probes by fluorescence [33].

ination within a limited area. Environmental protection agencies generally accept natural attenuation as an in situ remediation strategy, if the concentrations of harmful chemicals stay below limit values at points of interest. Such points of compliance are typically the aquifer below a contaminated site, a well in the aquifer at a certain distance downgradient from a contaminated site, a nearby public drinking well or the cellar of a nearby house.

Site investigation methods. Natural attenuation has become a popular concept for an in situ remediation. It relies on naturally occurring processes and can be much more cost-effective than active remediation measures. It is, however, generally understood that such a passive approach requires a careful *risk assessment, monitoring and control of remediation objectives*. The environmental engineer needs a number of *tools and investigation methods* to accurately describe the initial situation at contaminated sites and to predict and monitor the future development of natural attenuation processes such as diffusive spreading of contaminant vapors, volatilization, sorption, and degradation. Typical site investigation methods for the vadose zone are listed in Table 1.1. In the following chapters, these well-established methods will be discussed in greater detail and compared to a new method for the investigation of the vadose zone.

Chapter 2

Objectives, Innovation and Outline

Objectives. The objective of this thesis is to develop new inexpensive investigation methods for the *in situ determination* of soil parameters, which are important for risk assessment and the monitoring of remediation efforts. In a nutshell, the approach is the following: A small volume of gaseous tracers is injected into the soil. The tracers are observed, while they diffuse away from the injection point. Data gained from such experiments are interpreted with mathematical equations. The specific goals are

1. to learn more about gas-phase diffusion in the investigated soil, and
2. to use gaseous tracers for the detection and quantification of liquid contaminant phase.

The practical application could be the following:

1. An environmental engineer investigates a large-scale gasoline spill. He would like to calculate whether diffusive oxygen supply from the atmosphere is sufficient to meet the oxygen demand of gasoline degrading microorganisms. He also wants to know how fast vapors of the carcinogenic compound benzene will reach the aquifer or a nearby cellar.
2. The same environmental engineer wants to monitor the decline in the amount of liquid gasoline retained in the soil pores, in order to verify the progress of natural attenuation.

In technical terms: Gaseous tracer diffusion from a point source is tested as an *in situ* method to determine *effective* and *sorption-affected gas-phase diffusion coefficients* and the *residual NAPL saturation* in the vadose zone.

Innovation. The innovation of this work is the combined use of *conservative and partitioning* gaseous tracers¹ in instantaneous point source diffusion experiments. The theory and methodology of diffusive tracer experiments is extended to account for partitioning into stationary phases and degradation. This makes the method a versatile tool for the investigation of the vadose zone.

Outline of the thesis. The content of this thesis has been organized by presenting first the common theoretical basis and a data base with partitioning coefficients measured in batch experiments. Results of the in situ method are then presented in later chapters. The content of the next chapters can be characterized as follows:

Chapter 3 lists the relevant assumptions for the derivation of the theory, formulates the differential equation describing gas-phase diffusion in a porous medium and presents the analytical solutions to this equation for the boundary conditions of interest.

Chapter 4 presents the results of batch experiments, which were performed to investigate the sorption of gaseous compounds in the relevant porous media: a sand used in laboratory column studies, a sand used in a large scale lysimeter and a sand from a Danish field site. Also presented are experimentally determined air-NAPL partitioning coefficients for a few partitioning tracers of interest.

Chapter 5 documents a first application of the in situ method: the determination of effective and sorption-affected gas-phase diffusion coefficients. Results are reported for a sand-filled lysimeter and a Danish field site.

Chapter 6 contains laboratory results for a second application of the new method: the diffusive partitioning tracer test (DPTT). This method allows a localization and quantification of NAPLs in the vadose zone. The method was evaluated in a number of sand-filled laboratory columns with different NAPL and water content.

Chapter 7 documents the application of the DPTT in a more natural setting: a Danish field site, where an artificial contamination has been embedded in the sandy unsaturated zone. The DPTT was performed

¹A conservative gaseous tracer is a non-degradable compound. In a soil which consists of different phases such as solids, soil water and soil air this compound is only found in the gas-phase. Contrary to the conservative tracer, the partitioning tracer is also found in phases other than the soil air.

within the contamination and away from the contamination in the natural subsurface. The compatibility of the new method with traditional soil gas monitoring was also investigated.

Chapter 8 discusses the performance of the DPTT in a sand-filled lysimeter with a well-defined heterogeneous NAPL distribution. Two different ways to obtain the NAPL saturation from a DPTT are presented. The chapter characterizes these two approaches and compares them with a well established partitioning tracer method, the partitioning interwell tracer test (PITT).

Chapter 9 summarizes and discusses the results and formulates open questions.

Publications. The chapters of this thesis do not correspond to scientific publications, because it seemed preferable to combine each, the common basic theory and similar batch experiments in single chapters. The content of the thesis has been worked into three scientific articles:

Werner, D., Höhener, P., 2002. An in situ method to measure effective and sorption-affected gas-phase diffusion coefficients in sandy soils. *Environ. Sci. Technol.*, submitted.

Werner, D., Höhener, P., 2002. Diffusive partitioning tracer test for nonaqueous phase liquid (NAPL) detection in the vadose zone. *Environ. Sci. Technol.*, 36: 1592-1599.

Werner, D., Höhener, P., 2002. Diffusive partitioning tracer test: Extension of the concept, the effect of heterogeneity and field experiments. In prep.

Additional publications. Luckily the three years of this thesis also allowed to collaborate and contribute to the work of others. The following scientific articles or book chapters are the crop of such activities and address topics that are not directly part of this manuscript:

Werner, D., Höhener, P., 2002. The influence of water table fluctuations on the volatilization of contaminants from groundwater. In: Thornton, S.F., Oswald, S.E. (Eds.), *Proceedings of the Groundwater Quality 2001 Conference held at Sheffield. Natural and enhanced restoration of groundwater pollution*. IAHS Press, Wallingford. IAHS Publ. no 275.

Höhener, P., Werner, D., Balsiger C., Pasteris, G., 2002. Occurrence and fate of chlorofluorocarbon plumes in groundwater. In: Thornton, S.F., Oswald, S.E. (Eds.), *Proceedings of the Groundwater Quality 2001 Conference held at Sheffield. Natural and enhanced restoration of groundwater pollution*. IAHS Press, Wallingford. IAHS Publ. no 275.

Pasteris, G., Werner, D., Kaufmann K., Höhener, P., 2002. Vapor phase transport and biodegradation of volatile fuel compounds in the unsaturated zone: a large scale lysimeter experiment. *Environ. Sci. Technol.*, 36: 30-39.

Höhener, P., Werner, D. Balsiger, C. Pasteris, G., 2002. Worldwide occurrence and fate of volatile fluorinated organic compounds in groundwater. *Crit. Rev. Env. Sci. Control.*, in press.

Chapter 3

Basic Theory

Relevant assumptions. For the derivation of the theory, the pore space of the soil is described as a homogeneous three-phase system consisting of air, water, and nonaqueous phase liquid (NAPL). The properties of the soil are assumed to be constant over the distance and timescale of interest. Partitioning of gaseous tracers between the three phases of the pore space and the solids is described with partitioning constants and an instantaneous, reversible, linear equilibrium is assumed. Degradation is described with a single first-order rate constant for the water-phase. It is assumed that degradation occurs in the water-phase only. Gas-phase diffusion is considered to be the only relevant transport mechanism.

Partitioning of gaseous tracers in soil. Assuming an instantaneous, reversible, linear equilibrium between the soil air, water, NAPL and the wetted solids, the partitioning of a gaseous tracer can be described using the air-water partitioning coefficient or Henry constant H , the air-solid partitioning coefficient K_s , and the air-NAPL partitioning coefficient K_n . Dimensions and definitions are given under Notation. The mass fraction of the tracer in the soil air f_a can be calculated:

$$f_a = \frac{1}{1 + \frac{\rho_s(1-\theta_t)}{K_s\theta_a} + \frac{\theta_w}{H\theta_a} + \frac{\theta_n}{K_n\theta_a}} , \quad (3.1)$$

where θ_a , θ_w , θ_n and θ_t denote the air-filled, water-filled, NAPL-filled, and total porosity and ρ_s denotes the density of the solids. The air-solid partitioning coefficient K_s is defined as the ratio of the Henry constant H and the distribution coefficient K_d between the solid and the water-phase. The mass

fraction in the soil water f_w is

$$f_w = \frac{\frac{\theta_w}{H\theta_a}}{1 + \frac{\rho_s(1-\theta_t)}{K_s\theta_a} + \frac{\theta_w}{H\theta_a} + \frac{\theta_n}{K_n\theta_a}} , \quad (3.2)$$

the mass fraction in the NAPL f_n is

$$f_n = \frac{\frac{\theta_n}{K_n\theta_a}}{1 + \frac{\rho_s(1-\theta_t)}{K_s\theta_a} + \frac{\theta_w}{H\theta_a} + \frac{\theta_n}{K_n\theta_a}} , \quad (3.3)$$

the mass fraction on the solids f_s is

$$f_s = \frac{\frac{\rho_s(1-\theta_t)}{K_s\theta_a}}{1 + \frac{\rho_s(1-\theta_t)}{K_s\theta_a} + \frac{\theta_w}{H\theta_a} + \frac{\theta_n}{K_n\theta_a}} . \quad (3.4)$$

Diffusion of gaseous tracers in soil. General equation. With the above assumptions and using the modified form of Fick's second law to describe the diffusive transport of gaseous tracers, the general equation for gas-phase diffusion in soils becomes

$$\frac{\partial C_a}{\partial t} = (f_a \tau D_m \Delta) C_a - f_w k_w C_a , \quad (3.5)$$

where (Δ) denotes the Laplace operator, τ denotes the tortuosity factor, k_w the first-order degradation rate constant for the soil water and D_m the molecular diffusion coefficient. The parameters accounting for degradation can be lumped into an apparent first-order degradation rate constant

$$k_{app} = f_w k_w . \quad (3.6)$$

Analytical solutions to this kind of differential equation have been generated for many boundary conditions and initial conditions [8].

Solution for an instantaneous plane source. If one assumes a mass $M = m_0/A$ released in a plane at $x = 0$ then the concentration in the soil air C_a at distance x from the plane and at time t is given by:

$$C_a(x, t) = \frac{m_0 f_a}{2A\theta_a \sqrt{f_a \tau D_m \pi t}} \exp\left(\frac{-x^2}{4f_a \tau D_m t} - k_{app} t\right) . \quad (3.7)$$

The tracer mass fraction $f_{x'}$ within $-x' \leq x \leq x'$ is given by:

$$f_{x'}(x', t) = \operatorname{erf}\left(\frac{x'}{2\sqrt{f_a \tau D_m t}}\right) . \quad (3.8)$$

The tracer mass fraction within a certain distance x' from the plane and in a certain soil compartment such as the soil air or the soil water can be obtained by multiplying $f_{x'}$ with the respective tracer mass fraction f_a , f_w and so on. When degradation is negligible ¹ the concentration in the soil air at the location of the plane $C_a(0, t)$ is given by:

$$C_a(0, t) = \frac{m_0 f_a}{2A\theta_a \sqrt{f_a \tau D_m \pi t}} . \quad (3.9)$$

Solution for an instantaneous point source. If one assumes an instantaneous point source of mass m_0 released at $r = 0$, then the concentration in the soil air C_a at distance r from the injection point and at time t is given by:

$$C_a(r, t) = \frac{m_0 f_a}{8\theta_a (f_a \tau D_m \pi t)^{1.5}} \exp\left(\frac{-r^2}{4f_a \tau D_m t} - k_{app} t\right) . \quad (3.10)$$

The tracer mass fraction $f_{r'}$ within a certain distance r' from the injection point is given by:

$$f_{r'}(r', t) = \operatorname{erf}\left(\frac{r'}{2\sqrt{f_a \tau D_m t}}\right) - \frac{r'}{\sqrt{f_a \tau D_m \pi t}} \exp\left(\frac{-r'^2}{4f_a \tau D_m t}\right) . \quad (3.11)$$

The tracer mass fraction within a certain radius r' from the injection point and in a certain soil compartment such as the soil air or the soil water can be obtained by multiplying $f_{r'}$ with the respective tracer mass fraction f_a , f_w and so on ². When degradation is negligible the concentration in the soil air at the injection point $C_a(0, t)$ is given by:

$$C_a(0, t) = \frac{m_0 f_a}{8\theta_a (f_a \tau D_m \pi t)^{1.5}} . \quad (3.12)$$

Extended initial distribution. Neither a perfect plane source nor a perfect point source of tracer gas is practically feasible. Therefore analytical solutions to eq (3.5) have been derived for some extended initial distributions of the diffusing substance. In the following, degradation is considered to be negligible. If the diffusing substance is initially confined to the region

¹Here and henceforth in this chapter: Otherwise one writes an additional exponential factor $\exp(-k_{app} t)$.

²The method of Hers et al. [20] for the determination of apparent diffusion coefficients is based on the assumption that by sampling the soil air volume $\frac{4}{3}\pi\theta_a r'^3$ around the injection point one retrieves the tracer mass fraction $f_{r'}$. It is however more plausible that one retrieves something in between $f_{r'} \cdot f_a$ and $f_{r'}$ and that this method only works for conservative tracers with $f_a \approx 1$.

$-h < x < +h$ with a constant soil air concentration $C_0 = m_0 f_a / 2hA\theta_a$ the soil air concentration at $x = 0$ is given by

$$C_a(0, t) = \frac{m_0 f_a}{2hA\theta_a} \operatorname{erf} \left(\frac{h}{2\sqrt{f_a \tau D_m t}} \right). \quad (3.13)$$

If the diffusing substance is initially confined to the region $0 < r < a$ with a constant soil air concentration $C_0 = 3m_0 f_a / 4\pi a^3 \theta_a$ the soil air concentration at $r = 0$ is given by

$$C_a(0, t) = \frac{m_0 f_a}{\frac{4}{3}\pi a^3 \theta_a} \left[\operatorname{erf} \left(\frac{a}{2\sqrt{f_a \tau D_m t}} \right) - \frac{a}{\sqrt{f_a \tau D_m \pi t}} \exp \left(\frac{-a^2}{4f_a \tau D_m t} \right) \right]. \quad (3.14)$$

It can however be shown that for $t \rightarrow \infty$ eq (3.13) tends towards eq (3.9) and eq (3.14) towards eq (3.12)³. It is therefore plausible that the soil air concentrations measured at the injection point are, after an initial time lag, accurately described by the equations for a plane source or a point source even if there is some deviation from the assumed initial condition.

Practical application of the theory. The equations derived in this chapter will be used to interpret data from gas-phase diffusion experiments. Two distinct experimental set-ups are sketched in Figure 3.1. In laboratory experiments the gaseous tracers are injected into the center of sand-filled columns. Tracer concentrations in the soil air change mainly along the axis of the column and are interpreted with eq (3.7) derived for the plane source. In a large scale lysimeter or in the field, gas-phase diffusion spreads the tracers in all directions and is interpreted with eq (3.10) derived for the point source. Figure 3.1 shows a few concentration profiles for a partitioning and a non-partitioning tracer, with an identical total tracer mass m_0 and with identical properties, except for the mass fraction in the air f_a , which is 0.25 for the partitioning tracer and 1 for the non-partitioning tracer. The dilution or concentration decline of the gaseous tracers is faster for the point source as compared to the plane source. In both situations, the non-partitioning tracer migrates further than the partitioning tracer. However, for the situation with a point source a higher concentration of the partitioning tracer results at the injection point as compared to the non-partitioning tracer. The opposite is true for the plane source. Furthermore, the concentration ratio of the non-partitioning and partitioning tracer at the injection point is time independent in both situations, see also eq (3.9) and eq (3.12).

³This can be seen by developing eq (3.13) and eq (3.14) into their polynoms. With respect to large time t eq (3.9) and eq (3.12) are the leading contribution to the respective polynom.

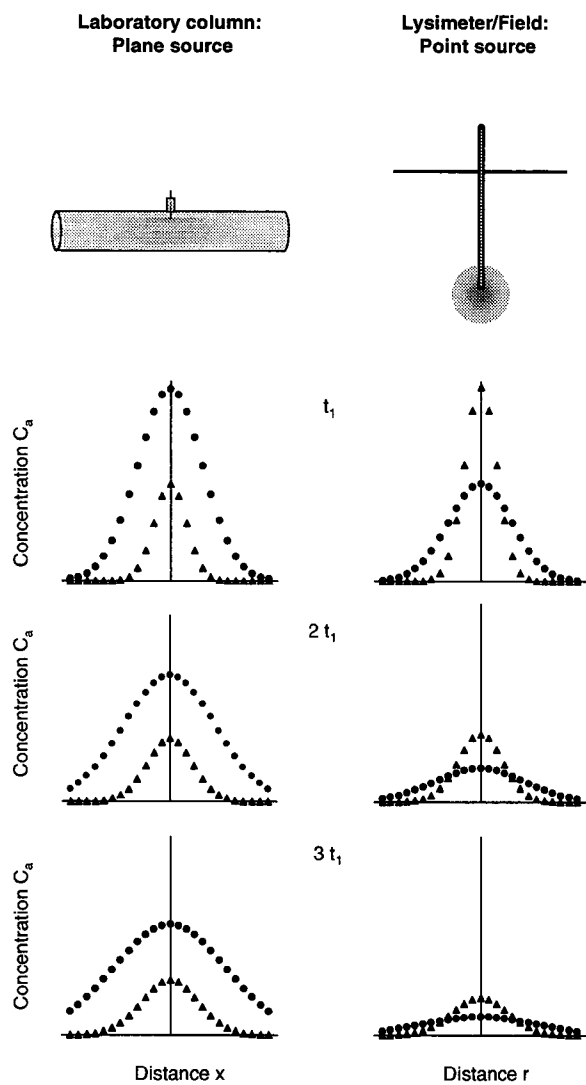


Figure 3.1: Diffusion from a plane source and from a point source for a non-partitioning tracer (\bullet) and a partitioning tracer (\blacktriangle), both with $k_{app} = 0$.

Chapter 4

Batch Experiments

4.1 Introduction

Partitioning behavior of volatile organic compounds in soil. Partitioning of volatile organic compounds (VOCs) between the soil water, the solids, the NAPL-phase and the soil air is a key issue when discussing the fate and impact of these chemicals in the subsurface. Partitioning affects the migration of organic compounds, as shown in Figure 4.1. Gas-phase diffusion will spread compounds only at times, when they are actually present in the soil air. Therefore knowledge of the mass fraction f_a of a compound in the soil air is crucial, when studying gas-phase diffusion in the vadose zone.

Air-water partitioning equilibrium. The partitioning of a compound between the soil air and the bulk soil water-phase is typically described with the Henrys law constant H , the partitioning coefficient between air and water. Measured Henrys law constants H and their temperature dependency are available from literature for many volatile organic compounds [54].

Air-solid partitioning equilibrium. In moist soils with a high relative humidity the solid surfaces are covered with water films and there is no direct contact between the soil air and the solid surface. Assuming an equilibrium distribution between soil air, soil water and the water-coated solids, one can still define an air-solid partitioning coefficient K_s as introduced in Chapter 3 equal to the ratio of the Henrys law constant H and the solid-water partitioning coefficient K_d . This coefficient is a constant and independent of the compound concentration in the case of linear sorption isotherms, which are often observed at low compound concentration [52]. Sorption in a complex medium such as soil is most likely the result of several mechanisms acting

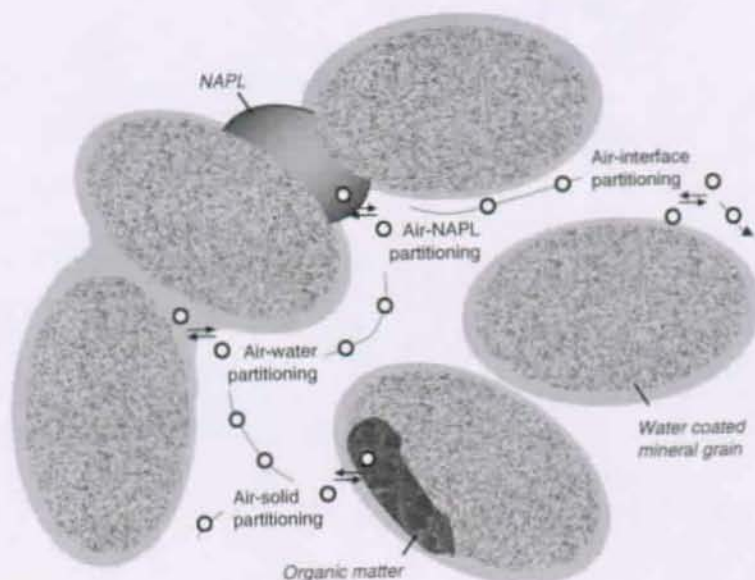


Figure 4.1: Partitioning of a volatile organic compound (o) in the soil.

in parallel. However, as long as each of these mechanisms can be described with a linear sorption isotherm, the combined effect can also be described by a single constant K_s , made up of several contributions. For *small* and *non-polar* organic compounds as investigated in this study sorption to natural, water-coated solids is often dominated by absorption into natural organic matter. Sorption to mineral surfaces may become important at a low relative humidity [45] or in moist soil with a low organic matter content [53], typically if the organic matter content f_{om} is $< 0.2\%$ [52].

Air-interface partitioning equilibrium. Adsorption to the air-water interface is considered to be relevant for hydrophobic compounds in soils with a low volumetric water content, a large air-water interfacial area and a low organic matter content f_{om} [22], [45]. Adsorption to the air-water interface is concentration dependent, with cooperative solute-solute association at very high gas-phase concentrations, but linear adsorption isotherms can be obtained at low concentrations [53]. Experimental results on the relevance of this adsorption mechanism in low f_{om} geomeedia are controversial: Silva et al. [53] suggest that previous studies have overestimated the relevance of adsorption to the air-water interface, because sorption to the mineral surface

was not considered in the data evaluation [45] or because the reported air-water interfacial area was unrealistically high [7]. Air-interface partitioning has not been considered as a mechanism in the theory developed in Chapter 3, mainly because this investigation focuses on in situ methods. It is difficult to determine the air-water interfacial area in situ. An eventual compound mass adsorbed to the interface will therefore be wrongly attributed to the mass sorbed to the solids.

Air-NAPL partitioning equilibrium. The presence of a nonaqueous phase liquid (NAPL) such as fuel, oil or solvent in the subsurface of contaminated sites has a significant impact on the partitioning behavior of nonpolar organic compounds. Even though the composition can vary considerably among the various types of NAPL, they generally provide an environment similar to the pure liquid phase of such compounds. The affinity to a NAPL-phase is therefore mainly a function of their volatility, being high for compounds with a low vapor pressure and vice versa.

Partitioning kinetics. The use of partitioning coefficients for the description of the compound mass distribution in a soil is based on the assumption that time was sufficient to achieve equilibrium between the different soil compartments. Mass transfer from the soil air through the water films to sorption sites within solids can, however, inhibit sorptive equilibrium, especially if sorption sites are located within particles or particle aggregates, for instance organic matter located in macropores of mineral grains [19]. Slow desorption of organic compounds from high affinity sorption sites can also inhibit sorptive equilibrium [50]. For air-NAPL partitioning, the kinetics have been investigated by researchers interested in the advective migration of air-NAPL partitioning tracers in contaminated soils [55]. Their main conclusion is that partitioning equilibrium is reached at low advective migration velocities, typically in the same range as gas-phase diffusion.

Aims. The following chapters focus on gas-phase diffusion in the vadose zone. As mentioned above, gas-phase diffusion of an organic compound is affected by the partitioning between the soil air and other soil compartments, where the compound is considered to be immobile. The mass fraction of a compound in the soil air f_a is therefore of particular interest. The aim of this chapter is to present a data base with air-solid partitioning coefficients K_s and air-NAPL partitioning coefficients K_n measured in batch experiments for the sands and NAPLs of interest. This data can later be used to interpret and validate f_a measured in situ. The comparison of f_a measured in batches

with live and sterilized soils as a function of time allowed the investigation of biodegradation rates and slow sorption kinetics.

4.2 Theory

Degradation rate constants. If one assumes that the organic compounds in a soil-filled batch are spatially evenly distributed at all times the solution to eq (3.5) is given by:

$$C_a(t) = C_0 \exp(-k_{app} t) , \quad (4.1)$$

where C_0 is the initial concentration in the soil air. The apparent first-order degradation rate k_{app} can thus be obtained from a linear regression $\ln(C_a(t))$ vs t .

Partitioning coefficients. For a batch filled with sterilized soil, the air-solid partitioning coefficient K_s can be determined from the mass fraction of tracer i in the soil air $f_{a,i}$ as follows:

$$K_{s,i}^{-1} = \frac{\theta_a}{\rho_s(1 - \theta_t)} \left(\frac{1}{f_{a,i}} - 1 - \frac{\theta_w}{H\theta_a} \right) . \quad (4.2)$$

If sorption of a compound to natural organic matter is the dominating sorption mechanism in a porous medium, the air-solid partitioning coefficient K_s can also be estimated [57]:

$$K_{s,i} = \frac{H}{K_d} \approx \frac{H}{1.72 f_{oc} K_{om}} . \quad (4.3)$$

The organic matter-water partitioning coefficient K_{om} can be estimated from the octanol-water partitioning coefficient K_{ow} , for instance with the formula [52]

$$\log K_{om,i} \approx 0.82 * \log K_{ow} + 0.14 . \quad (4.4)$$

The air-NAPL partitioning coefficients K_n can be determined from the mass fraction of tracer i $f_{a,i}$ in the headspace of a batch with a volume V_n of NAPL and a volume V_a of headspace as follows:

$$K_{n,i}^{-1} = \frac{V_a}{V_n} \left(\frac{1}{f_{a,i}} - 1 \right) . \quad (4.5)$$

4.3 Materials and Methods

Chemicals. All chemicals were obtained in the highest available purity. Chlorofluorocarbons CFC-11, CFC-12, CFC-114, petroleum hydrocarbons and chlorinated ethenes were obtained from Fluka (Buchs, Switzerland). CFC-113 was obtained from Merck (Dietikon, Switzerland). SF_6 was obtained from Carbagas (Lausanne, Switzerland). Relevant physicochemical properties of the compounds are given in Table 4.1 and Table 4.2. Besides dodecane, two different artificial fuel mixtures were used in the experiments as a NAPL. They were a mixture of typical linear and branched alkanes and aromatic hydrocarbons. One (fuel 1, composition reported in [44]) contained MTBE (5 % w/w), the other one (fuel 2) MTBE and Ethanol (5 % w/w each) as additive. Furthermore, trace amounts of CFC-11 (fuel 1) or CFC-113 (fuel 2) were added to the mixtures for experimental purposes, and the liquids were dyed red with Sudan IV.

Sands. Three different porous media are investigated in this and following chapters: Sand-filled laboratory columns, a sand-filled lysimeter and a field site with a sandy unsaturated zone. These porous media can be characterized as follows:

Laboratory columns were packed with a sand originating from the southern shore of Lake Geneva. Typical resulting porosities were $\theta_t = 0.47$ and $\theta_w = 0.04$. The sand had a f_{oc} of $0.06 \pm 0.03\%$ and the following grain size distribution: < 4 mm: 99.0% of weight; < 2 mm: 91.3%; < 1 mm: 85.0%; < 0.5 mm 58.1%; < 0.2mm: 20.0%; < 0.05 mm: 1.3%.

A large-scale lysimeter was packed with a sand originating from the Rhone river delta in Lake Geneva. The resulting porosities were $\theta_t = 0.42$ and $\theta_w = 0.06$. The sand had a f_{oc} of $0.2 \pm 0.1\%$ and the following grain size distribution: < 4 mm: 99.0% of weight; < 2 mm: 89.7%; < 1 mm: 78.5%; < 0.5 mm 50.2%; < 0.25 mm: 19.1%; < 0.1 mm: 2.5%.

A field site near Lyngby, Denmark had a sandy C horizon with porosities $\theta_t = 0.31$ and $\theta_w = 0.06$. The sand had a f_{oc} of $0.04 \pm 0.02\%$ and the following grain size distribution: < 5 mm: 98% of weight; < 2 mm: 97%; < 1 mm: 96%; < 0.5 mm 90%; < 0.2mm: 59%; < 0.1 mm: 16%; < 0.05 mm: 4%.

Determination of apparent first-order degradation rates. Glass vials (64 mL) with Mininert-valves (Fluka, Buchs, Switzerland) were filled to the top with sand. The sand was settled as good as achievable by shaking and

Table 4.1: Physicochemical properties. Data from [59].^a

Compound	MW	V_m	$D_m(25^\circ C)^b$	$\log K_{ow}(25^\circ C)$	$\log p^0(25^\circ C)$
SF ₆	146.1	79.2	0.089	n.a.	1.38
CFC-12	120.9	81.4	0.089	2.16	0.80
CFC-114	170.9	112.6	0.076	2.82	0.33
CFC-11	137.4	92.9	0.083	2.53	0.02
CFC-113	187.4	119.8	0.073	3.16	-0.36
Chloroethene	64.5	71.2	0.102	1.62	0.59
trans-Dichloroethene	96.94	77.9	0.093	2.09	-0.36
cis-Dichloroethene	96.94	76.6	0.094	1.86	-0.57
Benzene	78.1	89.5	0.090	2.13	-0.90
Toluene	92.1	106.6	0.082	2.73	-1.43
n-Octane	114.2	163.5	0.067	5.18	-1.99

^aThe dimension is [g/mol] for MW , [cm³/mol] for V_m , [(mol cm⁻³ octanol)/(mol cm⁻³ water)] for K_{ow} , [atm] for p^0 , which is $p^0(L)$ for gases; n.a. means not available.

^bMolecular diffusion coefficients D_m are estimated according to Fuller et al. [17], who suggest $D_m(T)/D_m(298.15K) \approx (T/298.15)^{1.75}$ for the temperature dependency. According to [38] measured $D_m(25^\circ C)$ in N₂ are 0.091 for CFC-12 and 0.082 for CFC-114.

Table 4.2: Henry constant H for different temperatures. Data from [54], CFC-114 data from [12], SF₆ data from [58].^a

Compound	$H(25^\circ C)$	$H(20^\circ C)$	$H(15^\circ C)$	$H(10^\circ C)$
SF ₆	168	147	126	105
CFC-12	13	11	9.1	7.5
CFC-114	51	43	36	31
CFC-11	3.8	3.2	2.7	2.2
CFC-113	12	10	8.5	7.1
Chloroethene	1.1	0.89	0.75	0.63
Trans-dichloroethene	0.45	0.36	0.29	0.23
Cis-dichloroethene	0.17	0.14	0.11	0.09
Benzene	0.24	0.19	0.15	0.12
Toluene	0.26	0.21	0.16	0.13
n-Octane	138	90	57	36

^aThe dimension of H is [(mol cm⁻³ air)/(mol cm⁻³ water)]. n-Octane: H from [54] · 10.

adding more sand, until it could not be settled any further. The air-filled, water-filled and total porosities θ_a , θ_w , θ_t were calculated from the weight and the water content of the sand filled into the batches assuming a density ρ_s of 2.5 for the solids. Resulting total porosities θ_t ranged from 0.40 to 0.50. Batches were kept at a constant temperature T . Equal amounts of a contaminant vapor mixture were injected into a sand-filled and an empty flask, and the concentrations were monitored over a period of 34 hours. The empty vial served as a control. The vials were initially shaken to facilitate a homogeneous distribution of the compounds. The apparent first-order degradation rate k_{app} was calculated from the concentration decline in the sand-filled vial. The soil was thereafter dried overnight at 105 °C and moistened again to allow germination of microorganism spores. This procedure was repeated three times and an identical control experiment was performed thereafter with the sterilized, re-moistened sand.

Determination of air-solid partitioning coefficients. Vials (64 mL) with Mininert-valves were filled with sterilized, moistened sand as described in the previous paragraph. Resulting total porosities θ_t ranged from 0.40 to 0.50. Equal amounts of a contaminant vapor mixture were injected into a sand-filled and an empty vial, the batches were kept at a constant temperature T , and the concentrations were monitored over a period of 8 h. The mass fraction f_a of each compound in the soil air was determined by dividing the mass in the gas-phase (calculated from soil air concentrations and θ_a) through the mass injected (calculated from the gas concentrations and the volume of the empty batch). Air-solid partitioning coefficients K_s were calculated using eq (4.2) and the Henry constants given in Table 4.2 for the respective temperatures.

Determination of air-NAPL partitioning coefficients. Dodecane in quantities of 0.1, 0.5, 1 and 2 mL was added to 14.5 mL glass vials with Mininert-valves. Equal amounts of the gaseous tracers were injected into the headspace of dodecane containing and an empty vial. The vials were gently shaken at 25°C for 6 hours and the concentrations in the headspace were determined. Control measurements after 48 hours yielded similar values. For each vial and each compound the fraction in the gas-phase was determined and air-dodecane partitioning coefficients K_n were calculated using eq (4.5). Air-fuel partitioning coefficients K_n were determined accordingly, but vials were equilibrated at 20°C and 10°C and the artificial fuel mixture replaced the dodecane.

4.4 Results

Apparent first-order degradation rates. Apparent first-order degradation rates $k_{app, live}$ and $k_{app, sterile}$ were measured in the lysimeter sand and in the sand from the field site. For both sands, apparent first-order degradation rates k_{app} were $< 1 \text{ d}^{-1}$ with no obvious difference between pristine and sterilized soil. The error is given as the error of the slope of the linear regression line used for the determination of k_{app} . The results of the batch experiments are summarized in Table 4.3. An initial decrease in the soil air concentrations was observed in both the pristine and the sterilized soils for the less volatile, hydrophilic compounds, resulting in a positive value for k_{app} . Figure 4.2 shows the time trend of the measured soil air concentrations for the batch experiments with sterilized lysimeter sand at 10°C . In these batches the time trends were most distinct.

Air-solid partitioning coefficients. Air-solid partitioning coefficients K_s were determined for three batches (replica) with sterilized soil. Results are reported in Table 4.3. The error for K_s is given as the standard deviation of the three measurements. The air-solid partitioning coefficients K_s for the lysimeter sand were studied at 10°C and 25°C . The air-solid partitioning coefficients K_s measured at 10°C showed an approximately twofold decrease if compared to K_s measured at 25°C , see Table 4.3.

Air-NAPL partitioning coefficients. Air-NAPL partitioning coefficients K_n were determined for SF_6 , CFC-12, CFC-114, CFC-11 and CFC-113 in dodecane at 25°C and in artificial fuel at 20°C and 10°C . Results are reported in Table 4.4. The air-NAPL partitioning coefficients K_n were calculated as mean value from the batches with different air-NAPL ratios and the error of K_n is reported as twice the experimental standard deviation. For SF_6 , results indicated $K_n > 0.4$ for all of the investigated NAPLs, but the experimental error was too high to determine reliable values. SF_6 results are therefore not reported in Table 4.4. Furthermore the artificial fuel 1 used for the determination of K_n at 20°C contained CFC-11 and the fuel 2 used for the determination of K_n at 10°C contained CFC-113. The air-NAPL partitioning coefficients K_n of these compounds are therefore not reported for the respective temperatures. In addition to the CFC-tracers, K_n were determined for trans-dichloroethene and cis-dichloroethene in dodecane at 25°C to validate the method. The results are $K_n(25^\circ\text{C}) = 0.0047 \pm 0.0007$ for trans-dichloroethene and $K_n(25^\circ\text{C}) = 0.0035 \pm 0.0005$ for cis-dichloroethene.

Table 4.3: Results of the batch experiments^a

Compound	T	$k_{app, live}$	$k_{app, sterile}$	K_s
Column sand:				
CFC-12	25	-	0.4 ± 0.5	22 ± 12
CFC-114	25	-	0.3 ± 0.5	21 ± 9
CFC-11	25	-	0.5 ± 0.6	30 ± 15
CFC-113	25	-	0.3 ± 0.5	22 ± 10
Lysimeter sand:				
SF ₆	25	-	0.1 ± 0.1	> 30
CFC-12	25	-	0.2 ± 0.1	23 ± 3
CFC-11	25	-	0.2 ± 0.1	> 30
Chloroethene	25	-	0.2 ± 0.1	17 ± 2
Trans-dichloroethene	25	-	0.6 ± 0.1	3.9 ± 0.6
Cis-dichloroethene	25	-	0.6 ± 0.1	2.7 ± 0.4
Lysimeter sand:				
SF ₆	10	0.1 ± 0.2	-0.1 ± 0.2	15 ± 8
CFC-12	10	0.1 ± 0.2	-0.3 ± 0.2	14 ± 3
CFC-11	10	0.2 ± 0.2	-0.3 ± 0.3	24 ± 6
Chloroethene	10	0.3 ± 0.2	-0.1 ± 0.2	13 ± 3
Trans-dichloroethene	10	0.5 ± 0.2	0.9 ± 0.3	2.3 ± 0.2
Cis-dichloroethene	10	0.6 ± 0.2	1.0 ± 0.3	1.5 ± 0.2
Field sand:				
CFC-12	15	0.1 ± 0.2	0.2 ± 0.2	22 ± 2
CFC-114	15	0.2 ± 0.2	0.2 ± 0.2	20 ± 4
CFC-11	15	0.2 ± 0.2	0.3 ± 0.2	24 ± 8
CFC-113	15	-0.1 ± 0.2	0.1 ± 0.2	20 ± 3
Benzene	15	0.1 ± 0.2	0.1 ± 0.2	4.1 ± 1.8
Toluene	15	0.2 ± 0.2	0.2 ± 0.2	2.9 ± 0.5
n-Octane	15	0.3 ± 0.2	0.2 ± 0.2	4.1 ± 0.9

^aDimensions are [°C] for T , [d⁻¹] for k_{app} and [(mol cm⁻³)/(mol g⁻¹ solid)] for K_s .

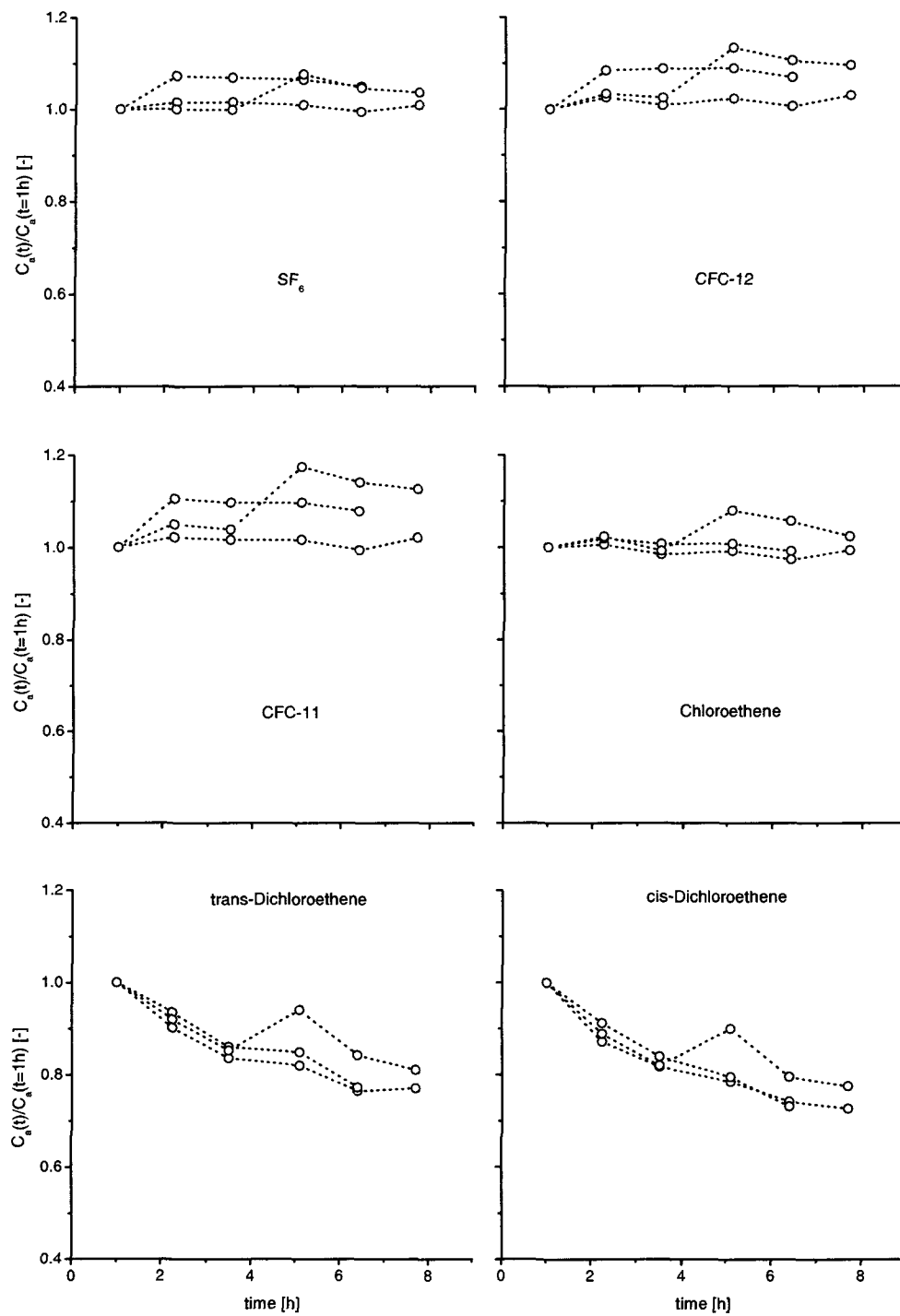


Figure 4.2: Time trend of the measured soil air concentration $C_a(t)$ (3 replica) for the sterilized lysimeter sand at 10°C.

Table 4.4: Measured Air-NAPL partitioning coefficients.^a

Compound	$K_n(25^\circ\text{C})$ for dodecane	$K_n(20^\circ\text{C})$ for fuel 1	$K_n(10^\circ\text{C})$ for fuel 2
CFC-12	0.082 ± 0.028	0.070 ± 0.030	0.033 ± 0.015
CFC-114	0.046 ± 0.012	0.032 ± 0.014	0.019 ± 0.009
CFC-11	0.010 ± 0.002	n.d.	0.0036 ± 0.0016
CFC-113	0.0061 ± 0.0010	0.0042 ± 0.0009	n.d.

^aDimensions are $[(\text{mol cm}^{-3} \text{ air})/(\text{mol cm}^{-3} \text{ NAPL})]$ for K_n ; n.d. means not determined.

4.5 Discussion

Apparent first-order degradation rates. No significant difference was found for apparent first-order degradation rates measured in pristine soil and in sterilized soil, see Table 4.3. It is concluded that biodegradation is negligible for the typical duration of the experiments ($<8\text{h}$). Apparent first-order degradation rates k_{app} measured in sterilized batches could be due to abiotic reactions, but are more likely explained with partially slow sorption kinetics, which will result in an initial slow decrease of the concentration in the soil air. Such a decrease was mainly observed in the first 5 hours for less volatile compounds in the lysimeter sand, which was the coarsest of the sands investigated and had the highest organic carbon content f_{oc} , see Section 4.3. As can be seen in Figure 4.2, soil air concentrations of volatile compounds such as the CFCs or SF_6 showed no significant time trend. Qualitatively similar results for batch experiments with VOCs and sterilized sand are reported by [21] and [42].

Air-solid partitioning coefficients. The main interest in determining K_s in this study was to have a reasonable estimate for the mass fraction f_a of the gaseous tracers and compounds in the different experimental systems. Figure 4.3 compares the mass fraction in the soil air f_a as calculated with measured or with estimated K_s for the different compounds and porous media of interest: a laboratory column at 25°C , the lysimeter at 10°C and the field site near Lyngby, Denmark at 15°C . Estimated K_s were calculated according to eq (4.3) and eq (4.4). As shown in Figure 4.3 the mass fraction in the soil air f_a calculated for three experimental systems with measured or estimated K_s compare reasonable well. The uncertainty is probably higher for f_a determined from estimated K_s , because the fraction of organic carbon f_{oc} was low

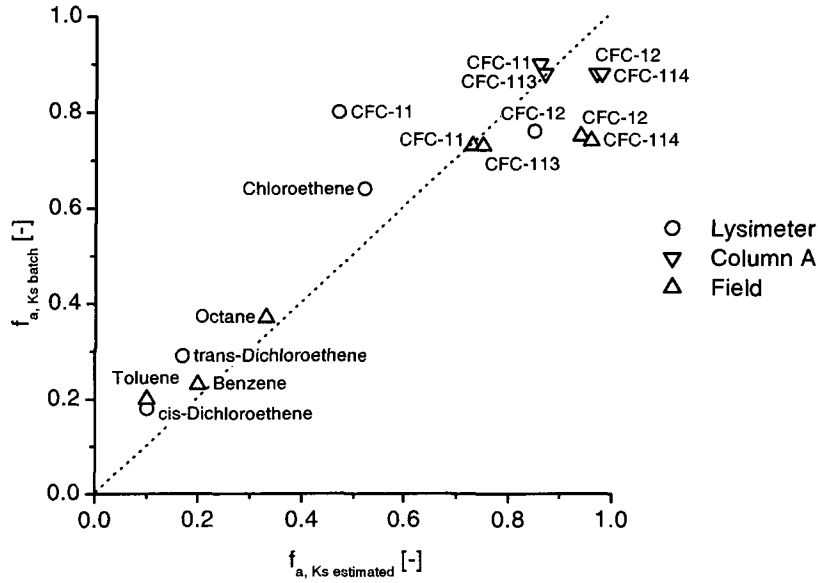


Figure 4.3: Comparison of the mass fraction in the soil air f_a as calculated with K_s from batch experiments (y-axis) or with K_s estimated according to eq (4.4) and eq (4.3) (x-axis).

for the investigated sands and close to the detection limit of the analytical method. Furthermore an empirical relation was used to estimate K_{om} . On the other hand, the uncertainty in determining air-solid partitioning coefficients K_s of very hydrophobic, volatile compounds (CFCs, SF_6) from batch experiments is also high due to the nonlinear nature of eq (4.2): if $f_{a,i}$ is close to 1, a small experimental error in the measured $f_{a,i}$ results in a large error for K_s . This explains relatively large error limits for the K_s of CFCs or SF_6 . The overall approach was to achieve similar air-water-solid ratios in batches as in the porous media of interest and to measure K_s at the temperature and compound concentrations typical for the later experiments. Simplifications such as the use of a single and concentration-independent K_s for the description of sorption processes and neglecting air-water interface adsorption in the evaluation of the batch data are then less problematic. For the sand from the field site the batches had a higher total porosity ($\theta_t = 0.4 - 0.5$) than the natural soil ($\theta_t = 0.31$). Furthermore, the accessibility of sorption sites can be altered by filling sand into batches as compared to the natural situation in the field. Therefore the uncertainty in predicting f_a is probably highest for the field site. Since degradation was negligible, K_s could also be calculated for the live batches (data not shown). They agreed within error limits with

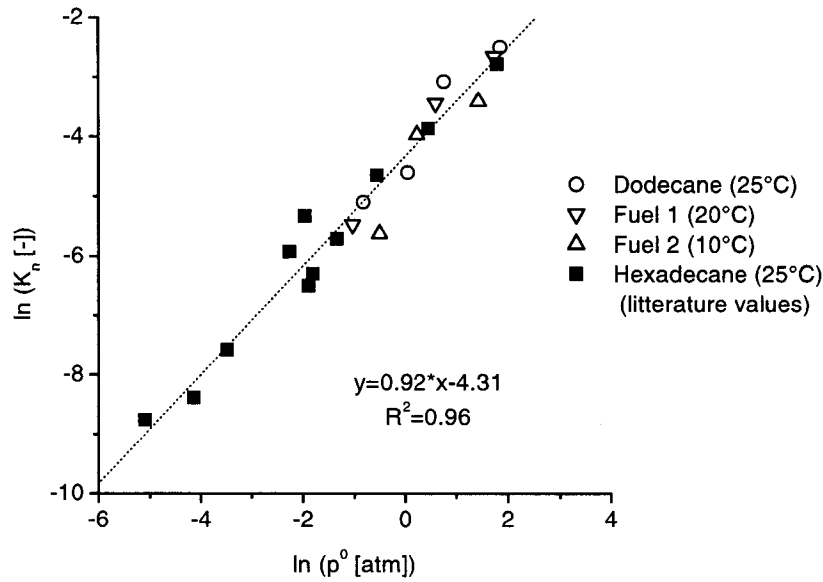


Figure 4.4: Vapor pressure dependency for the measured K_n and for K_n (hexadecane) of chlorinated methanes and ethanes from [1].

K_s determined in sterile batches, indicating that the sorptive capacity of the sands was not altered by the sterilization procedure.

Air-NAPL partitioning coefficients. The air-NAPL partitioning coefficients K_n reported in Table 4.4 show the expected vapor pressure dependency, being high for volatile and low for less volatile compounds. Figure 4.4 plots the measured K_n as a function of their vapor pressure at the respective temperature and compares them with air-hexadecane partitioning coefficients of chlorinated methanes and ethanes reported in [1]. Vapor pressure data is from reference [59]. The regression line in Figure 4.4 provides an estimate for the K_n of similar small, nonpolar compounds with an accuracy of a factor 2, if one knows the vapor pressure of the compound. Measured K_n of trans-dichloroethene and cis-dichloroethene in dodecane agree within error limits with air-hexadecane partitioning coefficients reported in [1], demonstrating the validity of the method. Abraham et al. [1] also report an air-hexadecane partitioning K_n of 1.3 for SF_6 at 25°C. This confirms the comparably low affinity of this volatile compound for the NAPL-phase and explains the difficulties in determining a reliable value for K_n of SF_6 experimentally.

Chapter 5

Determination of Apparent Diffusion Coefficients

5.1 Introduction

Gas-phase diffusion in soils. Gas-phase diffusion dominates the migration of natural gases and volatile pollutants in the unsaturated zone in the absence of pressure gradients. Gas-phase diffusion is relevant for vapor migration of volatile organic chemicals (VOCs) at contaminated sites [44], the supply of molecular oxygen to soil organisms [31], or ^{222}Rn migration from soil to houses [39]. Modelling of gas-phase diffusion in the unsaturated zone requires the knowledge of the apparent gas-phase diffusion coefficients. The molecular diffusion coefficients D_m in free air can be measured or estimated from empirical formulas [17], see Table 4.1. However, gas-phase diffusion in the unsaturated zone differs from diffusion through free air. Solid and liquid obstacles reduce the cross-sectional area and increase the mean path length in soils. This effect is identical for different gases, but specific for a certain soil at a specific water content. Furthermore, gas-phase diffusion in the unsaturated zone is affected by partitioning into the soil water, onto the soil-air interface, and into or onto the solids [18]. Gas-phase diffusion spreads only the contaminants in the gas-phase, and contaminants with a low mass fraction in the soil air will therefore diffuse slower than conservative gases, depending on the soil and the chemical properties of the diffusing substance [29]. Finally, methods to determine diffusion coefficients for non-conservative gases need to take into account degradation or reaction processes.

Apparent diffusion coefficients. Apparent diffusion coefficients are defined for gas-phase diffusion in a porous medium with proportionality fac-

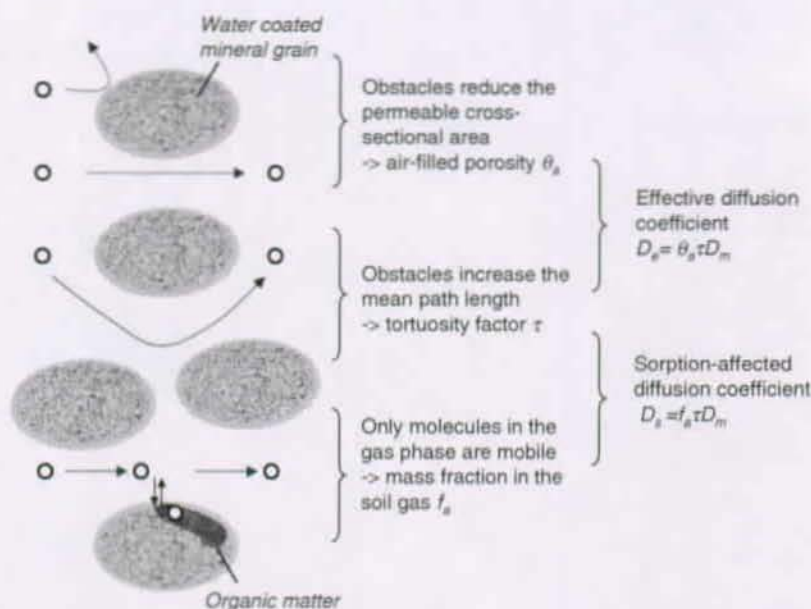


Figure 5.1: Different soil characteristics affecting the gas-phase diffusion of a volatile compound (o).

tors accounting for the effects of the physical reduction and/or partitioning [18],[30]. This is schematically shown in Figure 5.1. Effective diffusion coefficients D_e [18] account for the effect of reduced cross-sectional area and increased mean path length. They are used to calculate gas fluxes from Fick's first law or for the interpretation of *steady state* vapor concentration profiles. Sorption-affected diffusion coefficients D_s account for the effect of increased mean path length and partitioning into stationary phases such as the soil water-phase or the solids [30]. They describe the *transient* conditions such as the change of concentration profiles as a function of time.

Existing in situ methods. Large differences between the values for the effective diffusion coefficients D_e obtained from the various existing correlations [49], in laboratory tests [4], and field experiments explain the need for accurate *in situ* measurements of diffusion parameters. Flux chamber and point injection methods have been proposed to determine D_e directly in the field. Flux chamber methods are limited to surface soils. A cylinder is inserted into the soil and a gaseous tracer is supplied to the confined core from a well-stirred reservoir in a diffusion chamber placed over the cylinder [48].

Point injection methods make use of soil gas profilers or access needles to inject the gaseous tracer at the depth of interest. In the procedure reported by Lai et al. [31] a volume of gas containing the tracer is injected into the soil and the concentration change at the injection point is measured as a function of time. Jellick and Schnabel [24] find that the analytical solution for spherical diffusion used by Lai et al. [31] assumes unrealistic initial conditions and propose a finite difference model as an improvement. Ball et al. [3] use a special probe with a Geiger-Müller tube, which allows to measure the concentration decline of a radioactive tracer, ^{85}Kr , directly at the injection point. Hers et al. [20] evaluate an alternative method originally proposed by Johnson et al. [28], which determines the gas-phase diffusion coefficient from the mass fraction of the gaseous tracer found within a certain radius from the injection point rather than from the concentration change at the injection point itself. Kreamer et al. [30] use a continuous point source of gaseous tracer instead of an instantaneous point source and measure the tracer concentration in some distance from the source. Their method allows to study gas-phase diffusion over extended distances. Sorption and partitioning into the water-phase are only included in the theories of studies [30] and [20]. However, Hers et al. [20] report only data for He, which is generally considered to be a conservative tracer ¹. Kreamer and co-workers [30] conclude that the potential of their tracer test to determine in situ sorption characteristics remains undemonstrated as uncertainties in the data greatly outweigh any probable effect of dissolution or sorption. In summary, in situ methods are currently only available to measure effective diffusion coefficients, and no method has been proposed to obtain both effective and sorption-affected diffusion coefficients for partitioning gases in one in situ test.

Aims. The goal of this study is to develop the theory and to demonstrate the practical application of a new *in situ* method for the determination of *both* the effective and the sorption-affected diffusion coefficient. The method relies on the use of a gaseous compound of interest together with a conservative tracer. In this study, the compounds of interests were chlorinated ethenes or petroleum hydrocarbons, and the tracers were chlorofluorocarbons (CFCs) or sulfurhexafluoride (SF_6). The experimental set-up is similar to the one described by Lai et al. [31], with some modifications for the use of the method at greater depths. The theory is extended to include partitioning into the water-phase, sorption to solids and first-order degradation. The duration of the experiments is extended to several hours. This reduces the dependency of the results on the assumed initial condition. It reduces the velocity of the

¹Read also the footnote on page 9.

concentration change at the injection point and thus increases the probability that equilibrium conditions are reached. Furthermore it allows to investigate the relevance of degradation processes. The results of the in situ method are compared with a more conventional approach, where apparent diffusion coefficients are estimated from soil core data with empirical formulas for the tortuosity factor τ and with air-solid partitioning coefficients K_s measured in batch experiments.

5.2 Theory

Basics. The theory for the in situ determination of apparent diffusion coefficients is developed for two compounds, termed compound 1 and 2. For compound 1 the apparent diffusion coefficients and the degradation rate will be measured. Compound 2 serves as a tracer. A small volume of gas containing both compounds is injected into the soil to form a point source. It is assumed that the mass fraction in the soil air $f_{a,2}$ of the tracer and $k_{app,2}$ are known. Ideally, compound 2 is conservative, that is $f_{a,2} = 1$ and $k_{app,2} = 0$. Furthermore the method requires the knowledge of experimentally determined or estimated molecular diffusion coefficients D_m for both compounds.

Degradation. The soil air concentration C_a can be standardized with respect to the concentration of the compound in the injected gas mixture $C_{in} = m_0/V_{in}$ to obtain relative concentrations $C_r = C_a/C_{in}$. From eq (3.10) it follows that the relative concentration at the injection point $C_r(0, t)$ is given by

$$C_r(0, t) = \frac{V_{in} f_a}{8\theta_a (f_a \tau D_m \pi t)^{1.5}} \exp(-k_{app} t) . \quad (5.1)$$

From eq (5.1) it follows that

$$\ln \left[\frac{C_{r,1}(0, t)}{C_{r,2}(0, t)} \right] = \ln \left[\left(\frac{D_{m,2}}{D_{m,1}} \right)^{1.5} \left(\frac{f_{a,2}}{f_{a,1}} \right)^{0.5} \right] - (k_{app,1} - k_{app,2}) \cdot t . \quad (5.2)$$

According to eq (5.2) the difference in the apparent first-order degradation rate $k_{app,1} - k_{app,2}$ is equal to the slope of a linear regression line. Plotting data according to eq (5.2) allows to quantify the degradation.

Mass fraction in the soil air. In the following only the case, where degradation is slow over the timescale of the experiment ($k_{app,1} \cdot t \approx 0$ and

$k_{app,2} \cdot t \approx 0$) is discussed. The exponential factor in eq (5.1) can then be neglected. It follows that:

$$\frac{f_{a,1}}{f_{a,2}} = \left(\frac{C_{r,2}(0,t)}{C_{r,1}(0,t)} \right)^2 \left(\frac{D_{m,2}}{D_{m,1}} \right)^3. \quad (5.3)$$

Thus one obtains the ratio $f_{a,1}/f_{a,2}$ from the data, which explains the need to know $f_{a,2}$ in order to determine $f_{a,1}$.

Tortuosity factor. The tortuosity factor τ is obtained from the data of the tracer, for which one knows the mass fraction in the soil air $f_{a,2}$. The air-filled porosity θ_a needs to be determined independently. From eq (5.1) one finds with $k_{app} = 0$

$$\tau = \frac{V_{in}^{2/3}}{4\pi\theta_a^{2/3}C_{r,2}(0,t)^{2/3}f_{a,2}^{1/3}D_{m,2}} \cdot \frac{1}{t}. \quad (5.4)$$

Apparent diffusion coefficients. The apparent diffusion coefficients D_e and D_s can be calculated from the mass fraction in the soil air f_a , and the tortuosity factor τ , and the air-filled porosity θ_a [18]. Inserting the above expressions for f_a and τ it becomes evident that D_e can be obtained from the data as follows:

$$D_{e,1} = \theta_a \tau D_{m,1} = \frac{1}{4\pi} \left(\frac{V_{in}}{C_{r,2}(0,t)} \right)^{2/3} \left(\frac{\theta_a}{f_{a,2}} \right)^{1/3} \left(\frac{D_{m,1}}{D_{m,2}} \right) \cdot \frac{1}{t}, \quad (5.5)$$

and D_s is given by

$$D_{s,1} = f_{a,1} \tau D_{m,1} = \frac{1}{4\pi} \frac{C_{r,2}(0,t)^{4/3}}{C_{r,1}(0,t)^2} \left(\frac{D_{m,2}}{D_{m,1}} \right)^2 \left(\frac{V_{in}f_{a,2}}{\theta_a} \right)^{2/3} \cdot \frac{1}{t}. \quad (5.6)$$

Error analysis. Errors in parameters that appear with a high exponent in eq (5.5) and eq (5.6) will make a relevant contribution to the overall error of the apparent diffusion coefficients, whereas errors in parameters with a low exponent are less important. Assuming that the relative concentration $C_r(0,t)$, the air-filled porosity θ_a , $f_{a,2}$ and the ratio of the molecular diffusion coefficients $D_{m,1}/D_{m,2}$ can all be measured or estimated with an error of 10% whereas the injected volume V_{in} and the time t can be determined with negligible error, the theoretical overall error of the apparent diffusion coefficients as determined by this method is 13% for the effective diffusion coefficient D_e and 33% for the sorption-affected diffusion coefficient D_s . The method is therefore more robust for D_e . The error contribution of $C_r(0,t)$ can be reduced by calculating the apparent diffusion coefficients as an average of values measured at different times t .

5.3 Materials and Methods

Chemicals. The suppliers and the properties of the chemicals used in this study are listed in Section 4.3. All chemicals were obtained in the highest available purity.

Gaseous compound mixtures. In order to prepare mixtures of the gaseous compound and the tracer, the liquid organic compound (cis-dichloroethene, trans-dichloroethene, benzene, toluene, n-octane) was enclosed in a flask with a large headspace and a smaller quantity of the tracer (CFC-11, CFC-113) was added as liquid to the mixture or as gas (CFC-12, SF₆) to the headspace. The intention was to achieve the maximal headspace concentration for the less volatile compound, since concentrations of this compound were typically at the detection limit at the end of the experiment. The tracer was chosen to be the most volatile, fully halogenated compound (CFC or SF₆), which could be analyzed on the same GC run as the VOC and still be separated from unidentified initial peaks in the background signal of soil air. Due to the high vapor pressure and due to the low detection limits of the CFCs on GC-ECD systems, multiple mixtures of CFC-tracers could be prepared. The tracers were dissolve in octanol and the octanol was enclosed in a flask with a large headspace. Chloroethene was enclosed as pure gas in a flask and a small amount of SF₆-gas was added as the volatile, non-degradable tracer. Table 5.1 gives an overview over the different gaseous compound mixtures and the analytical system used for the measurements.

Table 5.1: Gaseous compound mixtures and the analytical system used for their detection.^a

Exp.	Compounds	C_a at 25°C	GC detector
A	CFC-11/CFC-12/SF ₆	500/2'000/1'500	ECD and FID.
B	Chloroethene/SF ₆	1'000'000/3'200	ECD and FID.
C	trans-Dichloroethene/SF ₆	44'000/1'000	ECD and FID.
D	cis-Dichloroethene/SF ₆	44'000/1'000	ECD and FID.
E	CFC-11/CFC-114/CFC-12	250/2'000/1'000	ECD.
F	CFC-113/CFC-12	250/800	ECD.
G	Benzene/CFC-11	120'000/40'000	FID.
H	Toluene/CFC-113	40'000/40'000	FID.
I	n-Octane/CFC-113	18'000/40'000	FID.

^aDimensions are [ppmv] for C_a ; Exp. means experiment.

Lysimeter. A cylindrical field lysimeter (1.2 m diameter, 2.5 m depth), similar to the one described in [44] was packed with the coarse sand originating from the Rhone river delta in Lake Geneva. See Section 4.3 for a characterization of the sand. The resulting total porosity of the porous medium was $\theta_t = 0.42 \pm 0.03$. Two stainless steel capillaries (1/16 in.) were installed at 1.5 m depth in the center of the lysimeter. One served as the injection capillary, the other one as the sampling capillary. Above ground, gastight sample lock syringes with removable needles (80727-series, Hamilton, Bonaduz, Switzerland) could be connected to the capillaries. Time domain reflectometry (TDR) probes (SDEC, Reignac s. Indre, France) were installed at 1.5 m and 1.3 m depth and a thermometer was installed at 1.5 m depth. The water-filled porosity θ_w determined with the TDR probes remained between 0.05 and 0.08, the temperature between 9 and 12 °C.

Field site. A sandy soil near Lyngby, Denmark, was used to test the method in a natural setting. The surface vegetation was a lawn. A dark brownish topsoil (30 cm) was followed by a loamy, orange colored transition zone (30 cm), which was followed by the actual sand layer, see Section 4.3 for a characterization of the sand. Two soil cores were taken before and 30 days later, after the field experiments to determine the water contents (3.3 and 3.5 percent by weight) and the total porosity θ_t (0.31 ± 0.03) at the depth of the injection point. Soil cores were homogeneous within the sandy layer to a depth of 2m. The water-filled porosity θ_w was 0.060 for the first core and 0.063 for the second core. The temperatures in a nearby sandy soil measured between 1 m and 1.5 m depth ranged from 10 to 15 °C [9], and outside temperatures ranged from 0 to 20 °C over the course of the experiments.

Soil gas probes. Soil gas probes were constructed from stainless steel tubes with an inner diameter of 4 mm, into which stainless steel capillaries (1/16 in.) were inserted. One of the capillaries was used to inject the gaseous compound mixture into the soil, the others to withdraw samples. Above ground, sample lock syringes with removable needles could be connected to the capillaries. At the bottom end, the tips of the capillaries were protected from clogging by soil with steel wool. Holes in the lowermost 5 cm of the outer tube allowed gases to diffuse in or out. Soil gas probes were installed at the field site by pre-drilling a hole of 3 cm diameter. The probes were inserted into the pre-drilled hole and then hammered an additional 35 cm into the sand, and the pre-drilled hole was backfilled with sand. This procedure reduced the risk of clogging the holes in the probe with topsoil. A schematic soil gas probe is shown in Figure 5.2.

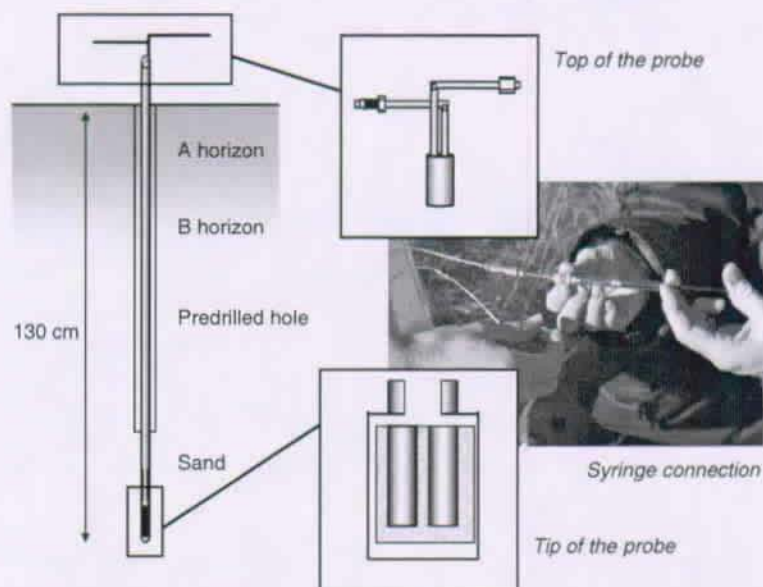


Figure 5.2: Experimental set-up at the Danish field site.

Experimental procedure. Before every experiment the flask with the mixture of gaseous compounds was equilibrated at the outside temperature. Then 5 mL of the headspace gas were sucked into a sample lock syringe, followed by 5 mL of clean air to reduce the risk of vapor condensation. The syringe was locked and the vapors were allowed to mix with the air by diffusion for 15 min. The concentration of the gaseous compounds in the syringe was determined by withdrawing three samples of 20 μL from the syringe, which were diluted and stocked in air-filled 64 mL flasks with Mininert-valves (Fluka, Buchs, Switzerland) until analysis. The gaseous compound mixture was then injected into the soil through the injection capillary, followed by 1 mL of clean air (approximately the dead volume of the stainless steel capillary). Samples were taken before the injection of the gaseous compounds (background) and at regular time intervals for 7 to 8 hours thereafter through the sampling capillary and stocked in sample lock syringes until analysis. Before every sample, 2.5 mL of soil air were withdrawn to flush the sampling capillary.

Analytical procedures. Gas samples from the lysimeter were analyzed on a Varian CP-3800 gas chromatograph equipped with an ECD and a FID

connected both to a 30 m capillary column GS-GasPro (J&W Scientific). The oven temperature was 130 °C. The injector was heated to 60 °C and the split ratio was 10. Carrier gas was Helium at a flow rate of 2 mL/min. Samples of non-halogenated compounds from the field site in Denmark were analyzed on a CarloErba gas chromatograph (AUTO/HRGC/MS) equipped with an injector heated to 200 °C in the splitless mode and a FID. A 30 m phenomenex 2B-5 capillary column was used for compound separation at a temperature of 35 °C. Carrier gas was Helium at a flow rate of 2 mL/min. Samples containing CFCs only were analyzed on a CarloErba gas chromatograph (HR GC 5300) with the injector heated to 200 °C at split ratio 5. A 25 m WCOT fused silica capillary column (CP-Sil-19 CB) (Chrompack) was used for the separation of the compounds at a temperature of 35 °C. Carrier gas was Helium at a flow rate of 2 mL/min.

5.4 Results

Relative concentrations. For the different gaseous compound mixtures the measured relative concentrations in the soil air $C_r(0, t)$ are plotted as a function of time in Figure 5.3, and results of the in situ method are reported in Table 5.2. The relative concentrations $C_r(0, t)$ are shown on a logarithmic scale, which provides more details at small concentrations. The relative concentrations $C_r(0, t)$ at the injection point fall by three orders of magnitude within the first hour and then decline more gradually with increasing time. At the end of the experiments the soil air concentrations $C_a(0, t)$ are 4 to 5 orders of magnitude lower than injected concentrations C_{in} and close to the detection limit of the analytical system. Differences in the plotted relative concentrations of the two compounds visualize differences in the molecular diffusion coefficient D_m and differences in the mass fraction in the soil air f_a . For instance, the relative concentrations of benzene, toluene and n-octane are higher than the concentrations of the respective CFC-tracers, indicating a more significant partitioning and thus a slower gas-phase diffusion of the former. Relative concentrations $C_r(0, t)$ calculated according to eq (5.1) with the fitted parameters τ and $f_{a,1}$ are shown as solid or dashed lines in the plots. It was assumed that degradation is negligible ($k_{app} \approx 0$). Molecular diffusion coefficients D_m from Table 4.1 corrected for 10 °C (lysimeter) and 13 °C (field experiment) and air-filled porosities θ_a of 0.36 for the lysimeter and 0.25 for the field site were used for the evaluation of the data. The tortuosity factor τ was determined from the data of the tracer assuming $f_{a,2} = 1$. The mass fraction in the soil air $f_{a,1}$ of compound 1 was then determined from the data of compound 1. As can be seen in Figure 5.3 the mathematical

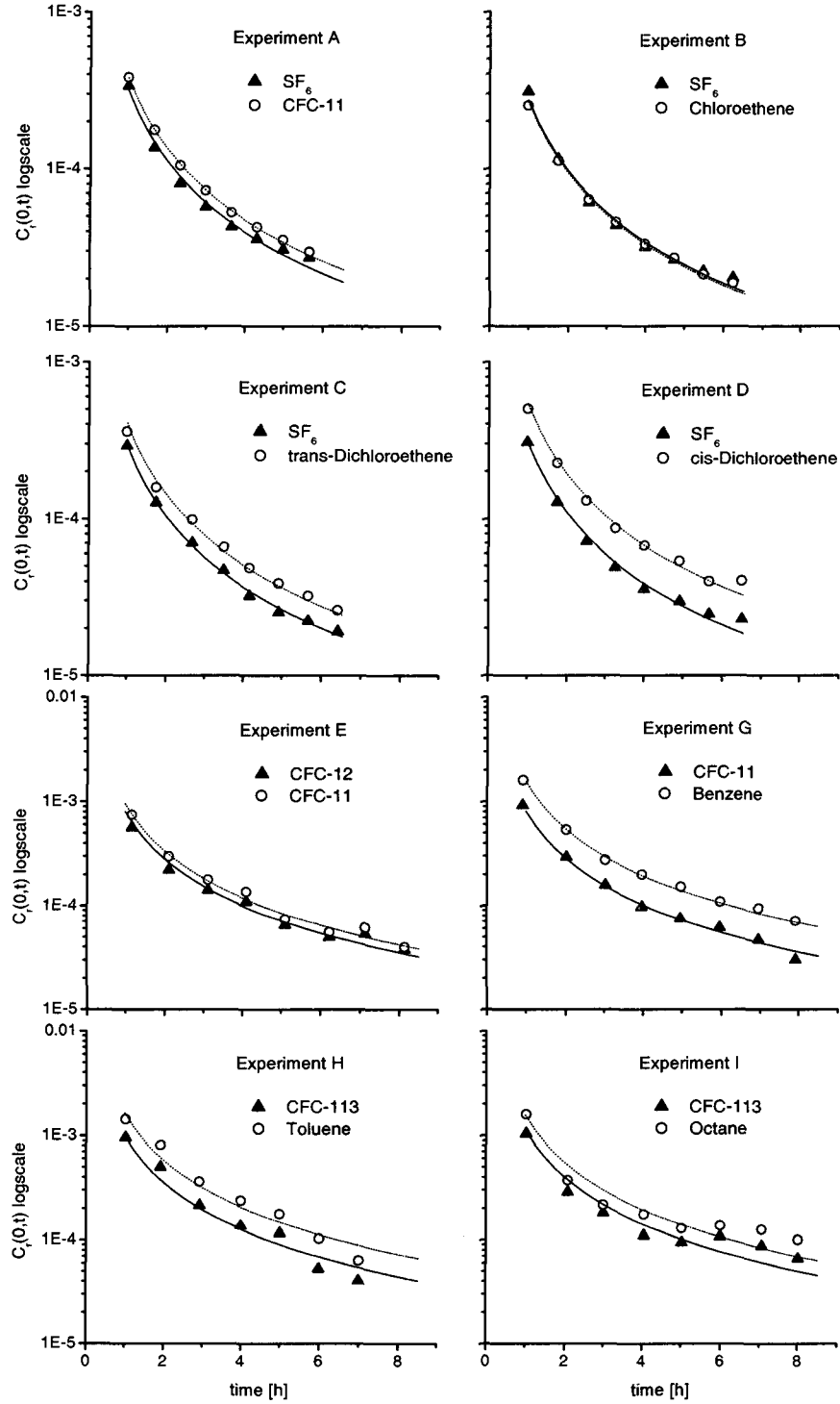


Figure 5.3: Measured $C_r(0,t)$ (symbols) and fitted model (eq (5.1) with $k_{app} = 0$; lines) from the lysimeter experiments A-D and the field experiments E-I. For experiments A, E+F data is shown for one exemplary CFC-tracer pair in each system. Data of experiments G_{rep} and H_{rep} are not shown.

Experiment	compound 1/2	$k_{app,1}^a$	$f_{a,1}/f_{a,2}^a$	$D_{e,1}/D_{m,1}^a$	$D_{s,1}/D_{m,1}^a$
Lysimeter:					
A	CFC-12/SF ₆	0.1 ± 0.4	0.82 ± 0.11	0.19 ± 0.01	0.44 ± 0.04
A	CFC-11/SF ₆	0.5 ± 0.3	0.84 ± 0.11	0.19 ± 0.01	0.45 ± 0.03
B	Chloroethene/SF ₆	-0.3 ± 0.5	0.70 ± 0.14	0.21 ± 0.01	0.41 ± 0.06
C	trans-Dichloroethene/SF ₆	-0.7 ± 0.3	0.45 ± 0.07	0.20 ± 0.01	0.26 ± 0.04
D	cis-Dichloroethene/SF ₆	-0.0 ± 0.3	0.27 ± 0.03	0.20 ± 0.01	0.15 ± 0.02
Field:					
E	CFC-114/CFC-12	0.0 ± 0.1	0.93 ± 0.03	0.09 ± 0.01	0.33 ± 0.03
E	CFC-11/CFC-12	0.8 ± 0.1	0.88 ± 0.15	0.09 ± 0.01	0.32 ± 0.05
F	CFC-113/CFC-12	-0.5 ± 0.4	0.83 ± 0.16	0.11 ± 0.01	0.38 ± 0.09
G	Benzene/CFC-11	-0.8 ± 0.3	0.22 ± 0.04	0.10 ± 0.01	0.08 ± 0.01
G _{rep}	Benzene/CFC-11	-1.1 ± 0.4	0.29 ± 0.09	0.09 ± 0.01	0.10 ± 0.03
H	Toluene/CFC-113	-0.4 ± 0.4	0.27 ± 0.05	0.10 ± 0.02	0.10 ± 0.02
H _{rep}	Toluene/CFC-113	0.1 ± 0.4	0.30 ± 0.03	0.11 ± 0.01	0.13 ± 0.02
I	n-Octane/CFC-113	-0.2 ± 0.4	0.66 ± 0.14	0.09 ± 0.02	0.23 ± 0.07

^aDimensions are [d⁻¹] for k_{app} ; ratios are dimensionless; $k_{app,1}$ calculated according to eq (5.2) with $k_{app,2} = 0$; $f_{a,1}/f_{a,2}$ calculated according to eq (5.3); $D_{e,1}$ calculated according to eq (5.5) with $f_{a,2} = 1$ and $\theta_a = 0.36$ (lysimeter), 0.25 (field); $D_{s,1}$ calculated according to eq (5.6) with $f_{a,2} = 1$ and $\theta_a = 0.36$ (lysimeter), 0.25 (field).

Table 5.2: Results of the in situ method.

model fits the data quite well. Deviations are observed in some data points from the field at low concentrations. Deviations affect both compounds in a similar way and therefore have less impact on parameters such as the apparent first-order degradations rate k_{app} or the ratio of the mass fraction in the soil air $f_{a,1}/f_{a,2}$, which are determined from concentration ratios.

Degradation. For every experiment the apparent first-order degradation rate of compound 1, $k_{app,1}$, was calculated according to eq (5.2). Results are reported in Table 5.2. Note that $k_{app,2} = 0$, because CFCs and SF_6 are not degraded under aerobic conditions. Errors are given as the error of the slope of the linear regression line used for the determination of $k_{app,1} - k_{app,2}$. An estimate for the overall uncertainty in measuring small k_{app} with the in situ method can be obtained from experiment A, E and F, where both compounds are non-degradable tracers. Experimental k_{app} between $\pm 1 \text{ d}^{-1}$ are observed, probably due to experimental error. Degradation rates $< 1 \text{ d}^{-1}$ can therefore not be determined reliably by this method. All the measured $k_{app,1}$ fell within this range, and are $< 1 \text{ d}^{-1}$. Moreover, $k_{app,1}$ is often negative, indicating an increase in the concentration of the degradable compound (chloroethenes, benzene, toluene or n-octane) at the injection point as a function of time with respect to the non-degradable, but more volatile tracer rather than a decrease. Degradation was neglected in the further evaluation of the data.

Mass fraction in the soil air. The ratio of the mass fraction in the soil air $f_{a,1}/f_{a,2}$ was calculated according to eq (5.3) with the molecular diffusion coefficients D_m listed in Table 1. The ratios were calculated for every measurement and then averaged. The error of the mean value was calculated as the experimental standard deviation for the eight measurements. Results are reported in Table 5.2. If only calculated for the measurements from 5 hours after the injection onwards, the average ratio $f_{a,1}/f_{a,2}$ is generally somewhat lower, with a difference of $< 15\%$ for all compounds (data not shown).

Apparent diffusion coefficients. Apparent diffusion coefficients were calculated from the measured data and the mean measured air-filled porosity θ_a with the approximation $f_{a,2} = 1$ for the mass fraction in the soil air of the tracer (compound 2). The apparent diffusion coefficients were calculated for every measurement according to eq (5.5) and eq (5.6) and then averaged and the experimental error of the mean value in Table 5.2 is given as the standard deviation of the measurements. The proportionality factors for the apparent diffusion coefficients and the molecular diffusion coefficient D_m are reported in Table 5.2 rather than apparent diffusion coefficients.

5.5 Discussion

Assumptions of the mathematical model. The evaluation of the data measured in situ relies on the mathematical model presented in Chapter 3, which is based on several assumptions.

Homogeneity: A first assumption is that the soil can be described as a homogeneous porous medium with uniform and constant properties. According to eq (5.1) the relative concentration $C_r(r, t)$ of CFC-12 falls to approximately 10% of the concentration $C_r(0, t)$ at the injection point within a radial distance of 80 cm after 8 hours at the field site. The other volatile organic compounds remain within a shorter radial distance. Thus, most of the compound mass remained in the sandy soil below the B horizon shown in Figure 5.2. Soil cores were homogeneous within the sandy layer to a depth of 2 m. Within the 8 hour duration of experiments, no changes of the soil properties are expected to occur. Therefore the assumption of a homogeneous medium was reasonable. The deviation of measured concentrations from model prediction observed in some field experiments for small concentrations are not systematic and attributed to increased experimental error for concentrations close to the detection limit of the analytical system. In the lysimeter, it is expected that the conservative tracer SF_6 reached the wall of the lysimeter at 60 cm distance towards the end of the experiments, but without affecting $C_r(0, t)$ significantly. A slight tendency towards higher than predicted concentrations at the end of the experiment can actually be observed in Figure 5.3.

Partitioning equilibrium: A second assumption is the instantaneous, reversible, linear equilibrium partitioning of the compounds between the different phases of the soil. Measured concentration ratios were relatively stable, suggesting that such an equilibrium exists. An initial decrease in f_a was found for the more hydrophilic and/or less volatile compounds, resulting in a negative k_{app} for many in situ experiments. This suggests that some slow kinetic processes may affect the soil air concentrations in the first hours. With increasing time the concentrations at the injection point change slower and equilibrium conditions are reached with a higher probability. Consequently, no significant time trend was found for mass fractions in the soil air determined from 5 h after the injection onward.

No advection: A third assumption is that gas-phase diffusion is the only relevant transport mechanism. Advective gas-phase transport can be

created due to gravity-driven, density dependent vapor transport [15]. Gravity-driven advection may be important in coarse soils with a high permeability [15], but is not expected to be important in the sandy soils investigated here. Furthermore the injected gaseous compounds are initially quickly diluted by diffusion due to steep concentration gradients. The concentrations measured at the injection point after one hour are far below the concentrations, where gravity-driven advection is important.

Point source: A fourth assumption is the instantaneous point source. An instantaneous point source is practically not feasible, however, the measured concentrations are well-described by eq (5.1). This is certainly due to the fact that the first samples were taken after a sufficient initial time lag (≥ 60 min). The discussion in Chapter 3 suggests that a deviation from the assumed initial condition becomes less relevant with increasing duration of the experiment.

Apparent first-order degradation rate. For the *in situ* method, the measured apparent first-order degradation rates k_{app} in the two unacclimated sandy soils were $<1 \text{ d}^{-1}$. The error in determining k_{app} from the results of the *in situ* method was too large to determine values below this limit accurately. Therefore, the potential use of the method for the *in situ* determination of degradation rates is only promising in highly active soils for easily degradable compounds. For instance, apparent first-order degradation rates of up to 8.7 d^{-1} for n-octane in a sandy soil [44] or 34 d^{-1} for toluene in a laboratory soil column [27] have been reported. In batch experiments reported in Chapter 4 no significant difference was found between k_{app} measured in live and sterilized sand. This confirms that biodegradation was negligible for the duration of the experiments ($\leq 8 \text{ h}$). Disappearance rates observed mainly over the first 5 hours in sterile batches are most likely explained by partially slow partitioning kinetics. For *in situ* experiments increased sorption will reduce the mass fraction in the soil air f_a . This will, according to eq (5.1), result in a higher gas-phase concentration $C_r(0, t)$ at the injection point. Therefore, a slow decrease for $f_{a,1}$ of the less volatile compound 1 (chlorinated ethenes, benzene, toluene or n-octane) with respect to $f_{a,2}$ of the tracer (CFCs, SF_6) can explain negative values for $k_{app,1}$, as have been measured in some *in situ* experiments. In summary, both batch experiments and *in situ* method indicate negligible degradation of the compounds and partially slow partitioning kinetics, which may affect soil air concentrations at the beginning of the experiments.

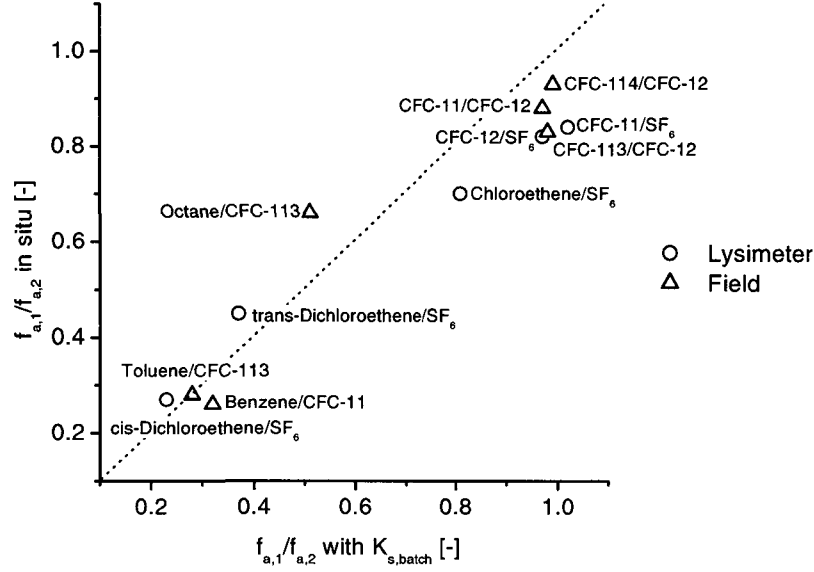


Figure 5.4: Comparison of ratios $f_{a,1}/f_{a,2}$ as measured in situ and as calculated from batch experiments and porosity data.

Mass fraction in the soil air. To further compare results of the in situ experiments with results of the batch experiments, the ratio of the mass fractions in the soil air $f_{a,1}/f_{a,2}$ was calculated according to eq (3.1) with the Henry coefficient H given in Table 4.2 for the respective temperatures, K_s determined in batch experiments (Table 4.3) and the measured porosity data (lysimeter: $\theta_w = 0.06, \theta_a = 0.36, \theta_t = 0.42$, field experiment: $\theta_w = 0.06, \theta_a = 0.25, \theta_t = 0.31$). The calculated ratios $f_{a,1}/f_{a,2}$ are compared with the corresponding ratios measured in situ in Figure 5.4. The ratios $f_{a,1}/f_{a,2}$ determined in situ and determined with partitioning coefficients measured in batch experiments agree well as shown in Figure 5.4. However, according to the batch experiments none of the tracers (CFCs, SF_6) was truly conservative: The calculated mass fraction in the soil air $f_{a,2}$ ranges from 0.73 for CFC-11 and CFC-113 at the field site to 0.79 for SF_6 in the lysimeter. Therefore one will systematically overestimate $f_{a,1}$ by 20 to 30%, if this parameter is calculated from $f_{a,1}/f_{a,2}$ with the approximation $f_{a,2} = 1$. CFCs and SF_6 , although used as conservative tracers in many studies [48], [28], [25], apparently partition into the water-phase or sorb to some extent to the solid matrix of the investigated sands or to the air-water interface at a temperature of 10 °C or 15 °C. Batch experiments with CFCs at 25 °C and lysimeter sand indicated negligible sorption, see Table 4.3.

Effective diffusion coefficient. The proportionality factors between the effective diffusion coefficient D_e and the molecular diffusion coefficient D_m measured in the lysimeter or at the field site on different days fall for each porous medium within a narrow range. This is expected, as soil conditions, namely the soil water content, did not change significantly over the whole experimental period. The effective diffusion coefficients D_e determined with the in situ method thus showed good reproducibility. Robustness with respect to errors in the input parameters is given by the nature of eq (5.5): uncertainty due to an error in the determination of θ_a decreases because θ_a is raised to the power of $1/3$. Likewise, an overestimation of the mass fraction in the soil air $f_{a,2}$ of the tracer by 25% due to the assumption $f_{a,2} = 1$ (see paragraph above) leads to an underestimation of D_e by 9% only. The proportionality factor between D_e and D_m is equivalent to the product of θ_a and the tortuosity factor τ . It can therefore be estimated from porosity data with empirical relationships for τ . Estimating τ with the empirical relation $\tau = \theta_a^{2.33}/\theta_t^2$ proposed by Millington & Quirk [37] one obtains a proportionality factor of 0.19 ± 0.02 for the lysimeter and 0.10 ± 0.03 for the field site. Estimation of τ with the empirical relation $\tau = 0.66$ proposed by Penman [43] one obtains a proportionality factor of 0.24 ± 0.01 for the lysimeter and 0.17 ± 0.02 for the field site. According to reference [25] those two relationships often define a lower and upper limit for the actual τ . The effective diffusion coefficients D_e in the soils investigated are better described by the Millington & Quirk relation as compared to the Penman relation. This good agreement between the measured D_e and D_e calculated according to Millington & Quirk may not be true in other soils [25]. In conclusion, there is a significant difference between D_e calculated from different relationships, but no obvious a priori choice for the best relationship. The in situ method avoids this uncertainty.

Sorption-affected diffusion coefficients. The sorption-affected diffusion coefficients D_s measured in situ using the approximation $f_{a,2} = 1$ for the evaluation of the in situ data are compared in Figure 5.5 with D_s calculated from the data of the batch experiments with the Millington & Quirk relationship for the tortuosity factor τ . The sorption-affected diffusion coefficients D_s determined from the data of the in situ method with the assumption $f_{a,2} = 1$ for the tracer are in qualitative agreement with D_s calculated from results of the batch experiments. The proportionality factor between D_s and the molecular diffusion coefficient D_m depends both on the properties and the condition of the soil and on the chemical properties of the compounds. Within a given porous medium the proportionality factor is highest for volatile and hydrophobic compounds such as the CFCs and lowest for

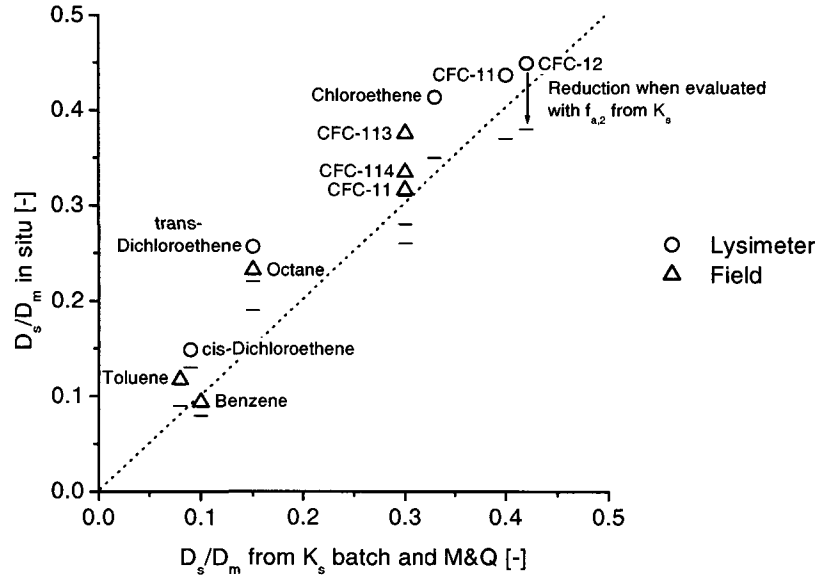


Figure 5.5: Comparison of D_s as measured in situ, evaluated with $f_{a,2} = 1$ and as calculated from batch experiments and soil core data.

less volatile and/or hydrophilic compounds such as toluene or benzene. For the repeated experiments G, G_{rep} and H, H_{rep} the D_s measured in situ agree within error limits, see Table 5.2. This is expected, as soil conditions didn't change significantly. Sorption-affected diffusion coefficients D_s determined in situ are, however, on average 18% higher if compared to D_s calculated from the batch data and with the Millington & Quirk relationship, see Figure 5.5. As discussed above, the Millington & Quirk relationship provided a good estimate for the tortuosity factor τ in the investigated soils and was therefore chosen for the comparison. The observed difference is explained by the approximation $f_{a,2} = 1$ in the evaluation of the field data, whereas batch experiments suggest $f_{a,2} \approx 0.75$ for the tracers used in this study. This results in a systematic overestimation of D_s . As shown in Figure 5.5, the sorption-affected diffusion coefficients D_s agree better, if $f_{a,2}$ as calculated with the air-solid partitioning coefficients K_s determined in batch experiments are used in the evaluation of the field data.

Practical implications. The applicability of the in situ method to determine apparent diffusion coefficients in sandy soils has been demonstrated in this study. Obtaining data in situ avoids the considerable uncertainty associated with choosing an empirical relation for the tortuosity factor. Further-

more, it avoids problems associated with establishing realistic soil conditions in laboratory experiments. The data in this study suggest that additional batch experiments with disturbed soil samples are useful to check whether the tracers are truly conservative. This reduces the uncertainty for the sorption-affected diffusion coefficient considerably. The effective diffusion coefficients were shown to be less affected by tracer sorption. More work is needed to understand the nature and kinetics of sorption for tracers and VOCs at temperatures around 10 °C.

Chapter 6

Diffusive Partitioning Tracer Test: Column Experiments

6.1 Introduction.

NAPL contaminated sites. The detection and quantification of non-aqueous phase liquids (NAPLs) in the subsurface is crucial for the management and remediation of contaminated sites [6]. During the downward migration of NAPLs through soil after an accidental release or spill, a certain amount of liquid is retained in the pore space by capillary forces. This fraction is known as residual saturation, and may occupy about 2-20% of the available pore space [36]. The presence of NAPLs defines the so-called source zone [57], from which gaseous and aqueous contaminant plumes are formed. Source zone delineation is a key procedure at NAPL contaminated sites. Delineation of source zones with traditional techniques such as soil core sampling presents considerable difficulties and costs [16].

Innovative methods for NAPL detection. Several innovative methods for NAPL detection based on partitioning tracers have been introduced and evaluated under laboratory and field conditions for the saturated and the vadose zone, see [47] for a review. Partitioning tracers may be naturally occurring gases such as ^{222}Rn [23] or a variety of harmless organic chemicals [47] with different affinities for NAPLs. The general principal of conventional partitioning tracer tests is that of chromatography [34]: a mixture of tracers is injected into a stream of gas or water created in the subsurface. The different tracers partition into the stationary NAPL-phases or other phases to different degrees, and the resulting difference in the migration of the tracers is used for the location and quantification of the phases of interest. The field

application of this concept is called partitioning interwell tracer test (PITT) [25]. An advective flow field in either the gas (vadose zone) or groundwater (saturated zone) is created between two or more wells, and the information obtained from the tracer data reflects the zone in between those wells. With an advective flow field subsurface environments of considerable spatial extensions can be assessed with a single tracer test. Practical problems associated with such a set-up are the incorrect interpretation in heterogeneous subsurface environments, especially when NAPLs are located in zones with low permeabilities that are bypassed by the tracers [40] and short tracer residence times with respect to partitioning kinetics. For the vadose zone, the generation of flow fields creating long residence times is difficult and biased by air pressure variations. Furthermore, the spreading of tracers by gas-phase diffusion has to be considered at low advective velocities [55]. Field applications of long duration are costly. The measurement of breakthrough curves requires a high number of analyzes and the use of sophisticated analytical equipment on site.

Aims. In this chapter, the theory of a new partitioning tracer test for the vadose zone, which is based on diffusion rather than advection, is presented and tested in laboratory column systems. This test obtains local information on NAPLs in the vadose zone. It is called diffusive partitioning tracer test (DPTT). The approach includes two or more gaseous tracers with known partitioning behavior into the stationary phases. Tracers are injected into the center of the column. The concentration change at the injection point is monitored, while tracers diffuse away. Data is interpreted with an analytical equation describing the gas-phase diffusion of partitioning tracers. Results are reported for six sand-filled columns with a range of NAPL and water contents.

6.2 Theory

Basics. The theory for the DPTT in laboratory columns is developed for two tracers with different affinities for the NAPL-phase, termed tracer 1 and 2. A small volume of gas containing both tracers is injected into the center of the column. The concentration decline at the injection point is interpreted with eq (3.7), which describes gas-phase diffusion from an instantaneous plane source. The soil air concentrations C_a are standardized with respect to the concentrations of the tracer in the injected gas mixture $C_{in} = m_0/V_{in}$ to obtain relative concentrations $C_r = C_a/C_{in}$.

NAPL saturation. The diffusive partitioning tracer test (DPTT) is a method for the indirect determination of the NAPL saturation S_n in a porous medium

$$S_n = \frac{\theta_n}{\theta_t}, \quad (6.1)$$

where θ_n denotes the NAPL-filled and θ_t the total porosity. The NAPL saturation S_n can be calculated from the mass fraction in the soil air $f_{a,1}$ and $f_{a,2}$ of two different gaseous tracers 1 and 2, see eq (3.1):

$$S_n = \frac{\frac{f_{a,1}}{f_{a,2}} b_1 - b_2}{\frac{1}{K_{n,2}} - \frac{f_{a,1}}{f_{a,2}} \frac{1}{K_{n,1}}} \cdot \frac{\theta_a}{\theta_t}, \quad (6.2)$$

where

$$b_i = 1 + \frac{\rho_s(1 - \theta_t)}{K_{s,i}\theta_a} + \frac{\theta_w}{H_i\theta_a}. \quad (6.3)$$

If partitioning into the water-phase and sorption into/onto the solids is negligible for both tracers, eq (6.2) simplifies to

$$S_n \approx \frac{\frac{f_{a,1}}{f_{a,2}} - 1}{\frac{1}{K_{n,2}} - \frac{f_{a,1}}{f_{a,2}} \frac{1}{K_{n,1}}} \cdot \frac{\theta_a}{\theta_t}. \quad (6.4)$$

Ratio of the mass fraction in the soil air. According to eq (3.9), which describes the concentration decline at ($x=0$) for an instantaneous plane source, and with $C_r = C_a V_{in}/m_0$, the ratio of the mass fraction in the soil air $f_{a,1}/f_{a,2}$ of tracer 1 and 2 is given by

$$\frac{f_{a,1}}{f_{a,2}} = \left(\frac{C_{r,1}(0,t)}{C_{r,2}(0,t)} \right)^2 \frac{D_{m,1}}{D_{m,2}}. \quad (6.5)$$

This ratio does not depend on soil physical parameters such as the tortuosity factor τ . The ratio $f_{a,1}/f_{a,2}$ determined according to eq (6.5) can be used to derive the NAPL saturation S_n according to eq (6.2) or eq (6.4).

Plots. To compare the measured data with the mathematical model a quantity $N^{plane}(0,t)$ is defined as follows:

$$N^{plane}(0,t) = \frac{C_r(0,t)\sqrt{D_m}}{V_{in}} = \frac{\sqrt{f_a}}{2A\theta_a\sqrt{\tau\pi}} \cdot \frac{1}{\sqrt{t}}. \quad (6.6)$$

The column data are evaluated by plotting $N^{plane}(0,t)$ against $1/\sqrt{t}$. This should yield a straight line through the origin. For two tracers released at the same location, differences in the slopes of the plotted linear graphs visualize the differences in the mass fraction in the soil air f_a and thus the different partitioning behavior.

Error Analysis. An error in parameters that appear with a high exponent in eq (6.5) will make a big contribution to the overall error of the ratio of the mass fraction in the soil air $f_{a,1}/f_{a,2}$, whereas an error in parameters with a low exponent is less relevant. The term in the first brackets is determined from measured concentration ratios of tracer 1 and 2 in the injected tracer gas mixture and in the soil air respectively. The determination of concentration ratios is generally more robust than the determination of absolute concentrations, especially so for gas samples, where any kind of dilution is the most probable error source. Assuming an error of 10% for the ratio $C_{r,1}(0,t)/C_{r,2}(0,t)$ and for the ratio of the diffusion coefficients $D_{m,1}/D_{m,2}$ the overall theoretical error for the ratio $f_{a,1}/f_{a,2}$ becomes 22%. The overall theoretical error for the NAPL saturation S_n depends on the choice of the tracers. If tracer 1 is a conservative tracer with $f_{a,1} \approx 1$ and tracer 2 an air-NAPL partitioning tracer with a high enough affinity to the NAPL-phase to obtain a mass fraction in the soil air $f_{a,2} \ll 1$, the overall theoretical error for S_n becomes 26%, if the partitioning coefficient K_n and the air saturation S_a were determined with an error of 10%. The error can be reduced by determining the ratio $C_{r,1}(0,t)/C_{r,2}(0,t)$ at different times t and by calculating S_n as an average from different tracer pairs.

6.3 Materials and Methods

Chemicals. The suppliers and the properties of the chemicals used in this study are listed in Section 4.3. All chemicals were obtained in the highest available purity.

Tracer mixtures. For the convenient use of CFC-tracers in the diffusion experiments a standard mixture was prepared in a vial with a Mininert-valve (Fluka, Buchs, Switzerland). The vial contained CFC-11, CFC-12, CFC-113 and CFC-114 dissolved in octanol (4.5 mL) and a headspace above the octanol (10 mL). The CFC-content in the octanol was adjusted to obtain for each compound a headspace concentration approximately 6000 times higher than the detection limit of the GC-ECD method. Before withdrawing gas from the headspace, the headspace concentration was equilibrated with the concentration in the octanol phase by gently shaking the vial for 30 min, avoiding any contact between the Mininert-valve and the octanol. To calibrate the GC before a DPTT, 160 μL , 120 μL , 80 μL and 40 μL of gas were withdrawn from the headspace with a gas-tight syringe and diluted in 64 mL glass vials equipped with Mininert-valves. The concentrations in these vials were determined by injecting 100 μL of each vial in the GC-ECD.

Table 6.1: Characterization of the porous media used in the laboratory column experiments.^a

Column	θ_t	S_n	θ_n	θ_a	θ_w
A	0.47	0	0	0.43	0.04
B	0.46	0	0	0.28	0.18
C	0.47	1.0	0.005	0.30	0.17
D	0.51	1.4	0.007	0.44	0.06
E	0.47	2.6	0.012	0.42	0.04
F	0.47	4.0	0.019	0.41	0.04

^aThe dimension is $[\text{cm}^3/\text{cm}^3 \text{ soil}]$ for θ_t , θ_n , θ_a , θ_w and $[\text{cm}^3/\text{cm}^3 \text{ total porosity in \%}]$ for S_n .

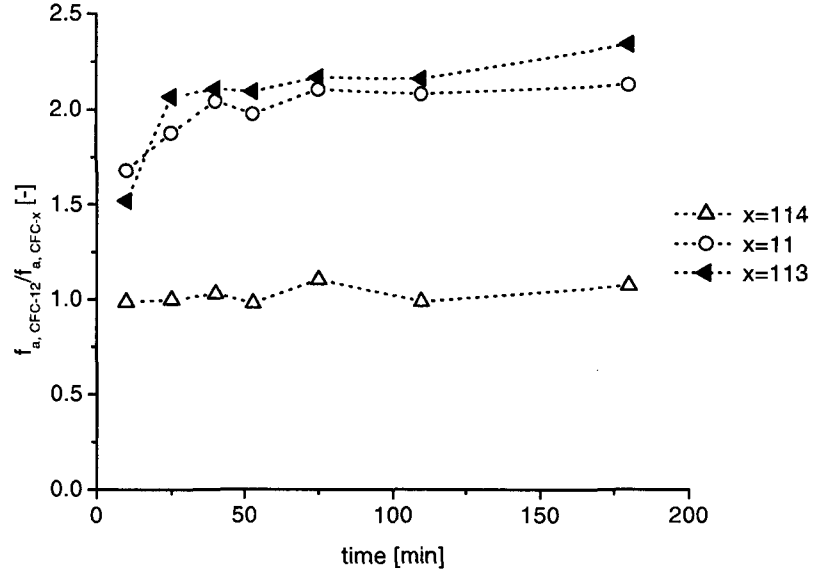
Column experiments. Cylindrical glass columns (120 cm, 6.84 cm inner diameter) with a sampling port located at 60 cm were used for the column experiments in the laboratory at 25°C. They had a ground glass joint at one side and a teflon-lined screw-cap opening at the other side and were placed horizontally in the lab. The sampling port was equipped with a needle connectable to gas-tight syringes. All material in contact with the gas inside the column was either glass, stainless steel or teflon. The columns A and B were filled with clean, moist sand, the columns C to F with a mixture of moist sand and dodecane. See Section 4.3 for some characteristics of the sand. The sand was packed by manual shaking and more sand was added until the sand could not be settled any further. This resulted in a uniformly packed column with no visible discontinuities. The water content was determined by drying a sand sample at 105°C for 12 hours. The total porosity θ_t was calculated from the dry weight of the sand filled into the column, assuming a density of 2.5 g cm^{-3} for the solids. Contaminated sand was prepared by manually mixing clean, moist sand with dodecane in an aluminium container. The water content was determined before mixing and the NAPL-saturation S_n was calculated from the amount of dodecane added. For columns C, D and F, dodecane was extracted with CH_2Cl_2 from 15 g of sand before or after the experiment and the extract was analyzed by GC-FID, see [44] for the method. Measured dodecane contents were on the average $104 \pm 9\%$ of the expected. The dodecane content of sand extracted after the experiment was on the average 3 % lower then the dodecane content of sand extracted before the experiment, indicating only small losses. Table 6.1 characterizes the columns used in the different experiments. Before a DPTT the concentrations of the gaseous tracers in the headspace of the standard were determined. A volume

of 1 mL was withdrawn from the headspace of the CFC-tracer mixture vial with a gas-tight syringe and injected through the sampling port located in the center of the column. After 40 min, 53 min, 75 min, 110 min and 180 min the soil air was sampled through the same port. To avoid artifacts due to the spatial limitation of the experimental system, the duration of the experiments was no longer than 3 hours. A volume of 50 μL was withdrawn in order to purge the needle and 100 μL of soil air were analyzed by GC-ECD.

Analytical procedures. Gas-phase concentrations of the CFC-tracers were analyzed by injecting 100 μL of gas into a Varian CP-3800 gas chromatograph equipped with an ECD detector. The injector was heated to 60°C and the split ratio was 10. A 30 m capillary column GS-GasPro (J&W Scientific) was used for the separation of the compounds at a temperature of 130°C. Carrier gas was Helium at a flow rate of 2 mL/min. Linearity of the detector response was checked with calibration standards.

6.4 Results

To study the appropriate time intervals for sampling, a preliminary experiment has been performed in the NAPL contaminated column D, where soil air sampling started 10 min after the injection. In Figure 6.1 the ratio of the mass fraction in the soil air $f_{a,CFC-12}$ of CFC-12 relative to $f_{a,CFC-x}$ of the three other tracers is plotted as a function of time. The ratio stabilizes after 40 min. In order to allow ample time for stabilization, the first data points used for data interpretation in all following experiments have been taken 40 minutes after injection of the tracers. Results are shown in Figure 6.2 and summarized in Table 6.2. The measured tracer concentration data were transformed to $N^{plane}(0, t)$ using eq (6.6) and plotted as outlined in the theory section. As predicted by the theory, the data points lay on straight lines for all tracers examined. Correlation coefficients R^2 for the linear regression lines are 0.98 or better and the extrapolated lines cross the axes close to the origin. If the regression lines are forced through the origin, R^2 is 0.96 or better. The regression lines and error bars for $N^{plane}(0, t)$ have been omitted from the plots to increase readability. In the columns A and B where the NAPL saturation was 0, the slope of the lines for all 4 tracers are identical. In the NAPL contaminated columns C to F, CFC-12 and CFC-114 data lie on lines with similar slopes. CFC-11 and CFC-113 data lie on lines with smaller slopes. In column C, the experiment was terminated after 75 min because of a problem with the GC, and the result was calculated from three measurements only. Repetition of the experiments in columns A and E

Figure 6.1: Ratios $f_{a,1}/f_{a,2}$ as a function of time for column D.Table 6.2: NAPL saturation S_n in the laboratory experiments as determined from the DPTT.^a

Column ^b	CFC-12/11	CFC-12/113	CFC-114/11	CFC-114/113	(average) DPTT	Actual
	S_n	S_n	S_n	S_n	$S_n \pm 2\sigma$	$S_n \pm 2\sigma$
A	-0.1	-0.1	0.0	0.0	0.0 ± 0.1	0.0 ± 0.0
A _{rep}	-0.1	-0.0	0.0	0.0	0.0 ± 0.1	0.0 ± 0.0
B	0.1	-0.0	0.2	0.0	0.1 ± 0.2	0.0 ± 0.0
C	0.8	0.5	1.1	0.6	0.8 ± 0.5	1.0 ± 0.1
D	1.3	0.8	1.6	0.9	1.2 ± 0.7	1.4 ± 0.1
E	1.7	1.4	2.6	1.8	1.9 ± 1.1	2.6 ± 0.3
E _{rep}	2.3	1.5	3.3	1.8	2.2 ± 1.5	2.6 ± 0.3
F	4.0	3.1	6.4	4.1	4.4 ± 2.8	4.0 ± 0.4

^a The dimension for S_n is $[\text{cm}^3/\text{cm}^3 \text{ total porosity in } \%]$. ^b rep. means repeated experiment.

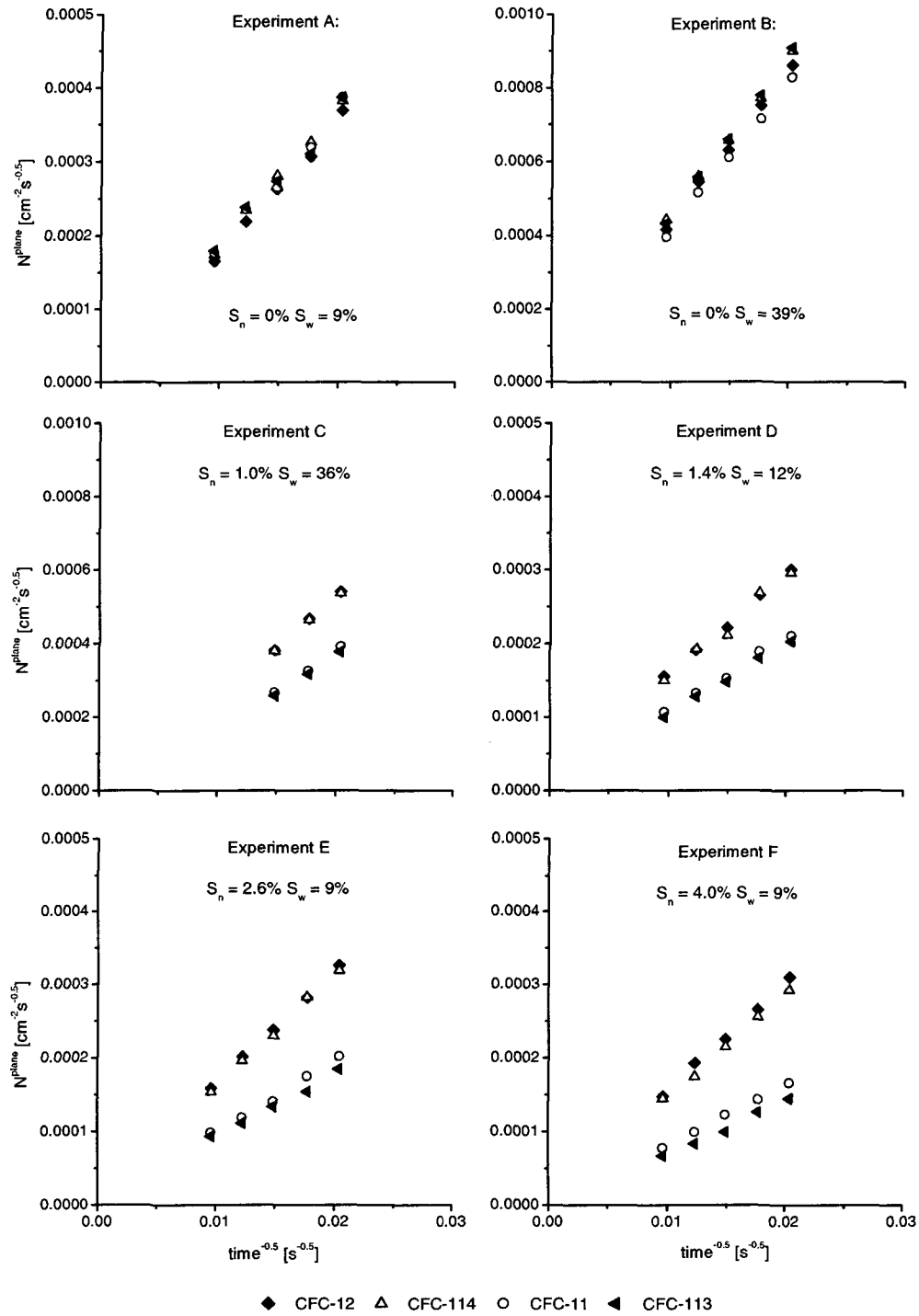


Figure 6.2: Results of the DPTTs in laboratory columns A-F. Data of repeated experiments A_{rep} and E_{rep} are not shown.

yielded similar results (data not shown in the plots). The experimental error for $N^{plane}(0, t)$ can be determined from the repeated experiments and is 12%. The ratio $f_{a,1}/f_{a,2}$ has been calculated according to eq (6.5) as the average of the five individual measurements at 40 min, 53 min, 75 min, 110 min and 180 min and not from the slopes of the regression lines, thus avoiding errors due to dilution, which will not affect the ratios. From this averaged ratio the NAPL saturation S_n was calculated according to eq (6.4) and eq (6.5) with the molecular diffusion coefficients D_m given in Table 4.1, using the measured D_m , if available, the air-dodecane partitioning coefficients K_n given in Table 4.4, and the air-filled and total porosity θ_a and θ_t given in Table 6.1. The NAPL saturation S_n has been calculated for each pair of tracers with a sufficient difference in f_a . Calculated S_n for each tracer pair are compared with actual S_n in Table 6.2. For individual tracer pairs, calculated and actual S_n agree within a factor 2 or better. The maximal deviation between actual S_n and S_n calculated as an average from all tracer pairs is 30 percent. The error for this averaged S_n is given as twice the standard deviation σ of S_n as calculated from the individual tracer pairs.

6.5 Discussion

Assumptions. A number of critical assumptions were made in the derivation of the basic analytical equation and for the evaluation of the DPTT data. These assumptions are discussed in the following.

Homogeneity: The first assumption is the homogeneity of the porous medium.

This could be ascertained in laboratory experiments. Measured dodecane contents of small soil samples were close to the expected average, indicating a homogeneous distribution of the NAPL. Using eq (3.7), which describes gas-phase diffusion from a instantaneous plane source, one can estimated that the soil air concentration $C_a(x, t)$ of the most volatile tracer CFC-12 falls to approximately 10% of the concentration at the injection point $C_a(0, t)$ within a distance of 60 cm after 3h (at the end of the experiments). Thus, a small fraction of the tracer mass has reached the column end towards the end of the experiment, but no obvious effect on $N^{plane}(0, t)$ could be observed, see Figure 6.2.

Partitioning equilibrium: The second assumption concerns the instantaneous equilibrium partitioning of the tracers between the gas-phase and the stationary phases. The results in Figure 6.1 indicate that in this NAPL contaminated sand column a time period of about 40 minutes was sufficient to achieve a stable concentration ratio of all four

tracers. In all further experiments, the experimental data for $t \geq 40$ min fell on straight lines when plotted according to the theory and measured concentration ratios varied by less than 15%. This shows that an equilibrium will be reached after an initial stabilization period. When preparing the laboratory columns, the dodecane was added to the porous medium by manually mixing the moist sand with the organic liquid. This procedure will maximize the NAPL surface coating. At field sites, longer stabilization times might be required to achieve equilibrium in the pore space. The required stabilization time can be determined by plotting the ratio $f_{a,1}/f_{a,2}$ as a function of time as shown in Figure 6.1. With increasing time the tracer concentration at the injection point will change more slowly, increasing the probability, that an instantaneous linear equilibrium between the different phases in the subsurface will eventually be reached.

Sorption to soil not relevant: As a third important assumption the sorption to the solids and partitioning into the water-phase is neglected in the derivation of eq (6.4). The experimental results show that for the sand used in this study it was possible to get good estimates of the NAPL saturation S_n . The higher water content in column experiment B and C did not affect this result. The sand used in this study contained relatively little organic matter compared to many soils. Air-solid partitioning coefficients K_s determined in batch experiments were in the order of $20 \text{ (mol cm}^{-3}\text{)}/(\text{mol g}^{-1} \text{ solid})$, see Table 4.3. Inserting the measured K_s and the Henry coefficients H from Table 4.2 into eq (6.2), one finds that the simplified eq (6.4) underestimates the NAPL saturation S_n by 15% for columns D, E and F and by 25% for column C with a higher water saturation. In many practical situations values for K_s are not available. For this reason the simplified eq (6.4) was used to evaluate the results. One should, however, keep in mind how such simplifications can affect the final result. In soils with a high content of organic matter, K_s should be determined. This can for example be done with a DPTT in the uncontaminated soil, since organic material should affect the diffusion of the gas tracers in a similar way as a NAPL.

No advection: A fourth assumption is that gas-phase diffusion is the only relevant process for tracer movement. This assumption is certainly valid in the closed and horizontally positioned laboratory columns, where pressure gradients or gravity-driven advection can be excluded.

Plane source: Finally an instantaneous plane source was assumed as an initial condition. A perfect Dirac input of tracers is practically impos-

sible. However, the observation of a linear dependency of the data in Figure 6.2 demonstrates that the derived equations also work for an nonperfect tracer input ¹.

Suitability of the DPTT for NAPL quantification. Measured and actual NAPL saturation in the laboratory experiments agree within a factor 2 or better with a tendency to underestimate the actual saturation, as can be seen in Table 6.2. The tracer pair CFC-12/CFC-11 yielded the best results. For this tracer pair the maximal deviation from the actual NAPL saturation was 30%. The accuracy of the DPTT can be improved significantly by calculating S_n as an average from different tracer pairs. If tracers can be separated and quantified in one GC run, the use of several tracers for the DPTT requires hardly any additional effort. The NAPL saturation calculated from the four different tracer pairs underestimated actual S_n by 17% on the average. Some of this systematic underestimation can be explained by the fact that sorption to the solids has been neglected in the data evaluation. Slow sorption kinetics could be another explanation. Overall, it can be concluded that the DPTT provides a valuable method for NAPL quantification, when the basic assumptions of the mathematical model are valid. Contrary to the PITT, which demands the measurement of complete breakthrough curves, the DPTT allows to quantify the NAPL saturation S_n with a few measurements. The DPTT is thus a potentially inexpensive method. On the other hand, the error for S_n as determined by the DPTT (see Table 6.2) is higher than reported for the PITT in comparable laboratory set-ups [13], where the reported error is 1.7% for $f_{a,1}/f_{a,2}$ and 10% for S_n .

Suitability of chlorofluorocarbons for NAPL quantification. CFCs were chosen as partitioning tracers for the following reasons: They are not toxic and not biodegradable under aerobic conditions. They have high Henry constants, and partitioning into the water-phase can be neglected for a wide range of water saturations. They are volatile enough to be used as gaseous tracers and cover an interesting range of air-NAPL partitioning constants. Furthermore they have low detection limits when analysed by GC-ECD. Although the industrial use of CFCs is regulated, they are still easily available for research purposes. The results of the laboratory experiments demonstrate that CFC-12, CFC-114, CFC-11 and CFC-113 provide a useful set of tracers for the quantification of NAPL saturations between 0 and 4% in sandy soils with a low organic matter content f_{om} at both, low and high water content.

¹Read also the discussion on page 9.

Chapter 7

Diffusive Partitioning Tracer Test: Field Experiments

7.1 Introduction

Partitioning tracer methods in the vadose zone. Partitioning tracer methods or interfacial tracer methods are relatively well established as a tool to characterize the volume and surface area of nonaqueous phase liquids (NAPLs) in aquifers, see [47] and [13] for a review. In recent years, partitioning tracer methods have also been suggested for the vadose zone, namely for the quantification of either the water saturation S_w [41], [10] or the NAPL saturation S_n [55], [56] or for the simultaneous determination of S_n and S_w [11], [34]. These methods are based on the principle of the partitioning interwell tracer test (PITT), which is based on advection and has already been introduced in Section 6.1. Field applications of the PITT in the vadose zone are reported in [11] and [34]. Mariner et al. [34] quantify the residual dense nonaqueous phase liquid (DNAPL) saturation between two multilevel monitoring wells, which were 16.8 m apart from each other. Tracer concentrations at the extraction well were monitored with two online gas chromatographs for 15 days, with increasing extraction rates towards the end of the experiment. Chromatographic separation of conservative and NAPL partitioning tracer in the shallow zone indicated an average DNAPL saturation S_n of $0.21 \pm 0.05\%$. Deeds et al. [11] installed a total of 6 multilevel wells, which were 4.6 m apart from each other, to investigate a NAPL-contaminated vadose zone. The total duration of the PITT was 7 days. Slight peak separation for conservative and NAPL partitioning tracers and especially a less pronounced decline in the breakthrough curve for the NAPL partitioning tracer at late times indicated a significant NAPL saturation. While these investigations

demonstrate the feasibility and value of the PITT in the vadose zone, especially its potential to sample large volumes in the subsurface environment, some drawbacks are also evident. The PITT requires sophisticated installations for the establishment and maintenance of the flow field and analytical equipment for the on site analysis of samples. The tracer-swept volume can be different for two consecutive investigations [11]. Data interpretation often relies on differences in the tail of breakthrough curves at low concentrations that are difficult to measure precisely or are below detection limits, requiring extrapolation [13]. Finally, gas-phase diffusion will spread gaseous tracers over a substantial distance for the typical duration of a PITT and should be considered in the data evaluation. The advective velocity of the tracers in a PITT needs to be low to achieve equilibrium partitioning and to avoid preferential flow. Laboratory investigations suggest that equilibrium partitioning between NAPL and soil air occurs at velocities, where gas-phase diffusion may not be neglected in vadose zone experiments [55]. A method relying on gas-phase diffusion as the sole transport mechanism for the spreading of partitioning tracers in the vadose zone might therefore be advantageous. Diffusion is the slowest achievable migration velocity and one has the highest chance to obtain a partitioning equilibrium. Diffusion is less susceptible to preferential flow as compared to advection. And finally, diffusion is occurring naturally and does not require the technical equipment used for establishing flow fields in the subsurface.

Aims. The goal of this chapter is to describe the theory and demonstrate the practical application of a diffusive partitioning tracer test (DPTT) for NAPL detection in the vadose zone. Results of homogenously packed laboratory columns have already been discussed in Chapter 6. The theory is now developed for field applications. The practical feasibility of the DPTT is tested at a field site in Værløse, Denmark, with a sandy unsaturated zone and an artificially embedded contamination. Furthermore it is demonstrated that the DPTT is compatible with traditional soil gas investigations, adding valuable information with little additional effort.

7.2 Theory

NAPL saturation. The calculation of the NAPL saturation S_n in a porous medium from the measured ratio of the mass fraction in the soil air $f_{a,1}/f_{a,2}$ of two tracers 1 and 2 with different affinities for the NAPL has already been discussed in Section 6.2. The ratio $f_{a,1}/f_{a,2}$ is obtained from the data of a DPTT in an analogous way as described for the laboratory columns,

however the basic equation used for the data evaluation is different: In the field diffusive spreading of the tracers is possible in any direction. Therefore, eq (3.10), which describes gas-phase diffusion from an instantaneous point source, is used for the data evaluation. From eq (3.12) it follows with $C_r = C_a V_{in}/m_0$ that the ratio $f_{a,1}/f_{a,2}$ can be obtained from the measured data:

$$\frac{f_{a,1}}{f_{a,2}} = \left(\frac{C_{r,2}(0,t)}{C_{r,1}(0,t)} \right)^2 \left(\frac{D_{m,2}}{D_{m,1}} \right)^3. \quad (7.1)$$

The ratio $f_{a,1}/f_{a,2}$ is calculated from the data of a DPTT with eq (7.1) and is used to derive the NAPL saturation S_n according to eq (6.2) or eq (6.4).

Plots. To compare the measured data with the mathematical model a quantity $N^{point}(0,t)$ is defined as follows:

$$N^{point}(0,t) = \frac{C_r(0,t)D_m^{1.5}}{V_{in}} = \frac{1}{8\theta_a(\tau\pi)^{1.5}\sqrt{f_a}} \cdot \frac{1}{t^{1.5}}. \quad (7.2)$$

The data are evaluated by plotting $N^{point}(0,t)$ against $1/t^{1.5}$. This should yield a straight line through the origin. For two tracers released at the same location, differences in the slopes of the plotted linear graphs visualize the differences in f_a and thus the different partitioning behavior. This slope will henceforth be referred to as slope s .

Estimation of the air saturation. When the NAPL saturation is calculated according to eq (6.2) or eq (6.4), one needs to know the air saturation $S_a = \theta_a/\theta_t$. In the field this parameter is not easily available. Therefore it is outlined how S_a can be estimated from the results of a DPTT, if one knows or has an estimate for the total porosity θ_t . According to Millington and Quirk [37], the tortuosity factor τ can be estimated with the following empirical formula:

$$\tau \approx \frac{\theta_a^{2.33}}{\theta_t^2}. \quad (7.3)$$

For a nonpartitioning tracer f_a equals 1. Making use of eq (7.2) and eq (7.3), S_a can be estimated from the slope s of the regression line of a nonpartitioning tracer

$$S_a \approx \left(\frac{1}{8\pi^{1.5}\theta_t^{1.5}s} \right)^{0.22}. \quad (7.4)$$

Accordingly, one can use other empirical relations for τ to estimate S_a . Furthermore, $S_a \approx 0.75$ provides a reasonable first estimate in many situations.

Error Analysis. Errors in parameters that appear with a high exponent in eq (7.1) will make the most relevant contribution to the overall error of the ratio of the mass fraction in the soil air $f_{a,1}/f_{a,2}$. Using the same analytical errors and assumptions as in Section 6.2, the overall theoretical error for the ratio $f_{a,1}/f_{a,2}$ as determined from the DPTT is 36%. The main contribution comes from the ratio of the molecular diffusion coefficients $D_{m,1}/D_{m,2}$, because it is raised to the power of 3. The overall theoretical error for the NAPL saturation S_n becomes 39%. The error can be reduced by using several tracers and building different tracer pairs. This can be done with hardly any additional effort, if all tracers can be quantified in the same GC run. Furthermore the ratio of the relative tracer concentration in the soil air $C_{r,2}(0,t)/C_{r,1}(0,t)$ can be determined at different times t and averaged, thereby reducing the experimental error.

7.3 Materials and Methods

Chemicals. The suppliers and the properties of the chemicals used in this study are listed in Section 4.3. All chemicals were obtained in the highest available purity.

Tracer mixtures. For the convenient use in the diffusion experiments CFC-tracers were dissolved in octanol and enclosed in vials with Mininert-valves from Fluka (Buchs, Switzerland). The headspace above the octanol was 50 mL. Headspace concentrations were approximately 1000 ppmv of CFC-12, 2000 ppmv of CFC-114 and 250 ppmv of CFC-11.

Værløse field site. A field site in Værløse, Denmark, was chosen to test the combined use of the DPTT and soil gas measurements as a tool for site investigation and source zone delineation. This site is a glacial sand deposit covered by extensively used grassland. Dark brown topsoil of 30-40 cm thickness is overlying a 2.5 - 2.8 m thick homogeneous sand layer, followed by gravel-sand layers below 2.8 to 3 m. The total porosity θ_t of the sand layer is 0.37 and the fraction of organic carbon f_{oc} is 0.02% of the dry weight [5]. The unconfined groundwater is at about 3.5 m below surface. A controlled hydrocarbon spill experiment is conducted at this site by the Danish Technical University (DTU) to investigate the natural attenuation of volatile hydrocarbons in the vadose zone [9]: Artificial fuel (composition reported in [9]) mixed with sand from the site was packed in a cylindrical hole with a diameter of 75 cm at a depth between 0.8 and 1.3 m below the surface to form a source of hydrocarbons. The initial NAPL saturation S_n

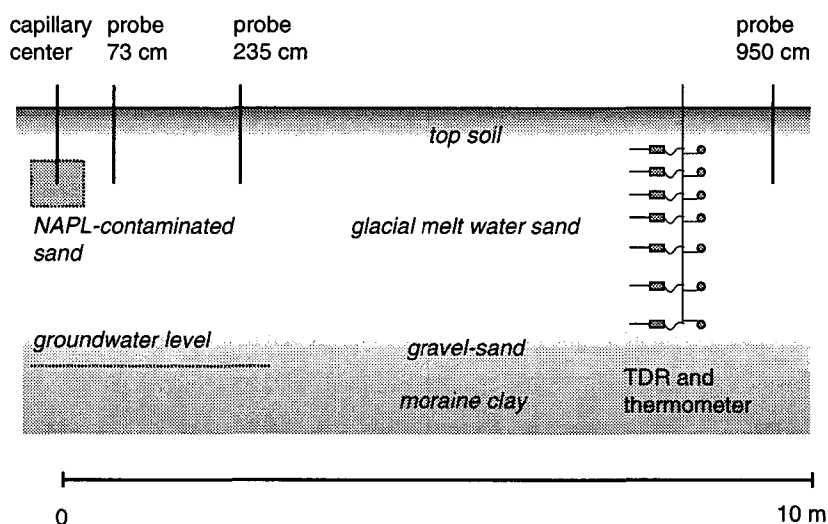


Figure 7.1: Experimental set-up at the Værløse field site.

was approximately 12% of the total porosity. Stainless steel capillaries (1/16 in.) were installed near the center of the contaminated sand to perform a DPTT in the NAPL contaminated zone. Soil gas probes as previously described in Section 5.3 were used to perform a DPTT away from this zone. The experimental set-up is shown in Figure 7.1. Experiments combining soil gas measurements with the DPTT were performed 25 days after the emplacement of the contaminated sand in the center of the contamination and at 9.5 m distance from the center and 102 days after the emplacement, in the center of the contamination, and 73 cm, 2.35 m and 9.5 m away from the center.

Field protocol. A DPTT at the Værløse field site was performed as follows: The headspace concentrations in the CFC-tracer mixture vial were determined by withdrawing three times 20 μL from the headspace, which were diluted and stocked in 64 mL vials with Mininert-valves until analysis. A volume of 5 mL was withdrawn from the headspace of the CFC-tracer mixture vial with a gas-tight syringe and injected into the soil through the

injection capillary. A volume of 0.7 mL of clean air was injected thereafter to purge the dead volume of the capillaries. Two to four soil air samples were withdrawn from each location at times > 53 min but < 180 min after the tracer injection. A volume of 2.1 mL was withdrawn to purge three times the dead volume of the capillaries and 100 μL of soil air were withdrawn thereafter and stocked in sample lock syringes (Hamilton, Bonaduz, Switzerland) until analysis. Samples were analyzed on a GC equipped with a FID and ECD, which allowed simultaneous detection of non-halogenated and halogenated compounds on separate chromatograms.

Analytical procedures. Samples from the field site were analyzed on a CarloErba gas chromatograph (HR GC 5300) with the injector heated to 200 °C at split ratio 5. A 25 m WCOT fused silica capillary column (CP-Sil-19 CB) (Chrompack) was used for the separation of the compounds at a temperature of 35 °C. The column was connected to an ECD and a FID. Carrier gas was Helium at a flow rate of 2 mL/min.

7.4 Results

Soil physical parameters. The temperature and water content at the Værløse field site was closely monitored with thermometers and TDR probes as a function of time and depth [9], see Figure 7.1. For the first 102 days after source emplacement the water-filled porosity θ_w measured with TDR probes remained between 0.07 and 0.13 at a depth between 0.5 and 1.5 m below surface. The air saturation S_a calculated from TDR measurements in the uncontaminated sand at the depth of the embedded contamination with a total porosity $\theta_t = 0.37$ was 0.78 on day 25 and 0.73 on day 102. The temperature measured at the depth of the embedded contamination declined from 17°C on day 25 to 13°C on day 102.

DPTT in the NAPL contaminated sand. A DPTT in the NAPL contaminated sand was performed at the Værløse field site 25 days and 102 days after the emplacement of the contamination. The data was interpreted with eq (3.12) derived for the point source. The measured $N^{point}(0, t)$ are shown in Figure 7.2. Also shown are linear regression lines for the measured data, which were forced through the origin. Correlation coefficients R^2 are 0.98 or better. As can be seen in Figure 7.2, the regression line of CFC-11, the tracer with the highest affinity for the NAPL-phase, has a significantly higher slope than the line going through the data points of CFC-114 or CFC-12. This indicates the presence of a NAPL. The ratio $f_{a,1}/f_{a,2}$ was calculated

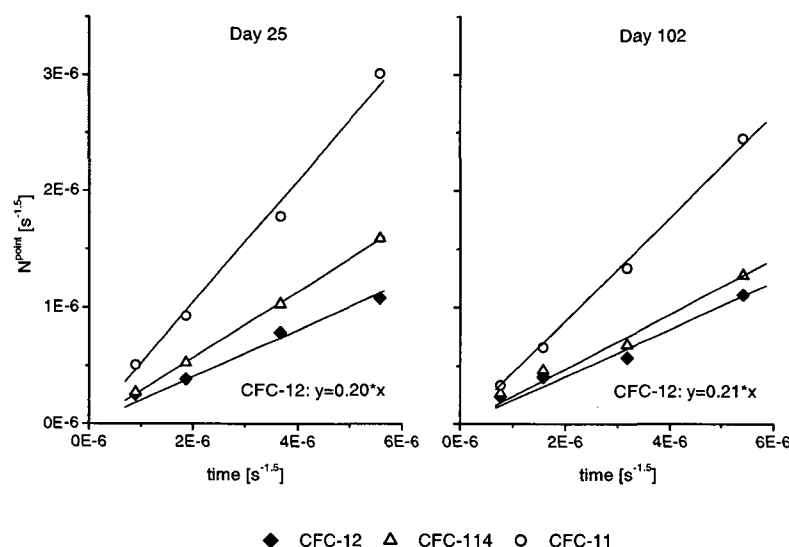


Figure 7.2: Results of the DPTT at the Værløse field site in the contaminated sand 25 and 102 days after the emplacement of the contamination.

as an average of the individual measurements. From this ratio, the NAPL saturation S_n was calculated according to eq (6.4). Thus sorption to the solids or partitioning into the water-phase was neglected. Air-fuel partitioning coefficients K_n measured at 10°C, listed in Table 4.4 were corrected for the actual temperature (17°C on day 25, 13°C on day 102) with the formula $K_n(T_1) \approx K_n(T_2) \cdot p^0(T_1)/p^0(T_2)$ and vapor pressure data from [59]. Furthermore, the air saturation S_a determined from TDR measurements in the uncontaminated sand at the depth of the emplaced contamination was used for the data evaluation. Results are reported in Table 7.1. In the contaminated sand, an average S_n of 3.1% was measured on day 25 and an average S_n of 1.1% was measured on day 102. In comparison with the initial S_n of 12%, the DPTT indicates a drastic decrease of the NAPL quantity in the first 25 days and a slower decrease over the next 77 days¹. The air saturation S_a can also be estimated from the slope s of the regression line of the most volatile tracer CFC-12 according to eq (7.4) with $f_a = 1$ and the total porosity $\theta_t = 0.37$. The estimated S_a , 0.86 for day 25 and 0.85 for day 102, is approximately 15% higher than S_a determined from TDR measurements.

¹According to pentane extracts from soil cores, the NAPL content decreased by a factor 5 to 6 within the first 24 days, oral communication Dr. M. Broholm, E&R, DTU, Lyngby, Denmark.

Table 7.1: NAPL saturation S_n and effective diffusion coefficient D_e as determined at the Værløse field site by DPTTs.^a

distance	0	73	235	950
Day 25:				
S_n CFC-12/11	4.1	n.d.	n.d.	-0.1
S_n CFC-114/11	2.1	n.d.	n.d.	-0.1
S_n (average)	3.1 ± 1.4	n.d.	n.d.	≤ 0.2
D_e/D_m ^b	0.14 ± 0.02	n.d.	n.d.	0.10 ± 0.01
Day 102:				
S_n CFC-12/11	1.2	0.2	0.2	0.0
S_n CFC-114/11	1.0	0.2	0.2	0.0
S_n (average)	1.1 ± 0.2	≤ 0.2	≤ 0.2	≤ 0.2
D_e/D_m ^b	0.14 ± 0.01	0.08 ± 0.02	0.13 ± 0.01	0.15 ± 0.01

^a The dimension for S_n is [cm^3/cm^3 total porosity in %]; the distance from the center of the contamination is given in [cm], the extension of the contamination is 38 cm from the center; n.d. means not determined. ^bCalculated from CFC-12 data according to eq (5.5) with $f_{a,2} = 1$ and $\theta_a = 0.29$ (day 25), 0.27 (day 102).

DPTT in the uncontaminated sand. DPTT were also performed in the uncontaminated sand, in 9.5 m distance from the center of the contamination on day 25 and in 0.73 m, 2.35 m and 9.5 m distance on day 102. Only 2-3 samples were taken at irregular time intervals for $t > 53$ min after the injection of the tracers. The data was evaluated as described for the DPTT in the contaminated sand and results are reported in Table 7.1. The apparent S_n measured by the DPTT in uncontaminated soil remains between -0.1 and 0.2% of the total porosity, which is in the range of the experimental error. Average results are therefore reported as $\leq 0.2\%$.

Effective diffusion coefficient. Effective diffusion coefficients D_e were calculated from the data of the most volatile compound, CFC-12, with the assumption $f_{a,CFC-12} = 1$ for both, the measurements in the contaminated and uncontaminated sand. The air-filled porosity θ_a used for the data evaluation was 0.29 for day 25 and 0.27 for day 102, as determined from TDR measurements at the depth of the embedded contamination. The proportionality factor D_e/D_m reported in Table 7.1 is the average of D_e/D_m calculated from the individual measurements (2-4 at one location). The error is given as the standard deviation of the single measurements.

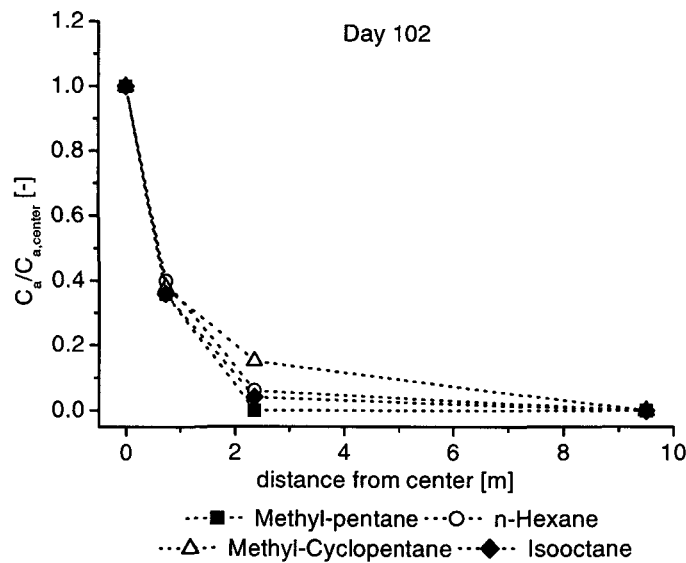


Figure 7.3: VOC concentrations measured at the Værløse field site 102 days after the emplacement of the contamination.

VOC measurements. Soil air concentrations of the CFCs were analyzed on a GC equipped with an ECD and FID connected to the same column. Thus VOC concentrations in the soil air could be measured with the FID at the same time as the tracer concentrations on the ECD. On day 25 VOC were only detected in the source zone and not at 9.5 m distance from the center of the contamination. The VOC concentrations measured on day 102 at some distance from the center of the contamination relative to the concentration measured in the contaminated sand are shown in Figure 7.3. Data points are the average of the 2-4 measurements at each location. Methylcyclopentane could be detected in all soil air samples. Isooctane and n-Hexane were below the detection limit in 9.5 m distance from the contamination, methylpentane already at 2.35 m distance. The relative concentration profiles of the four compounds are, however, similar.

7.5 Discussion

Assumptions. The derivation of the theory used for the evaluation of the DPTT relies on a number of critical assumptions, which are discussed in the following.

Homogeneity: The first assumption is the homogeneity of the porous medium.

Given the specific situation at the Værløse field site, the most relevant question is, whether the air-NAPL partitioning tracer CFC-11 spread beyond the contaminated sand layer. For the more volatile tracers, the presence or non-presence of a NAPL is less relevant. The distance over which the CFC-11 concentration falls to approximately 10 percent of the concentration at the injection point can be estimated from eq (3.10). One estimates a distance of 22 cm after 3 h for CFC-11 in the contaminated sand on day 25 and 26 cm on day 102. Comparing this distance with the extension of the contaminated sand layer (38 cm from the center) it can be concluded that CFC-11 has not diffused out of the contaminated sand. For the DPTT in the uncontaminated sand one estimates accordingly, that CFC-tracers were spread over a distance of 55 cm at the end of the experiments. Tracers were injected at a depth of 1.1 m below surface and are thus expected to remain within the glacial melt water sand layer. Thus the assumption of a homogeneous medium was reasonable in both, the contaminated and uncontaminated sand.

Partitioning equilibrium: The second assumption concerns the instantaneous equilibrium partitioning of the tracers between the gas-phase and the other phases of the vadose zone. Previous results presented in Chapter 6 indicated equilibrium conditions after an initial stabilization period, which resulted in stable ratios $f_{a,1}/f_{a,2}$ for times $t > 40$ min after the injection of the tracers into laboratory columns. For the DPTT at the Værløse field site, samples were taken at $t > 53$ min. No obvious time trend was observed for the ratios $f_{a,1}/f_{a,2}$. The measured $N^{point}(0, t)$ were well described by linear regression lines going through the origin, when plotted according to the theory. This suggests that the model based on equilibrium partitioning provided a reasonable description for the tracer diffusion at the field site. Before the emplacement of the contamination, the NAPL was mixed with the moist sand in a concrete mixer [9], probably maximizing the NAPL surface coating in favor of the partitioning equilibrium. At field sites, where the contamination results from an accidental spill, longer stabilization times may be required to achieve equilibrium in the pore space.

Sorption to soil not relevant: As a third assumption sorption to the solids and partitioning into the water-phase was neglected in the data evaluation. The sand had a low organic carbon content f_{oc} of 0.02% and sorption is thus not expected to be very important for the CFC-tracers. A slightly positive “apparent” S_n as measured in some of the DPTTs

in the uncontaminated sand would indicate sorption of the less volatile tracer CFC-11, however, the “apparent” S_n measured in the uncontaminated sand were all within the range of the experimental error.

No advection: A forth assumption is that gas-phase diffusion is the only relevant process for tracer movement. Advective gas transport can be created due to gravity-driven density-dependent vapor transport [15], [32]. An increase of the density of organic vapors, particularly of halogenated compounds, over the density of soil air can create vertical gas transport in the vadose zone [32]. However, this process is only relevant in relatively coarse soils. Considering the quick initial decrease of the tracers concentrations due to steep concentration gradients, one does not expect gravity-driven vapor transport to be important.

Point source: A fifth assumption is the instantaneous point source as initial condition. A perfect point source is practically impossible. However, the observation of a linear dependency of the data in Figure 7.2 demonstrates that the derived equations also work for an nonperfect tracer input.

Suitability of the DPTT for site investigation. Both, on day 25 and day 102 after the emplacement of the contamination, the DPTT in the contaminated sand indicated the presence of a NAPL, whereas a number of DPTTs in the uncontaminated sand yielded much lower “apparent” NAPL saturations S_n in the range of the detection limit of the method. Furthermore the DPTT in the contaminated sand showed a decrease in S_n between day 25 and 102 as expected for a weathering source zone [44]. This suggests that the DPTT is a suitable tool for source delineation and for the monitoring of natural attenuation in a NAPL-contaminated sand. On day 25 the S_n calculated for the two different tracer pairs deviated by almost a factor 2, on day 102 the agreement was better, see Table 7.1. Given the additional uncertainties in assumptions made for the data evaluation, such as neglecting sorption, the averaged S_n of the DPTT at the Værløse field site is expected to be within a factor 2 of the actual S_n .

Estimation of the air saturation. A method to estimate the air-saturation S_a from the results of the DPTT and the total porosity θ_t has been tested at the Værløse field site. The estimated S_a agree reasonably well with the θ_a determined from TDR readings. The deviation is in the order of 15 %. It is possible that the total porosity is somewhat higher and the water content somewhat lower in the embedded contamination as compared to the natural

glacial melt water sand, which would explain the observed difference. Overall it can be concluded that the estimation provides a reasonable value for S_a and can be useful, if no other data is available.

Effective diffusion coefficients. The proportionality factors between effective and molecular diffusion coefficient D_e/D_m measured in situ range from 0.08-0.15. Estimating τ with the empirical relation $\tau = \theta_a^{2.33}/\theta_t^2$ proposed by Millington & Quirk [37] one obtains a proportionality factor of 0.12 for day 25 and 0.09 for day 102. Estimating τ with the empirical relation $\tau = 0.66$ proposed by Penman [43] one obtains a proportionality factor of 0.19 for day 25 and 0.18 for day 102. The differences between D_e/D_m measured at different locations may be the result of experimental error, since D_e were determined from only two measurements at some locations. However, the experimental standard deviation is relatively small. Another explanation is an actual variation in D_e due to spacial variations in the water content of the glacial melt water sand.

Compatibility with soil gas investigations. The combination of the DPTT with traditional soil gas investigations is a promising application of this new method. Soil air samples withdrawn from the injection point during a DPTT contain not only the tracers, but also the other components of soil air. If the analytical system allows the separation and simultaneous detection of tracers and VOCs, *one obtains the combined information with hardly any additional effort.* The results of the DPTT in Table 7.1 add valuable additional information to the measured VOC concentrations shown in Figure 7.3. For instance, the combination of the NAPL saturation data with VOC concentration profiles allows a localization of the contamination, and the combination of VOC concentration profiles with effective diffusion coefficients D_e measured in situ allows the calculation of diffusive contaminant fluxes from Fick's first law.

Chapter 8

Diffusive Partitioning Tracer Test: Lysimeter Experiments

8.1 Introduction

Heterogeneous NAPL distribution. The spatial distribution of non-aqueous phase liquid (NAPL) in the subsurface of contaminated sites can be very heterogeneous, with pools of locally high residual NAPL saturations, for instance along preferential flow paths, surrounded by uncontaminated soil. A heterogeneous NAPL distribution makes site investigations difficult. Some traditional methods such as core sampling [2] or cone penetrometer testing [33] characterize a relatively small volume of the subsurface. For a sufficient number of sampling points with a high spatial resolution a detailed characterization of the NAPL distribution can be obtained. This is for instance important for source delineation at contaminated sites. Interpolation between point measurements can, on the other hand, be very inaccurate in heterogeneous environments. Indirect methods for NAPL detection such as soil gas measurements [2] have a wider, but ill-defined range. Large spatial volumes can be investigated with interwell partitioning tracer tests (PITT), see Section 6.1 for an introduction. This indirect method determines an average NAPL saturation S_n for the tracer swept volume between an injection and an extraction well [13]. For instance, the decrease in the average NAPL saturation can be assessed on a large scale by performing a PITT before and after remediation measures, see [35] for an example of this approach in a highly heterogeneous aquifer. Averaging methods such as the PITT can be more cost-effective as compared to a high number of point measurements. The detection of locally high NAPL saturations in an elsewhere uncontaminated environment can, however, be problematic, if the average S_n is low

and thus close to the detection limits of an averaging method [34]. The accuracy of the PITT in a heterogeneous environment is controversially discussed. Laboratory experiments indicate that the presence of porous media heterogeneity and a variable distribution of the NAPL can lead to a reduced accuracy of the PITT [40]. Other authors report the successful application of the PITT in a highly heterogeneous aquifer [35]. Many successful investigations of heterogeneous sites use point measurements and large-scale averaging methods in parallel, taking advantage of the specific merits of each method [35], [11].

Aims. The goal of this chapter is to characterize the performance of the DPTT in a porous medium, where the distribution of the NAPL is heterogeneous, but well defined. For the DPTT reported in Chapter 6 and 7 the NAPL partitioning tracer spread within either the contaminated or uncontaminated sand and the NAPL could therefore be considered to be homogeneously distributed, even if this was not necessarily the case on a larger scale. From those experiments it was not evident, which volume of soil was actually represented by the measured NAPL saturation S_n . In this chapter results from a lysimeter study are reported, where the NAPL is located within a 20 cm thick contaminated sand layer, surrounded by uncontaminated sand. DPTT were performed by injecting tracers inside and outside of the contaminated zone and the effect on S_n , as determined from the tracer data with equations derived for a homogeneous medium, was investigated. Besides monitoring the decline of the tracer concentration at the injection point, diffusive tracer breakthrough curves were also measured in some distance from the injection point. This alternative for the determination of S_n can be seen as a conceptual extension of the DPTT described so far. For both approaches, the experiments in the lysimeter allow to better define the volume of soil represented by the measured S_n . Such knowledge is crucial for the proper use of the method in heterogeneous environments.

8.2 Theory

NAPL saturation from diffusive breakthrough curves. In Chapter 6 and 7 the DPTT has been described as a method to determine the NAPL saturation S_n from the ratio of the mass fraction in the soil air $f_{a,1}/f_{a,2}$ of two tracers 1 and 2 with different affinities for the NAPL. This ratio was obtained from the relative concentrations of the tracers at the injection point $C_r(0, t)$, see eq (7.1). The ratio of the mass fraction in the soil air $f_{a,1}/f_{a,2}$ can also be determined by measuring the diffusive tracer breakthrough curves in some

distance r from the injection point. According to eq (3.10) the maximum concentration of a *non-degradable* tracer in some distance r from the injection point is measured after the time t_{max} ¹

$$t_{max} = \frac{r^2}{6f_a\tau D_m} . \quad (8.1)$$

For two tracers 1 and 2 one finds

$$\frac{f_{a,1}}{f_{a,2}} = \frac{t_{max,2}D_{m,2}}{t_{max,1}D_{m,1}} . \quad (8.2)$$

This ratio does not depend on r , and there is no need to determine r accurately. The measurement of diffusive breakthrough curves in some distance r from the injection point provides an alternative for the determination of S_n , even if r is not known exactly. This approach is similar to the PITT with the difference, that gas-phase diffusion instead of advection is the relevant transport mechanism for the partitioning tracers.

Tortuosity factor and apparent diffusion coefficients. Although the determination of apparent diffusion coefficients D_e and D_s is not in the focus of this chapter, it is shortly sketched how they can be obtained from the measured diffusive breakthrough curves. By transforming eq (8.1) one obtains the tortuosity factor τ from the measured diffusive breakthrough curve of a non-degradable tracer 2, for which the mass fraction in the soil air $f_{a,2}$ is known

$$\tau = \frac{r^2}{6f_{a,2}t_{max,2}D_{m,2}} . \quad (8.3)$$

The effective diffusion coefficient $D_{e,1}$ of a compound 1 can also be determined, if one knows the air-filled porosity θ_a :

$$D_{e,1} = \theta_a\tau D_{m,1} = \frac{\theta_a r^2}{6f_{a,2}t_{max,2}} \frac{D_{m,1}}{D_{m,2}} . \quad (8.4)$$

By transforming eq (8.1) one obtains the sorption-affected diffusion coefficient D_s of compound 1, if degradation is negligible:

$$D_{s,1} = f_{a,1}\tau D_{m,1} = \frac{r^2}{6t_{max,1}} . \quad (8.5)$$

Note that for the determination of D_e and D_s one needs to know the distance r between the injection point and the monitoring point.

¹At time t_{max} , the first derivative of eq (3.10) with respect to t equals zero, for $k_{app} = 0$.

Error analysis NAPL saturation. The determination of the ratio $f_{a,1}/f_{a,2}$ from diffusive breakthrough curves is more robust with respect to analytical errors as compared to the determination of $f_{a,1}/f_{a,2}$ from $C_r(0, t)$. With an analytical error of 10% for both the ratio $t_{max,2}/t_{max,1}$ and the ratio $D_{m,1}/D_{m,2}$ one calculates a theoretical error of 14% for the ratio $f_{a,1}/f_{a,2}$ as determined from diffusive breakthrough curves. Using the same assumptions as in Section 6.2, the overall theoretical error for S_n becomes 20%.

Error analysis apparent diffusion coefficients. Assuming that the distance r , the air-filled porosity θ_a , the mass fraction in the soil air $f_{a,2}$, the time of the maximal tracer concentration t_{max} and the ratio of the molecular diffusion coefficients $D_{m,1}/D_{m,2}$ can all be determined or estimated with an error of 10%, one calculates an overall theoretical error of 28% for the effective diffusion coefficient D_e and an overall theoretical error of 22% for the sorption-affected diffusion coefficient D_s as determined from diffusive breakthrough curves.

8.3 Materials and Methods

Chemicals. The suppliers and the properties of the chemicals used in this study are listed in Section 4.3. All chemicals were obtained in the highest available purity.

Tracer mixtures. For the convenient use in the diffusion experiments CFC-tracers were dissolved in octanol and enclosed in vials with Mininert-valves (Fluka, Buchs, Switzerland). The headspace above the octanol was 50 mL. Headspace concentrations were approximately 1500 ppmv of SF₆, 2000 ppmv of CFC-12 and 500 ppmv of CFC-11.

Lysimeter. A large scale, cylindrical field lysimeter with a diameter of 1.2 m and a 2.5 m depth was used as the experimental system, see Figure 8.1. The lysimeter was filled with a coarse alluvial sand, see Section 4.3 for the characterization. The resulting total porosity θ_t was 0.41 ± 0.03 . At depths between 1.0 and 1.2 m, 0.226 m³ of the same sand contaminated with an artificial fuel mixture (fuel 2, see Section 4.3) were embedded. Fuel and sand were mixed in a concrete mixer to obtain a residual NAPL saturation S_n of approximately 3.5% of the total porosity. A 1.5 m long capillary made of stainless steel (1/16 in.) was installed in order to allow a point injection at 1.1 m depth in the center of the contaminated zone (capillary A). An identical capillary allowed to withdraw samples. The dead volume of the capillaries

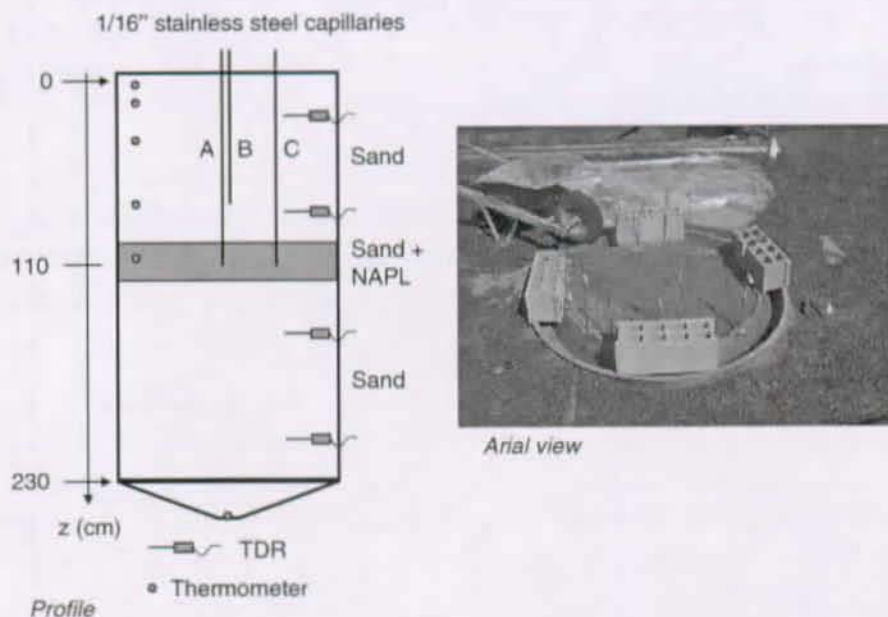


Figure 8.1: Experimental set-up for the lysimeter study.

was 0.7 mL. Additional pairs of capillaries allowed the injection or sampling at 0.8 m depth in the center of the lysimeter (capillaries B) and at 1.1 m depth, but 30 cm from the center of the lysimeter (capillaries C). Several time domain reflectometry (TDR) probes (SDEC, Reignac s. Indre, France) and thermometers were installed at different depths to measure the water-filled porosity θ_w and temperature T . This experimental set-up is shown in Figure 8.1.

Experimental procedure. Basically, the DPTT was performed as described for the field site in Chapter 7. After 40 min, 53 min, 75 min, 110 min and 180 min the soil air at the injection point was sampled through the sampling capillary. Additional soil air samples were withdrawn every 20 min over a period of 8 h from the sampling capillary in 30 cm distance from the injection point to measure the diffusive tracer breakthrough curves. Samples were stocked in sample lock syringes (Fluka, Buchs, Switzerland) and analyzed by GC-ECD. The DPTT was performed 8, 14 and 19 days after the emplacement of the contaminated sand in the lysimeter (experiment L1-L3).

In experiment L1 the tracers were injected through capillary A and the concentrations were monitored at the injection point (capillary A) and 30 cm from the injection point through capillary C. For this experiment the shortest diffusive pathway between the two capillaries remains within the NAPL-contaminated sand layer.

In experiment L2 the tracers were injected through capillary B and the concentrations were monitored at the injection point (capillary B) and 30 cm from the injection point through capillary A. For this experiment 1/3 of the shortest diffusive pathway between the two capillaries is within the contaminated sand layer.

In experiment L3 the tracers were injected through capillary A and the concentrations were monitored at the injection point (capillary A) and 30 cm from the injection point through capillary B. For this experiment also 1/3 of the shortest diffusive pathway between the two capillaries is within the contaminated sand layer.

Analytical procedures. For the lysimeter experiments, concentrations of the CFC-tracers were analyzed by injecting 100 μL of gas into a Varian CP-3800 gas chromatograph equipped with an ECD detector. The injector was heated to 60°C and the split ratio was 10. A 30 m capillary column GS-GasPro (J&W Scientific) was used for the separation of the compounds at a temperature of 130°C. Carrier gas was Helium at a flow rate of 2 mL/min. Linearity of the detector response was checked with calibration standards.

8.4 Results

Soil physical parameters. In the lysimeter experiment the water-filled porosity θ_w as determined with the TDR probes remained between 0.04 and 0.07 in the center of the lysimeter for the first 45 days after the installation of the contaminated sand. The air saturation S_a calculated from TDR measurements and with a total porosity $\theta_t = 0.41$ was 0.86, 0.85 and 0.85 on day 8, 14 and 19 after the source emplacement. The temperature T remained near 10 °C.

NAPL saturation from measurements at the injection point. DPTTs were performed 8, 14 and 19 days after the emplacement of the contaminated sand and eq (3.12) derived for the point source was used to interpret data measured at the injection point. The measured $N^{point}(0, t)$ are shown in

Figure 8.2 and results are reported in Table 8.1. Also shown in Figure 8.2 are linear regression lines, which were forced through the origin. Correlation coefficients R^2 are 0.98 or better. For the capillary A, located in the center of the contaminated sand, the regression line of the tracer with the highest affinity for the NAPL-phase, CFC-11, has the highest slope, and the regression line of the tracer with the lowest affinity for the NAPL-phase, SF_6 , has the lowest slope. This can be seen for both, experiment L1 and L3, where tracers were injected through capillary A. For the capillary B, located in the center of the lysimeter, but 20 cm above the upper limit of the contaminated sand layer, the regression lines fall together (experiment L2). The ratio $f_{a,1}/f_{a,2}$ has been calculated as an average of the five individual measurements. From this ratio, the NAPL saturation S_n was calculated for the tracer pairs with a sufficient difference in f_a using eq (6.4) and the air-fuel partitioning coefficients K_n measured at 10°C , listed in Table 4.4, and the air saturation S_a as determined from TDR measurements. For SF_6 , the air-hexadecane partitioning coefficient published in [1] was corrected for a temperature of 10°C using $K_n(T_1) \approx K_n(T_2) \cdot p^0(T_1)/p^0(T_2)$ and vapor pressure data from [59]. The NAPL saturation S_n calculated for the different tracer pairs agree within $\pm 40\%$. The error of the average S_n is given as the standard deviation of S_n as calculated from the two tracer pairs. According to the results in Table 8.1, the NAPL saturation S_n in the vicinity of capillary A decreases from 2.8% to 2.3% of the total porosity between day 8 and day 19. A comparison with S_n determined from the NAPL extracted from soil cores on day 0 and day 30 shows agreement within at least a factor 2, see footnote in Table 8.1. In the vicinity of capillary B, no NAPL was detected by the DPTT on day 14. The air saturation S_a as estimated from the slope s of the regression line for SF_6 with eq (7.4) and $\theta_t = 0.41$ is 0.89, 0.89 and 0.84 on day 8, 14 and 19. Estimated S_a and S_a determined from TDR measurements thus agree within $\pm 5\%$.

NAPL saturation from diffusive breakthrough curves. In the lysimeter experiment, tracer concentrations were monitored not only at the injection point, but also in 30 cm distance from the injection point. Diffusive tracer breakthrough curves measured in 30 cm distance from the injection point are shown in Figure 8.3. For all experiments, a separation is observed for the different tracers, and the observed difference in the migration behavior is by far greater than what can be attributed to differences in the molecular diffusion coefficient D_m . This indicates the presence of a NAPL between the injection point and the observation point, where the diffusive tracer breakthrough curves were measured. The tracer with the lowest affin-

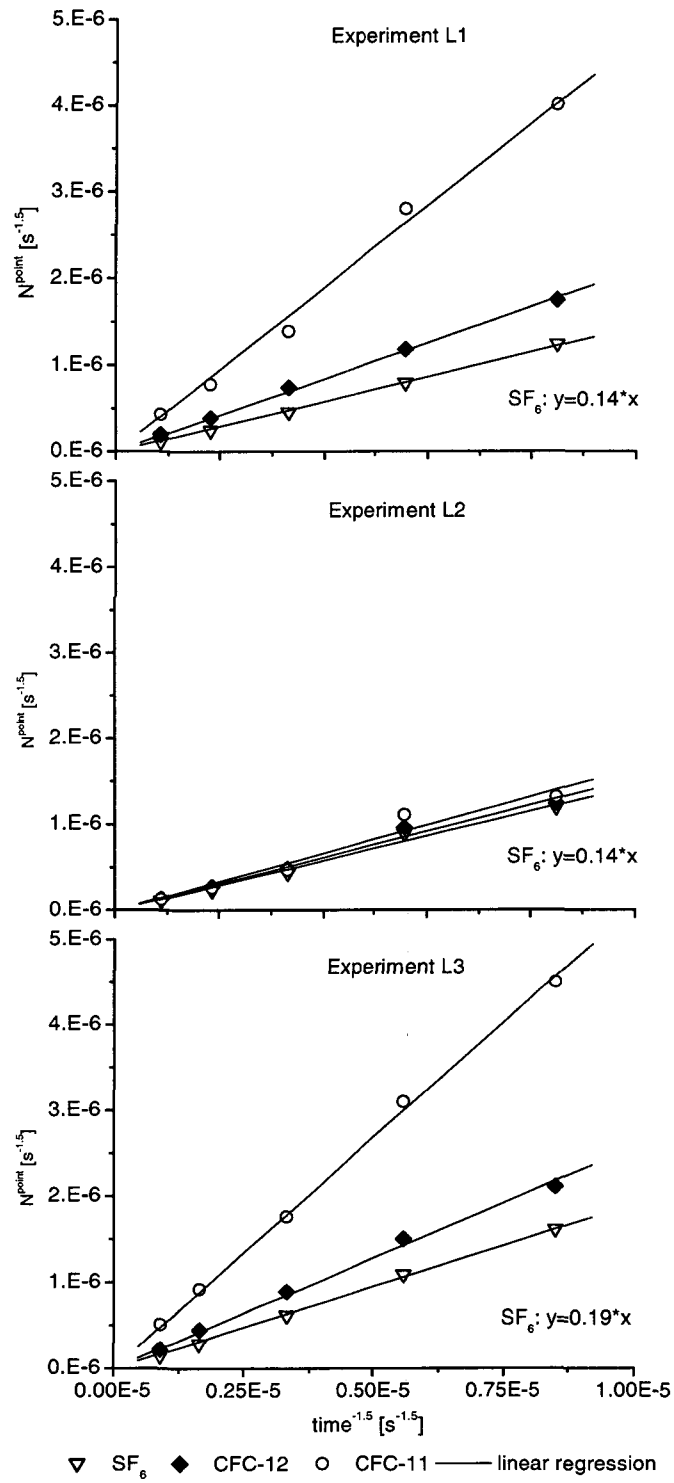


Figure 8.2: $N^{point}(0, t)$ measured at the injection point for the DPTTs in the lysimeter.

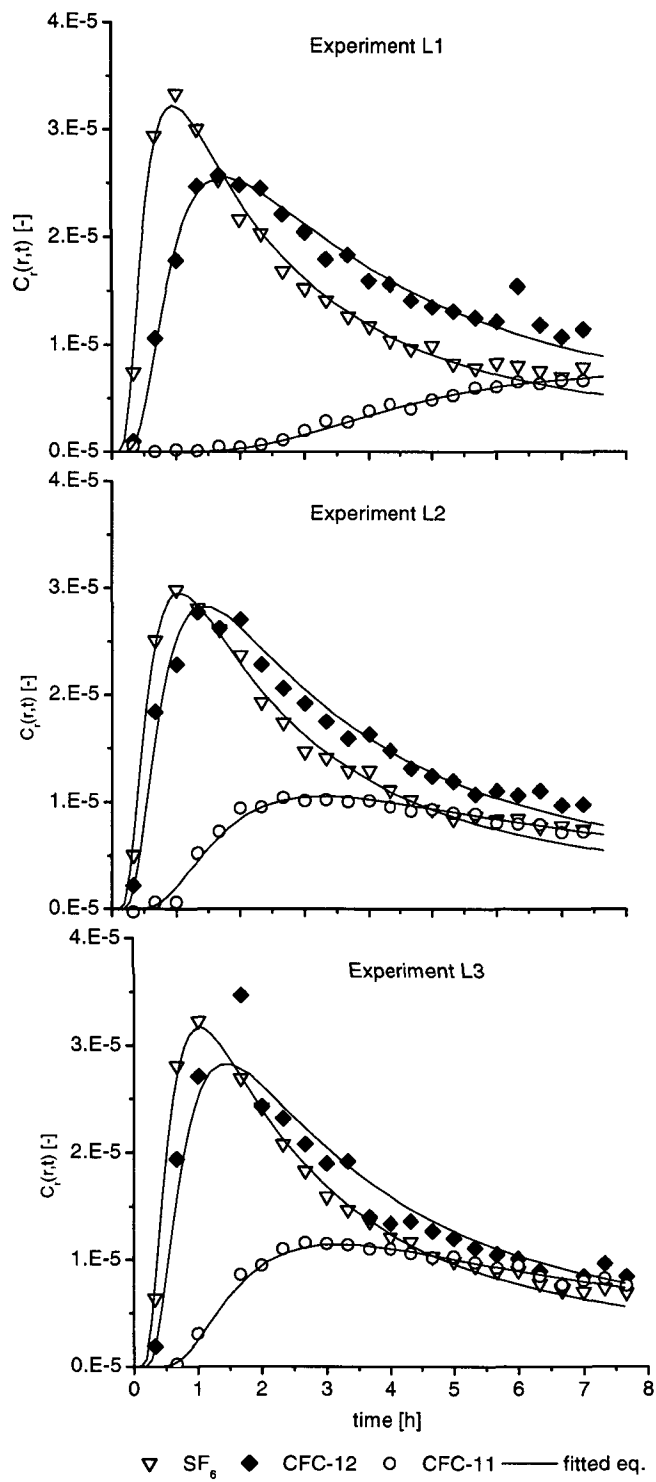


Figure 8.3: Measured diffusive breakthrough curves in 30 cm distance from the injection point for the DPTTs in the lysimeter.

Table 8.1: NAPL saturation S_n and proportionality factor D_e/D_m as determined in the lysimeter from DPTTs.^a

	L1, day 8	L2, day 14	L3, day 19
Injection capillary	A	B	A
Sampling capillary	A + C	B + A	A + B
From $C_r(0, t)$ at the injection point:			
S_n DPTT from SF ₆ /CFC-11	3.4	0.1	2.6
S_n DPTT from CFC-12/CFC-11	2.3	0.0	2.1
S_n DPTT (average)	2.8 ± 0.8	0.1 ± 0.1	2.3 ± 0.4
D_e/D_m ^b	0.21 ± 0.01	0.21 ± 0.01	0.17 ± 0.01
From $C_r(r, t)$ in 30 cm distance:			
S_n DPTT from SF ₆ /CFC-11	2.7	0.6	0.6
S_n DPTT from CFC-12/CFC-11	3.0	0.4	0.4
S_n DPTT (average)	2.8 ± 0.1	0.5 ± 0.1	0.5 ± 0.1
D_e/D_m ^c	0.19	0.18	0.17

^a The dimension for S_n is [cm³/cm³ total porosity in %]. The initial S_n in the contaminated layer calculated from the total amount of NAPL added is 3.5% of the total porosity. However, some volatile compounds evaporated while the NAPL was mixed with the sand. S_n as determined by NAPL extraction from sand was 2.4% immediately after source emplacement and 0.8% 30 days after the source emplacement. ^bCalculated from SF₆ data according to eq (5.5) with $f_{a,2} = 1$ and $\theta_a = 0.35$. ^cCalculated from SF₆ data according to eq (8.4) with $f_{a,2} = 1$ and $\theta_a = 0.35$.

ity for the NAPL, SF₆ is spreading fastest by gas-phase diffusion. For SF₆, the measured diffusive breakthrough curves are very similar in all experiments. For CFC-11, the tracer with the highest affinity for the NAPL, the diffusive breakthrough curves are similar in experiment L2 and L3, but diffusive spreading is clearly slower in experiment L1. For experiment L1, the 8 h duration of the experiment was not sufficient to observe a maximum in the breakthrough curve of CFC-11. Measured diffusive breakthrough curves were evaluated by fitting the equation $y = (a/t^{1.5})\exp(-b/t)$, which corresponds to eq (3.10) with $k_{app} = 0$ and a number of time-independent parameters lumped into the fitting parameters a and b , with a least-squared error routine to the measured data and determining t_{max} for the fitted equation. As can be seen in Figure 8.3, the equation fits the data well and the maximum of the fitted equation is close to the maximal measured tracer concentration. From the ratio $t_{max,1}/t_{max,2}$ the S_n was calculated according to eq (8.1) and eq (6.4) with the same air-fuel partitioning coefficients K_n and porosity

data as used for the evaluation of the measurements at the injection point. Results are reported in Table 8.1. The NAPL saturation S_n calculated for the different tracer pairs agree within $\pm 15\%$. The error of the average S_n is given as the standard deviation of S_n as calculated from the two tracer pairs. For experiment L1, where both, the capillaries A and C are located in the contaminated sand, the calculated S_n agrees well with S_n determined from the tracer concentrations at the injection point. For experiments L2 and L3, where only approximately 1/3 of the shortest diffusive pathway between the capillaries A and B is located in the contaminated sand layer, there's an obvious discrepancy.

Effective diffusion coefficient from measurements at the injection point. In the lysimeter experiment, the air-filled porosity θ_a was known, because the water content was monitored with TDR measurements. The effective diffusion coefficient D_e could therefore be calculated according to eq (5.5) from the concentrations $C_r(0, t)$ of the most volatile tracer SF_6 . Results are reported in Table 8.1. The proportionality factor D_e/D_m reported in Table 8.1 is the average of the five individual measurements. The error is given as the experimental standard deviation of these measurements.

Effective diffusion coefficient from breakthrough curves. The effective diffusion coefficient D_e was calculated according to eq (8.4) from the time t_{max} of the most volatile tracer SF_6 and the air-filled porosity θ_a as calculated from TDR measurements. Results are reported in Table 8.1. Because only one value for D_e can be obtained per experiment, no experimental error is indicated. The D_e determined from diffusive breakthrough curves agree within $\pm 15\%$ with the values determined from the measurements at the injection point.

8.5 Discussion

Assumptions. The derivation of the theory used for the evaluation of the DPTT relies on a number of critical assumptions. In the lysimeter experiment, one of the assumptions (homogeneous NAPL distribution) was violated intentionally. This is discussed in the following:

Homogeneity: In the lysimeter, the NAPL distribution was highly heterogeneous, with a contaminated sand layer between 1.0 to 1.2 m from the surface and uncontaminated sand above and beyond this layer. The distance over which the tracer concentration falls to approximately

10% of the concentration at the injection point $C_r(0, t)$ can be used to characterize the extension of the tracer plume in a homogeneous medium. From eq (3.10) one estimates a distance of 20 cm after 3 h for CFC-11 in contaminated lysimeter sand with a NAPL saturation S_n of 2.5% and a distance of 60 cm in the uncontaminated lysimeter sand. Capillary A is placed in the center of the 20 cm thick contaminated sand layer. It can therefore be concluded that a part of the CFC-11 tracer mass diffused out of the contaminated sand layer during the 3 hour period, for which the soil air concentrations have been monitored at the injection point. Furthermore it is expected that a part of the CFC-11 tracer mass injected through capillary B into the uncontaminated soil will reach the contaminated sand in 20 cm distance from the injection point in experiment L2. The tracer SF_6 , which has a very low affinity for the NAPL, diffuses in all experiment at approximately the same velocity as CFC-11 in the uncontaminated sand, because their molecular diffusion coefficients D_m are approximately equal. One must therefore expect that part of the SF_6 tracer mass reaches the sidewall of the lysimeter in 60 cm distance from the injection point from 3 hours after the injection onwards. Thus the assumption of homogeneity was not valid in the lysimeter experiment. The effect on the results of the DPTT will be discussed in the next paragraphs.

Partitioning equilibrium: As in the previous experiments reported in Chapter 6 and 7, no obvious indication of non-equilibrium conditions can be observed in the measured data. The higher than predicted values for the *more volatile* tracers SF_6 and CFC-12 at times $> 5\text{h}$ in the measured diffusive breakthrough curves are probably due to the fact that these tracers reached the sidewall of the lysimeter after 3 hours, and thereafter concentrations decreased somewhat slower than predicted. This deviation is thus not interpreted as an indication of slow partitioning kinetics.

Sorption to soil not relevant: Of all the sand investigated, the lysimeter sand has the highest f_{oc} , see section 4.3. However, no separation was observed for the $N^{point}(0, t)$ of tracers with a different affinity to NAPL in uncontaminated sand, see experiment L2 in Figure 8.2. This indicates that as a first approximation, sorption to the solids can be neglected. Using the measured air-solid partitioning coefficients K_s in Table 4.3 and the Henry constants H in Table 4.2 to calculate the NAPL saturation S_n according eq (6.2), one finds that the simplified eq (6.4) used for the data evaluation underestimated S_n by approximately

20%. Furthermore, using f_{a,SF_6} as calculated from K_s and H for the determination of the effective diffusion coefficient D_e , one finds that D_e determined from the measurements at the injection point has been underestimated by 8% and D_e determined from breakthrough curves by 20% due to the approximation $f_{a,2} = 1$. In summary it can be said, that reasonable values for S_n and D_e could be obtained, even though sorption was neglected in the data evaluation.

No advection: Advective gas transport can be due to gravity-driven density-dependent vapor migration [15]. An increase of the density of organic vapors, particularly of halogenated compounds, over the density of soil air can create vertical gas transport in the vadose zone. The density of the gas tracer mixture injected into the lysimeter, estimated from the tracer concentration according to [15], was 1.19 g cm^{-3} as compared to 1.17 g cm^{-3} for air at 1 atm, 25°C . Using the equations given in [15], a maximum advective downward gas pore velocity of less than 0.01 m d^{-1} is estimated for the gaseous tracer mixture in the lysimeter, which had a soil permeability of $3 \cdot 10^{-12} \text{ m}^2$ [44]. The gaseous tracer mixture was initially quickly diluted due to diffusion. Thus gravity-driven vapor migration can be excluded in the lysimeter.

Point source: As in the previous experiments reported in Chapter 5, 6 and 7, no indication was found for problems arising from the assumed initial condition.

Effect of heterogeneity on measurements at the injection point.

As can be seen in Figure 8.2, the decline of the tracer concentration at the injection point is well described by the mathematical model, which has been derived for a homogeneous medium. For instance, no deviation from the predicted linear behavior is observed for the measured $N^{point}(0, t)$ of CFC-11, the tracer with the highest affinity for the NAPL. Thus, the concentration change at the injection point was little affected by the heterogeneous NAPL distribution, even though part of the CFC-11 tracer mass diffused out of the contaminated sand layer during the 3 hour monitoring period. The heterogeneity of the NAPL distribution in the lysimeter becomes only obvious, when comparing the results of all three experiments in Figure 8.2: Whereas the concentration ratios at the injection point in experiment L1 and L3 indicate the presence of a significant NAPL saturation S_n in the vicinity of capillary A, with a decrease between day 8 and 19, no NAPL is detected in the vicinity of capillary B in experiment L2 on day 14. Thus it is concluded that S_n as determined from the concentration ratio of the tracers

at the injection point represents a rather small volume of soil around the injection point, smaller than the total volume the tracers diffuse into. This approach to determine S_n must therefore be seen as a method, which acquires information on a small scale, having a high resolution, but requiring a high number of measurements for an accurate characterization of a heterogeneous environment.

Effect of heterogeneity on measured diffusive breakthrough curves.

The diffusive breakthrough curves in Figure 8.3 show the typical time dependency of diffusive breakthrough curves in a homogeneous medium, as can be seen by the good agreement of the measured data and the fitted equation. From the data of a single experiment, the heterogeneity of the NAPL distribution in the lysimeter is thus not evident. The heterogeneity of the lysimeter becomes only obvious, when comparing the different experiments. A significantly lower S_n is calculated for experiments L2 and L3, which investigate the soil between capillary A and B, as compared to experiment L1, which investigates the soil between capillary A and C. The empirical results in Table 8.1 suggest that S_n as calculated from the time t_{max} of the maximum in the diffusive breakthrough curve represents a somehow² averaged S_n for the soil between the injection and the monitoring capillary. For experiment L3 the S_n determined from the diffusive breakthrough curves is approximately one fourth of the S_n determined from the tracer concentration decline at the injection point. Interestingly, the diffusive breakthrough curves are very similar for experiment L2 and L3, even though the tracers were injected into the contaminated sand and measured in the uncontaminated sand in experiment L2 and vice versa in experiment L3. The concentration decline at the injection point was very different for the two experiments, see Figure 8.2. A better understanding of these phenomena may require numerical simulations, which are beyond the scope of this study. In summary it can be concluded that for the S_n obtained from diffusive breakthrough curves, the investigated soil volume is better defined as compared to the S_n obtained from the concentration ratios at the injection point. However, in heterogeneous media the “average” represented by S_n is ill-defined.

Comparison of partitioning tracer methods. The results presented in this and the previous chapters allow a characterization of the DPTT as a new method for the detection and quantification of NAPL in the vadose zone and a comparison with its well established counterpart, the PITT.

²The term “somehow” is used, because no theory has been presented for diffusion in a heterogeneous medium.

DPTT, injection point: The NAPL saturation S_n can be obtained from the concentration ratios at the injection point of tracers with different affinities for the NAPL. The method requires a minimum of 2 GC-analyzes, one to determine the concentration ratios of the tracers in the injected gas mixture and one to determine the concentration ratios at the injection point after a sufficient initial time lag. The error for S_n as determined by this method is estimated to be 39%, see Section 7.2. The error can be reduced by measuring the concentration ratios at different times, and by using several tracers, which can be done with little additional analytical effort. According to the results of the lysimeter study the S_n obtained from this method represents only a small volume of soil around the injection point. Experiments at the Værløse field site demonstrate the compatibility of the method with traditional soil gas investigations. Given the appropriate analytical equipment is available, VOC concentrations in the soil air samples can be measured in parallel to the tracer concentrations. Furthermore, effective diffusion coefficients can be obtained from conservative tracer data.

DPTT, diffusive breakthrough curves: The NAPL saturation S_n can also be determined from diffusive breakthrough curves of tracers with different affinities for the NAPL measured in some distance from the injection point. The measurement of diffusive breakthrough curves requires a high frequency and an elevated number of analyzes and realistically the use of analytical equipment on site. The error for S_n as determined by this method is estimated to be 20%, see Section 8.2. Several tracers can be used in one test. This can, however, increase the analytical effort, because the time t_{max} of the maximum tracer concentration needs to be determined for every tracer. According to the empirical results of the lysimeter study the S_n obtained from this method represents an “average” S_n between the injection and the monitoring point. However, this “average” is ill-defined in heterogeneous media. As demonstrated in the lysimeter study, the method is easily combined with the above method, with only a few additional measurements at the injection point. Furthermore, effective diffusion coefficients can be obtained from conservative tracer data.

PITT: The NAPL saturation S_n can also be obtained from a PITT, which is based on advection as transport mechanism for the partitioning tracers. Typically, the PITT requires the measurement of complete breakthrough curves, rather than the determination of a concentration maxi-

mum. Non-equilibrium partitioning is often observed in advective partitioning tracer tests due to the elevated migration velocity, and S_n is therefore determined from the first temporal moment of the tracer response data [13]. This demands an accurate measurement of the complete breakthrough curves, especially also at late and low tracer concentrations. In addition to the analytical equipment needed for the measurement of breakthrough curves, the PITT also requires equipment for establishing and maintaining the flow field in the subsurface. The error for S_n as determined by this method is estimated to be 10% [13]. Several tracers can be used in one test. However, complete breakthrough curves must be measured for all tracers. The NAPL saturation S_n obtained from a PITT represents an average for the tracer swept volume. Soil volumes of substantial spacial extension can be investigated by one single PITT.

In summary, both the volume of soil investigated and the accuracy of the determined S_n increase from method A to method B to method C, but so do the experimental effort and costs. A number of low-cost point measurements can yield a higher resolution and better characterization of a NAPL contamination as compared to one average S_n . In a very heterogeneous environment, the number of point measurements required for an accurate description of the NAPL contamination may, on the other hand, be so elevated that a wider ranging, averaging method becomes more cost-effective. The choice of the appropriate method depends on the goals of an investigation and on the specific situation at the contaminated site and requires the scientific judgment and expertise of the investigating engineer, as well as a good characterization of the merits and drawbacks of available methods.

Chapter 9

Synopsis, Conclusions and Outlook

Basic approach. The basic experiment described in this thesis is the injection of a mixture of gaseous compounds into an unsaturated porous medium, where they form an instantaneous point source. The gaseous compounds are monitored at the injection point or in some distance from the injection point, while they are spread by gas-phase diffusion. An analytical equation has been derived to describe gas-phase diffusion from such an instantaneous point source in a homogeneous porous medium. This analytical equation includes a number of parameters, namely the mass fraction of the injected compound in the soil air f_a , the air-filled porosity θ_a of the soil, the tortuosity factor τ , the apparent first-order degradation rate k_{app} , the molecular diffusion coefficient in free air D_m and the total mass of the compound m_0 . The derivation of the equation is based on a number of assumptions: homogeneous and time-constant properties of the soil, instantaneous reversible linear equilibrium partitioning, first-order degradation rate in the water-phase and the absence of advection. If those assumptions are valid or provide a reasonable description for the actual situation, the data obtained from point source diffusion experiments can be interpreted with the analytical equation, and some of the parameters, or a combination of the parameters, can be determined.

Accomplishments. In this study the basic approach described above has been used to measure either the effective diffusion coefficients D_e , the sorption-affected diffusion coefficients D_s , or the NAPL saturation S_n , or a combination of these parameters *in situ*. The method for the determination of S_n has been baptized diffusive partitioning tracer test (DPTT). The results can be summarized as follows:

Effective diffusion coefficient: The calculation of diffusive fluxes in soil from Ficks first law or the interpretation of steady state concentration profiles requires the knowledge of effective diffusion coefficients D_e [18]. This parameter can be obtained from point source diffusion experiments by monitoring the concentration decline of a conservative gaseous tracer at the injection point. The air-filled porosity θ_a of the soil needs to be determined independently. The method has been tested in a sand-filled lysimeter and at a field site with a sandy unsaturated zone. The measured data were well described by the analytical equation, suggesting that the basic assumptions used for the derivation of the equation were valid. The method showed good reproducibility. Because the “true” D_e of a soil is not known, the accuracy could not be determined. Assuming an error of 10% for the measured or estimated input parameters, the overall error for D_e as determined by this method is 13%. The method provides an alternative to existing in situ methods for the determination of D_e in the subsurface [3], [20], with the advantage, that this proposed new method is easily combined with a simultaneous determination of D_s for a compound of interest or the determination of the NAPL saturation S_n .

Sorption-affected diffusion coefficient: The simulation of the spreading of gaseous compounds in soil by gas-phase diffusion requires the knowledge of sorption-affected diffusion coefficients D_s [18]. This parameter can be obtained from point source diffusion experiments by simultaneously monitoring the concentration decline of a gaseous compound and a conservative gaseous tracer at the injection point. The air-filled porosity θ_a of the soil needs to be determined independently. The method has been tested in a sand-filled lysimeter and at a field site with a sandy unsaturated zone. The measured data were quite well described by the analytical equation. Some experiments indicated partially slow partitioning kinetics, which affect the soil air concentration of less volatile compounds at the beginning of the experiments. The method showed good reproducibility. Because the “true” D_s of a soil is not known, the accuracy could not be determined. However, a comparison with results from batch experiments suggested a systematic overestimation by 15% to 20%, because, according to the batch experiments, the tracers were not truly conservative. Assuming an analytical error of 10% for the measured or estimated input parameters, the overall error for D_s as determined by this method is 33%. To date no other validated method for the in situ determination of D_s in the subsurface is available.

NAPL saturation: The localization and quantification of residual NAPL in the pore space of soils is a crucial procedure for the investigation and monitoring of sites contaminated with organic liquids [57]. The NAPL saturation S_n can be obtained from point source diffusion experiments by simultaneously monitoring the concentration decline of air-NAPL partitioning tracers with different affinity for NAPL at the injection point. An alternative is the measurement of diffusive tracer breakthrough curves in some distance from the injection point. The air saturation S_a of the soil needs to be determined independently or estimated, for instance from the concentration decline of a conservative tracer. Furthermore the method requires the knowledge of molecular diffusion coefficients D_m and air-NAPL partitioning coefficients K_n . The method (DPTT) has been tested in laboratory columns, at a field site with an artificially embedded contamination in a sandy unsaturated zone and in a sand-filled lysimeter with a heterogeneous NAPL distribution. The measured data were well described by the analytical equations. Column experiment showed that a partitioning equilibrium is reached after an initial time lag < 1 h, when the concentration change at the injection point is slower. For repeated column experiments the determined S_n agreed within $\pm 20\%$. The NAPL saturation S_n as calculated from different simultaneously measured tracer pairs in column experiments agreed within a factor 2 or better. The NAPL saturation S_n calculated as an average from all tracer pairs was within $\pm 30\%$ of the actual S_n . Assuming an analytical error of 10% for the measured or estimated input parameters, the theoretical overall error for S_n is 39%, if determined from the concentration decline at the injection point and 20%, if determined from diffusive tracer breakthrough curves. Experiments with a heterogeneous NAPL distribution suggest that S_n determined from tracer concentrations at the injection point represents a small soil volume around the injection point, whereas S_n determined from diffusive breakthrough curves represents the soil between injection and monitoring point. The DPTT thus provides a potentially inexpensive method for the investigation of NAPL contaminated sites with other characteristics than existing methods such as soil core sampling [2] or the PITT [13]. Besides the S_n , effective diffusion coefficients D_e can be obtained from the data of a DPTT without an additional effort, and VOC concentrations can be analyzed simultaneously, if soil air samples are analyzed on a GC equipped with an ECD and FID connected to the same column.

Conclusions. The monitoring of gas-phase diffusion from an instantaneous point source as a method to determine effective diffusion coefficients D_e and sorption-affected diffusion coefficients D_s and as a method to localize and quantify NAPL in the subsurface has been successfully tested in both, laboratory systems and natural, sandy soils. The validity and value of the method has been proven in soils, which were reasonably well described by the basic assumptions of the mathematical model used for the data interpretation. This is an important *first step* in the evaluation of this innovative method. An investigation of more complicated systems has been undertaken for the localization and quantification of NAPL by means of a diffusive partitioning tracer test (DPTT): at a field site with an artificially embedded contamination and in a lysimeter study the NAPL distribution was heterogeneous. The results demonstrate that value of the method under circumstances, where not all of the basic assumptions are valid. The new method for the investigation of the vadose zone is compared with more traditional methods in Table 9.1.

Open questions. While the experimental results presented in this study address and clarify many important aspects of the proposed in situ methods some new questions arise from the experimental results and some of the observed phenomena are not yet fully understood:

Slow partitioning kinetics: The experimental data were generally well described by the analytical equation, derived for an instantaneous partitioning equilibrium. However, both batch experiments and the in situ determination of apparent diffusion coefficients indicated partially slow partitioning kinetics for some of the less volatile compounds. As compared to the sandy soils investigated, slow partitioning kinetics may be more pronounced in soils with a high organic matter content or large particle aggregates. The coexistence of fast and slow partitioning kinetics has also been observed in advective gas-phase migration experiments [19] and batch experiments [21], [42]. This may affect the determination of apparent diffusion coefficients D_s . Numerical models are often based on the partitioning equilibrium assumption. Experimental error excluded, the averaged D_s obtained from the in situ experiments provides the best value for D_s as input parameter to such models for the description of gas-phase diffusion over the timescale of the experiment. However, if slow partitioning kinetics affect the gas-phase concentrations of diffusing compounds on a much longer timescale, the D_s determined in situ may overestimate the actual D_s . Therefore the relevance of slow partitioning kinetics should be further investigated.

Method	Characterization	Shortcomings
Diffusion of gaseous tracers from a point source	Injection of gaseous tracers into the vadose zone through profilers. Measurement of soil air concentrations at the injection point, or measurement of diffusive breakthrough curves. In situ determination of S_n , D_e , D_s , (k_{app}). VOC concentrations can be measured simultaneously. Little equipment, few analytes.	Local information, porosities need to be determined independently, only evaluated in artificially contaminated sandy soils.
Soil core sampling [2]	Local investigation of the soil profile. Qualitative description, porosities, S_n from extractions, f_{oc} , microbial analyzes. Soil cores/samples can be used to determine D_e , D_s , k_{app} from empirical relationships or in follow-up laboratory studies.	Local information, can be technically demanding and costly, additional laboratory work often required.
Soil gas sampling [2]	Measurement of VOC concentrations, O_2 , CO_2 .	Local information.
Flux chambers [5]	Measurement of diffusive contaminant fluxes to the atmosphere.	Local information.
Partitioning interwell tracer test (PITT) [47]	Measures the chromatographic separation of air-NAPL, air-water partitioning and conservative tracers between two wells. Yields an average S_n for the tracer swept volume between the two wells. Relatively well defined volume and average.	Cost intensive, technically demanding.
^{222}Rn activities [51]	NAPL localization through analysis of naturally occurring ^{222}Rn .	Information mainly qualitative.
Fluorescence probe [33]	NAPL detection with special probes by fluorescence.	Local, qualitative information.

Table 9.1: Comparison of the new method with other site investigation methods for the vadose zone.

Tracer sorption: Batch experiments presented in this study suggest that the mass fraction in the soil air f_a of the tracers used in this study (CFCs, SF₆) is up to 25% smaller than 1 in the (uncontaminated) sandy soils investigated at temperatures between 10°C and 15°C. This has an effect on the determination of the apparent diffusion coefficients D_e and D_s and the NAPL saturation S_n . The error for the measured parameters is smaller or equal to the error in f_a , depending on the power to which f_a is raised in the data evaluation. Other researchers have used SF₆ and CFCs as conservative tracers in the vadose zone, however, sorption was either not investigated [26], [28], or investigated at room temperatures and found to be within the limit of experimental error [46]. A possible explanation for the reduced f_a of very volatile, but hydrophobic compounds could be adsorption to the air-water interface [45], [53]. A thorough investigation of tracer sorption or adsorption may require more sophisticated methods as compared to the reported batch experiments, where the precise determination of f_a , slightly smaller than 1, is difficult. A thorough investigation of tracer sorption will ultimately reduce unnecessary uncertainties in the data evaluation.

Effect of heterogeneity: The effect of a heterogeneous NAPL distribution on the results of the DPTT has been investigated in a lysimeter study. The empirical results suggest that the method, where the maximum of diffusive tracer breakthrough curves is determined in some distance from the injection point, yields a somehow averaged S_n for the distance between injection and observation point. However, from a theoretical point of view, the phenomenon is not yet understood and numerical simulations may be required for a better understanding of the performance of this test in heterogeneous media. Such numerical simulations were beyond the scope of this thesis, but will be performed in a follow-up project in cooperation with V. Burganos, Foundation of Research and Technology, Hellas, Greece.

Unexplored options. Besides the determination of apparent diffusion coefficients D_e and D_s and the NAPL saturation S_n , the general approach presented in this study has the potential to obtain additional parameters of interest from in situ experiments. A potentially rewarding, but challenging undertaking would be the in situ measurement of compound specific apparent degradation rates k_{app} for volatile organic compounds in the vadose zone. The results of this study suggest that this approach could be promising in highly active soils for easily biodegradable compounds. Another interesting option is the use of an air-water partitioning tracer for the determination of the

water saturation S_w . The combination of such a tracer with air-NAPL partitioning tracers would allow a determination of S_n , S_w and $S_a = 1 - S_w - S_n$ from one DPTT. It is the hope of the author that the reported results inspire other researchers to explore the various possibilities, how gas-phase diffusion from a point source can be used as a tool for vadose zone investigations.

Bibliography

- [1] Abraham, M. H., Andonian-Haftan, J. A., Whiting, G. S., Loe, A., Taft, R. S., 1994. Hydrogen bonding. Part 34. The factors that influence the solubility of gases and vapours in water at 298 K, and a new method for its determination. *J. Chem. Soc. Pekin Trans.*, 2: 1777-1791.
- [2] ASTM, 1998. ASTM Standards related to the phase II environmental site assessment process. American Society for Testing and Materials, West Conshohocken, PA 19428, USA, 336 pp.
- [3] Ball, B. C., Glasbey, C. A., Robertson, E. A. G., 1994. Measurement of soil gas diffusivity in situ. *European Journal of Soil Science*, 45: 3-13.
- [4] Batterman, S., Padmanagham, I., Milne, P., 1996. Effective gas-phase diffusion coefficients in soils at varying water content measured using a one-flow sorbent-based technique. *Environ. Sci. Technol.*, 30: 770-778.
- [5] Bjerre, T.M., Holtegaard, L. E., 2002. Transport og emission af flygtige organiske stoffer i den umættede zone. Master thesis Miljø & Ressourcer Danish Technical University, 125 pp.
- [6] Boulding, R.J., 1996. EPA environmental assessment sourcebook. Ann Arbor Press, Chelsea, 386 pp.
- [7] Brusseau, M.L., Popovicova, J., Silva, J. A., 1997. Characterizing gas-water interfacial and bulk-water partitioning for gas-phase transport of organic contaminants in unsaturated porous media. *Environ. Sci. Technol.*, 31: 1645-1649.
- [8] Crank, J., 1989. The mathematics of diffusion. Clarendon Press, Oxford, 414 pp.
- [9] Christophersen, M., Broholm, M., Kjeldsen, P., 2002. Migration and degradation of fuel vapors in the vadose zone. Field experiment at Værløse Airforce Base, Denmark. In: Halm, D., Grathwohl, P.

- (Eds.), Proceedings of the 1st International Workshop on Groundwater Risk Assessment at Contaminated Sites (GRACOS), Tübinger geowissenschaftliche Arbeiten (TGA), Heft 61: 83-87.
- [10] Deeds, N. E., McKinney, D. C., Pope, G. A., Whitley, G. A. Jr., 1999. Difluoromethane as partitioning tracer to estimate vadose water saturations. *J. Environ. Engin.*, 125: 630-633.
 - [11] Deeds, N. E., Pope, G. A., McKinney, D. C., 1999. Vadose zone characterization at a contaminated field site using partitioning interwell tracer technology. *Environ. Sci. Technol.*, 33: 2745-2751.
 - [12] Downing, R.C., 1988. Fluorocarbon refrigerants handbook. Prentice-Hall, Englewood Cliffs, New Jersey, 402 pp.
 - [13] Dwarakanath, V., Deeds, N. Pope, G. A., 1999. Analysis of partitioning interwell tracer test. *Environ. Sci. Technol.*, 33: 3829-3836.
 - [14] Elberling, B., Larsen, F. Christensen, S. Postma, D., 1998. Gas transport in a confined unsaturated zone during atmospheric pressure cycles. *Water Resour. Res.*, 34: 2855-2862.
 - [15] Falta, R.W., Javandel, I. Pruess, K. Witherspoon, P.A., 1989. Density-driven flow of gas in the unsaturated zone due to the evaporation of volatile organic compounds. *Water Resour. Res.*, 25: 2159-2169.
 - [16] Feenstra, S., Cherry, J.A., 1996. Diagnosis and assessment of DNAPL sites. In: Pankow, J.F., Cherry, J.A. (Eds.), Dense chlorinated solvents and other DNAPL sites. Waterloo Press, Portland: 395-473.
 - [17] Fuller, E.N., Schettler, P.D., Giddings, J.C., 1966. A new method for prediction of binary gas-phase diffusion coefficients. *Ind. Eng. Chem.*, 58: 19-27.
 - [18] Grathwohl, P., 1998. Diffusion in natural porous media. Kluwer Academic Publishers, Boston, 207 pp.
 - [19] Grathwohl, P., Reinhard, M., 1993. Desorption of trichloroethylene in aquifer material: rate limitation at the grain scale. *Environ. Sci. Technol.*, 27: 2360-2366.
 - [20] Hers, I., Zapf-Gilje, R., Li, L. and Atwater, J., 2000. Measurement of in situ gas diffusion coefficients. *Environ. Technol.* , 21: 631-640.

- [21] Höhener, P., Duwig, C. Pasteris, G. Kaufmann, K. Dakhel, N. Harms, H., 2002. Biodegradation of petroleum hydrocarbon vapors: laboratory studies on rates and kinetics in unsaturated alluvial sand. *J. Contam. Hydrol.*, submitted.
- [22] Hoff, J.T., Mackay, D., Gilham, R., Shiu, W.Y., 1993. Partitioning of organic chemicals at the air-water interface in environmental systems. *Environ. Sci. Technol.*, 27: 2174-2180.
- [23] Hunkeler, D., Hoehn, E. Höhener, P. Zeyer, J., 1997. ^{222}Rn as a partitioning tracer to detect mineral oil contaminations: laboratory experiments and field study. *Environ. Sci. Technol.*, 31: 3180-3187.
- [24] Jellick, G. J., Schnabel, R. R., 1986. Evaluation of a field method for determining the gas diffusion coefficient in soils. *Soil Sci. Soc. Am. J.*, 50: 18-23.
- [25] Jin, M., Delshad, M. Dwarakanath, V. McKinney, D.C. Pope, G.A. Sepehrnoori, K. Tilburg, C.E. Jackson, R.E., 1995. Partitioning tracer test for detection, estimation and remediation performance assessment of subsurface nonaqueous phase liquids. *Water Resour. Res.*, 31: 1201-1211.
- [26] Jin, Y., Jury, A., 1996. Characterizing the dependence of gas diffusion coefficient on soil properties. *Soil Sci. Soc. Am. J.*, 60: 66-71.
- [27] Jin, Y., Streck, T. Jury, W. A., 1994. Transport and biodegradation of toluene in unsaturated soil. *J. Contam. Hydrol.*, 17: 111-127.
- [28] Johnson, P. C. Bruce, C. Johnson, R. L. Kemblowski, M. W., 1998. In situ measurement of effective vapor-phase porous media diffusion coefficient. *Environ. Sci. Technol.*, 32: 3405-3409.
- [29] Kim, H. Annable, M.D. Rao, S.C., 2001. Gaseous transport of volatile organic chemicals in unsaturated porous media: Effect of water-partitioning and air-water interfacial adsorption. *Environ. Sci. Technol.*, 35: 4457-4462.
- [30] Kreamer, D. K., Weeks, E. P., Thompson, G. M., 1988. A field technique to measure the tortuosity factor and sorption-affected porosity for gaseous diffusion of materials in the unsaturated zone with experimental results from near Barnwell, South Carolina. *Water Resour. Res.*, 23: 331-341.

- [31] Lai, S.-H., Tiedje, J.M., and Erickson, E., 1976. In situ measurement of gas diffusion coefficient in soils. *Soil Sci. Soc. Amer. J.*, 40: 3-6.
- [32] Lenhard, R.J., Oostrom, M. Simmons, C.S. White, M.D., 1995. Investigation of density-dependent gas advection of trichloroethylene: Experiment and a model validation exercise. *J. Contam. Hydrol.*, 19: 47-67.
- [33] Lin, J., Hart, S.J., Kenny, J.E., 1996. Improved two-fiber probe for in situ spectroscopic measurement. *Anal. Chem.*, 68: 3098-3103.
- [34] Mariner, P.E., Jin, M. Studer, J.E. Pope, G.A., 1999. The first vadose zone partitioning interwell tracer test for nonaqueous phase liquid and water residual. *Environ. Sci. Technol.*, 33: 2825-2828.
- [35] Meinardus, H.W., Dwarakanath, V., Ewing, J., Hirasaki, G.J., Jackson, R.E., Jin, M., Ginn, J.S., Londergan, J. T., Miller, C.A., Pope, G.A., 2002. Performance assesement of NAPL remediation in heterogeneous alluvium. *J. Contam. Hydrol.*, 54: 173-193.
- [36] Mercer, J.W., Cohen, R.M., 1990. A review of immiscible fluids in the subsurface: properties, models, characterization, and remediation. *J. Contam. Hydrol.*, 6: 107-126.
- [37] Millington, R.-J., Quirk, J.P., 1961. Permeability of porous solids. *Trans. Faraday Soc.*, 57: 1200-1207.
- [38] Monfort, J. P., Pellegatta, J. L., 1991. Diffusion coefficients of the halocarbons CCl_2F_2 and $\text{C}_2\text{Cl}_2\text{F}_4$ with simple gases. *J. Chem. Eng. Data*, 36: 135-137.
- [39] Nazaroff, W.W., 1992. Radon transport from soil to air. *Reviews of geophysics*, 30: 137-160.
- [40] Nelson, N., Oostrom, M. Wietsma, T.W. Brusseau, M.L., 1999. Partitioning tracer method for the in situ measurement of DNAPL saturation: influence of heterogeneity and sampling method. *Environ. Sci. Technol.*, 33: 4046-4053.
- [41] Nelson, N. T., Brusseau, M. L., Carlson, T. D., Constanza, M. S., Young, M. H., Johnson, G. R., Wierenga, P. J., 1999. A gas-phase partitioning tracer method for the in situ measurement of soil-water content. *Water Resour. Res.*, 35: 3699-3707.

- [42] Ostendorf, D.W., Hinlein, E.S. Schoenberg, T.H., 2000. Aerobic biodegradation kinetics and soil gas transport in the unsaturated zone. In: Wise, D.L. Trantolo, D.J. Cichon, E.J. Inyang, H.I. Stottmeister, U. (Eds.), *Bioremediation of contaminated soils*, M. Dekker, New York: 607-632.
- [43] Penman, H.L., 1940. Gas and vapor movement in the soil. I. The diffusion of vapors through porous solids. *J. Agr. Sci.*, 30: 570-581.
- [44] Pasteris, G., Werner, D., Kaufmann, K., Höhener, P., 2002. Vapor phase transport and biodegradation of volatile fuel compounds in the unsaturated zone: a large scale lysimeter experiment. *Environ. Sci. Technol.*, 36: 30-39.
- [45] Pennell, K. D., Rhue, R. D., Rao, P.S.C., Johnston, C.T., 1992. Partitioning of organic chemicals at the air-water interface in environmental systems. *Environ. Sci. Technol.*, 26: 756-763.
- [46] Petersen, L.W., Rolston, D.E., Moldrup, P., Yamaguchi, T., 1994. Volatile organic vapor diffusion and adsorption in soils. *J. Environ. Qual.*, 23: 799-805.
- [47] Rao, P.S.C., Annable, M.D. Kim, H., 2000. NAPL source zone characterization and remediation technology performance assessment: recent developments and applications of tracer techniques. *J. Contam. Hydrol.*, 45: 63-78.
- [48] Rolston, D. E., Glauz, R. D., Grundmann, G. L., Louie, D. T., 1991. Evaluation of an in situ method for measurement of gas diffusivity in surface soils. *Soil Sci. Soc. Am. J.*, 55: 1536-1542.
- [49] Scanlon, B.R., Nicot, J.P., Massmann, J.M., 2000. Soil gas movement in unsaturated systems. In: Sumner, M. E. (Ed.), *Handbook of soil sciences*, CRC Press, Boca Raton, Florida: A277-A319.
- [50] Schlebaum, W., Schraa, G., van Riemsdijk, W. H., 1999. Influence of nonlinear sorption kinetics on the slow desorbing organic contaminant fraction in soil. *Environ. Sci. Technol.*, 33: 1413-1417.
- [51] Schubert, M., 2001. Erfassung von Untergrundkontaminationen durch Non-Aqueous Phase Liquids (NAPLs) mit Hilfe der Bestimmung des Radongehalts der Bodenluft. PhD thesis, Umweltforschungszentrum Leipzig-Halle, Leipzig-Halle: 116 pp.

- [52] Schwarzenbach, R.P. Gschwend, P.M. Imboden, D.M., 1993. Environmental organic chemistry. John Wiley & Sons, New York, 681 pp.
- [53] Silva, J.A.K., Bruant JR., R.G., Conklin, M. H., Corley, T. L., 2002. Equilibrium partitioning of chlorinated solvents in the vadose zone: Low foc geomeia. Environ. Sci. Technol., 36: 1613-1619.
- [54] Staudinger, J., Roberts, P.V., 2001. a critical compilation of Henry's law constant temperature dependence relations for organic compounds in dilute aqueous solutions. Chemosphere, 44: 561-576.
- [55] Whitley, G. A. Jr., 1997. An investigation of partitioning tracers for characterization of nonaqueous phase liquids in vadose zones. PhD thesis, The University of Texas at Austin: 338 pp.
- [56] Whitley, G. A. Jr., McKinney, D. C., Pope, G. A., Rouse, B. A., Deeds, N. E., 1999. Contaminated vadose zone characterization using partitioning gas tracers. J. Environ. Engin., 125: 574-582.
- [57] Wiedemeier, T.H., Rifia, H.S. Newell, C.J. Wilson, J.T., 1999. Natural attenuation of fuels and chlorinated solvents in the subsurface. Wiley, New York, 617 pp.
- [58] Wilhelm, E., Battion, R., Wilcock, J., 1977. Low-pressure solubility of gases in liquid water. Chemical reviews, 77: 219-262.
- [59] Yaws, C.L., 1999. Chemical properties handbook: physical, thermodynamic, environmental, transport, safety, and health related properties for organic and inorganic chemicals. McGraw-Hill, New York, 779 pp.

Appendix A

Notation

A	Cross-sectional area	$[\text{cm}^2]$
a	Initial extension from the point source	$[\text{cm}]$
C_a	Concentration of the compound in the soil air	$[\text{g cm}^{-3}]$
C_{in}	Concentration of the compound in the injected compound mixture	$[\text{g cm}^{-3}]$
C_r	Relative concentration of the compound C_a/C_{in}	$[-]$
C_0	Initial concentration of the compound in the soil air	$[\text{g cm}^{-3}]$
D_e	Effective gas-phase diffusion coefficient	$[\text{cm}^2 \text{s}^{-1}]$
D_m	Molecular gas-phase diffusion coefficient	$[\text{cm}^2 \text{s}^{-1}]$
D_s	Sorption-affected gas-phase diffusion coefficient	$[\text{cm}^2 \text{s}^{-1}]$
erf	Error function	
f_a	Mass fraction of the compound in the soil air	$[\text{g/g}]$
f_n	Mass fraction of the compound in the NAPL	$[\text{g/g}]$
f_{oc}	Organic carbon content	$[\% \text{ dry weight}]$
f_{om}	Organic matter content	$[\% \text{ dry weight}]$

$f_{r'}$	Mass fraction of the compound between $r = 0$ and $r = r'$	[g/g]
f_s	Mass fraction of the compound on/in the solids	[g/g]
f_w	Mass fraction of the compound in the soil water	[g/g]
$f_{x'}$	Mass fraction of the compound between $x = -x'$ and $x = x'$	[g/g]
H	Air-water partitioning coefficient (Henry constant)	$[(\text{mol cm}^{-3})/(\text{mol cm}^{-3})]$
h	Initial extension from the plane source	[cm]
k_{app}	Apparent first-order degradation rate constant	$[\text{s}^{-1}]$ sometimes $[\text{d}^{-1}]$
K_d	Solid-water partitioning coefficient	$[(\text{mol g}^{-1})/(\text{mol cm}^{-3})]$
K_{om}	Organic matter-water partitioning co- efficient	$[(\text{mol g}^{-1})/(\text{mol cm}^{-3})]$
K_n	Air-NAPL partitioning coefficient	$[(\text{mol cm}^{-3})/(\text{mol cm}^{-3})]$
K_{ow}	Octanol-water partitioning coefficient	$[(\text{mol cm}^{-3})/(\text{mol cm}^{-3})]$
K_s	Air-solid partitioning coefficient	$[(\text{mol cm}^{-3})/(\text{mol g}^{-1})]$
k_w	First-order degradation rate constant in the soil water	$[\text{s}^{-1}]$ sometimes $[\text{d}^{-1}]$
m_0	Total mass of the compound	[g]
MW	Molecular weight	$[\text{g mol}^{-1}]$
N^{plane}	Quantity used for plotting purposes	$[\text{cm}^{-2} \text{ s}^{-0.5}]$
N^{point}	Quantity used for plotting purposes	$[\text{s}^{-1.5}]$
p^0	Vapor pressure, $p^0(L)$ for gases	$[\text{Nm}^2]$ sometimes [atm]
r	Distance from the point source	[cm]
s	Slope of the regression line in eq (7.2)	[-]
S_a	Air saturation	$[\text{cm}^3/\text{cm}^3 \text{ tot. porosity}]$
S_n	NAPL saturation	$[\text{cm}^3/\text{cm}^3 \text{ tot. porosity}]$
S_w	Water saturation	$[\text{cm}^3/\text{cm}^3 \text{ tot. porosity}]$
T	Temperature	$[\text{°K}]$ sometimes $[\text{°C}]$
t	Time	[s] sometimes [h]
V_{in}	Volume injected	$[\text{cm}^3]$
V_m	Liquid molar volume	$[\text{cm}^3 \text{ mol}^{-1}]$
(Δ)	Laplace operator	
θ_a	Air-filled porosity	$[\text{cm}^3/\text{cm}^3 \text{ soil}]$
θ_n	NAPL-filled porosity	$[\text{cm}^3/\text{cm}^3 \text{ soil}]$
θ_t	Total porosity	$[\text{cm}^3/\text{cm}^3 \text{ soil}]$
θ_w	Water-filled porosity	$[\text{cm}^3/\text{cm}^3 \text{ soil}]$
ρ_s	Density of the solids	$[\text{g cm}^{-3}]$
τ	Tortuosity factor	[-]

Appendix B

Raw Data

Table B.1: Apparent diffusion coefficients. Results of the lysimeter experiments.^a

Exp A:								
time	1.0	1.7	2.3	3.0	3.7	4.3	5.0	5.7
$C_r(0, t)$ SF ₆	3.4E-4	1.4E-4	8.1E-5	5.7E-5	4.3E-5	3.6E-5	3.1E-5	2.7E-5
$C_r(0, t)$ CFC-12	3.4E-4	1.6E-4	9.5E-5	6.8E-5	5.0E-5	4.0E-5	3.2E-5	2.9E-5
$C_r(0, t)$ CFC-11	3.8E-4	1.8E-4	1.1E-4	7.3E-5	5.3E-5	4.3E-5	3.5E-5	3.0E-5
Exp B:								
time	1.0	1.8	2.6	3.3	4.0	4.8	5.5	6.3
$C_r(0, t)$ SF ₆	3.1E-4	1.2E-4	6.1E-5	4.3E-5	3.2E-5	2.6E-5	2.2E-5	2.0E-5
$C_r(0, t)$ Vinyl	2.5E-4	1.1E-4	6.4E-5	4.6E-5	3.3E-5	2.7E-5	2.1E-5	1.9E-5
Exp C:								
time	1.0	1.8	2.7	3.5	4.2	4.9	5.7	6.4
$C_r(0, t)$ SF ₆	2.9E-4	1.3E-4	7.0E-5	4.7E-5	3.2E-5	2.5E-5	2.2E-5	1.9E-5
$C_r(0, t)$ Trans	3.6E-4	1.6E-4	9.9E-5	6.6E-5	4.9E-5	3.9E-5	3.2E-5	2.6E-5
Exp D:								
time	1.0	1.8	2.5	3.3	4.0	4.9	5.7	6.5
$C_r(0, t)$ SF ₆	3.1E-4	1.3E-4	7.2E-5	4.9E-5	3.6E-5	3.0E-5	2.5E-5	2.3E-5
$C_r(0, t)$ Cis	5.0E-4	2.3E-4	1.3E-4	8.7E-5	6.7E-5	5.4E-5	4.0E-5	4.0E-5

^a $C_r(0, t)$ is dimensionless. The dimension of time t is [h].

The injected volume V_{in} was 10 [cm³].

Table B.2: Apparent diffusion coefficients. Results of the field experiments.^a

Exp E:									
time		1.2	2.1	3.1	4.1	5.1	6.3	7.2	8.2
$C_r(0, t)$ CFC-12		5.7E-4	2.2E-4	1.4E-4	1.1E-4	6.5E-5	4.9E-5	5.3E-5	3.8E-5
$C_r(0, t)$ CFC-114		7.8E-4	3.0E-4	1.9E-4	1.5E-4	8.8E-5	6.7E-5	7.0E-5	5.0E-5
$C_r(0, t)$ CFC-11		7.5E-4	3.0E-4	1.8E-4	1.4E-4	7.4E-5	5.5E-5	6.1E-5	4.0E-5
Exp F:									
time		1.1	2.0	3.1	4.1	5.0	6.0	6.9	8.0
$C_r(0, t)$ CFC-12		6.2E-4	1.9E-4	1.0E-4	6.6E-5	4.9E-5	3.8E-5	3.8E-5	2.6E-5
$C_r(0, t)$ CFC-113		9.3E-4	2.6E-4	1.4E-4	9.0E-5	7.4E-5	5.7E-5	7.3E-5	3.8E-5
Exp G:									
time		0.9	2.0	3.0	4.0	5.0	6.0	7.0	8.0
$C_r(0, t)$ CFC-11		9.2E-4	2.9E-4	1.6E-4	9.7E-5	7.5E-5	6.1E-5	4.7E-5	3.0E-5
$C_r(0, t)$ Benzene		1.6E-3	5.4E-4	2.8E-4	2.0E-4	1.5E-4	1.1E-4	9.4E-5	7.1E-5
Exp G _{rep} :									
time		1.0	2.0	3.0	4.0	5.0	6.0	7.0	8.0
$C_r(0, t)$ CFC-11		1.0E-3	3.3E-4	1.8E-4	9.2E-5	7.7E-5	6.4E-5	4.3E-5	4.1E-5
$C_r(0, t)$ Benzene		1.4E-3	5.0E-4	2.7E-4	1.8E-4	1.2E-4	1.2E-4	9.4E-5	7.2E-5
Exp H:									
time		1.0	1.9	2.9	4.0	5.0	6.0	7.0	
$C_r(0, t)$ CFC-113		9.6E-4	5.0E-4	2.1E-4	1.4E-4	1.2E-4	5.3E-5	4.1E-5	
$C_r(0, t)$ Toluene		1.4E-3	8.1E-4	3.6E-4	2.4E-4	1.8E-4	1.0E-4	6.3E-5	
Exp H _{rep} :									
time		1.0	2.0	2.9	4.0	5.0	6.0	7.0	
$C_r(0, t)$ CFC-113		8.5E-4	2.8E-4	1.6E-4	1.3E-4	8.2E-5	4.9E-5	3.1E-5	
$C_r(0, t)$ Toluene		1.4E-3	4.5E-4	2.4E-4	1.9E-4	1.2E-4	7.5E-4	5.1E-5	
Exp I:									
time		1.0	2.1	3.0	4.1	5.0	6.0	7.1	8.0
$C_r(0, t)$ CFC-113		1.0E-3	2.9E-4	1.8E-4	1.1E-4	9.4E-5	1.1E-4	8.7E-5	6.6E-5
$C_r(0, t)$ Octane		1.6E-3	3.7E-4	2.2E-4	1.8E-4	1.3E-4	1.4E-4	1.3E-4	1.0E-4

^a $C_r(0, t)$ is dimensionless. The dimension of time t is [h].

The injected volume V_{in} was 10 [cm³].

Table B.3: DPTT: Results of the column experiments.^a

time	2400	3180	4500	6600	10800
Exp A:					
$C_r(0, t)$ CFC-12	1.2E-3	1.1E-3	8.7E-4	7.2E-4	5.4E-4
$C_r(0, t)$ CFC-114	1.3E-3	1.1E-3	9.8E-4	8.2E-4	6.1E-4
$C_r(0, t)$ CFC-11	1.3E-3	1.1E-3	9.1E-4	8.1E-4	6.1E-4
$C_r(0, t)$ CFC-113	1.4E-3	1.1E-3	1.0E-3	8.7E-4	6.6E-4
Exp A _{rep} :					
$C_r(0, t)$ CFC-12	1.3E-3	1.1E-3	9.3E-4	7.4E-4	6.1E-4
$C_r(0, t)$ CFC-114	1.4E-3	1.2E-3	1.0E-3	8.1E-4	6.9E-4
$C_r(0, t)$ CFC-11	1.4E-3	1.2E-3	1.0E-3	8.0E-4	6.5E-4
$C_r(0, t)$ CFC-113	1.4E-3	1.2E-3	1.1E-3	8.4E-4	6.8E-4
Exp B:					
$C_r(0, t)$ CFC-12	2.9E-3	2.5E-3	2.1E-3	1.8E-3	1.4E-3
$C_r(0, t)$ CFC-114	3.1E-3	2.7E-3	2.3E-3	2.0E-3	1.5E-3
$C_r(0, t)$ CFC-11	2.8E-3	2.5E-3	2.1E-3	1.8E-3	1.4E-3
$C_r(0, t)$ CFC-113	3.3E-3	2.8E-3	2.4E-3	2.0E-3	1.6E-3
Exp C:					
$C_r(0, t)$ CFC-12	1.8E-3	1.5E-3	1.3E-3		
$C_r(0, t)$ CFC-114	1.9E-3	1.6E-3	1.3E-3		
$C_r(0, t)$ CFC-11	1.3E-3	1.1E-3	9.1E-4		
$C_r(0, t)$ CFC-113	1.4E-3	1.2E-3	9.4E-4		
Exp D:					
$C_r(0, t)$ CFC-12	1.0E-3	8.8E-4	7.3E-4	6.3E-4	5.2E-4
$C_r(0, t)$ CFC-114	1.0E-3	9.4E-4	7.4E-4	6.7E-4	5.2E-4
$C_r(0, t)$ CFC-11	7.2E-4	6.5E-4	5.2E-4	4.5E-4	3.7E-4
$C_r(0, t)$ CFC-113	7.4E-4	6.6E-4	5.4E-4	4.7E-4	3.6E-4
Exp E:					
$C_r(0, t)$ CFC-12	1.1E-3	9.4E-4	7.5E-4	6.6E-4	5.5E-4
$C_r(0, t)$ CFC-114	1.1E-3	9.7E-4	8.3E-4	7.3E-4	5.5E-4
$C_r(0, t)$ CFC-11	7.3E-4	6.4E-4	5.3E-4	4.5E-4	3.4E-4
$C_r(0, t)$ CFC-113	7.1E-4	5.9E-4	5.0E-4	4.3E-4	3.3E-4
Exp E _{rep} :					
$C_r(0, t)$ CFC-12	1.1E-3	9.3E-4	7.9E-4	6.7E-4	5.3E-4
$C_r(0, t)$ CFC-114	1.1E-3	9.9E-4	8.0E-4	6.8E-4	5.4E-4
$C_r(0, t)$ CFC-11	6.9E-4	6.0E-4	4.8E-4	4.1E-4	3.4E-4
$C_r(0, t)$ CFC-113	6.7E-4	5.6E-4	4.9E-4	4.1E-4	3.4E-4
Exp F:					
$C_r(0, t)$ CFC-12	1.0E-3	8.8E-4	7.5E-4	6.4E-4	4.9E-4
$C_r(0, t)$ CFC-114	1.0E-3	8.9E-4	7.5E-4	6.1E-4	5.1E-4
$C_r(0, t)$ CFC-11	5.7E-4	4.9E-4	4.2E-4	3.4E-4	2.7E-4
$C_r(0, t)$ CFC-113	5.3E-4	4.6E-4	3.6E-4	3.0E-4	2.4E-4

^a $C_r(0, t)$ is dimensionless. The dimension of time t is [s].
The injected volume V_{in} was 1 [cm³].

Table B.4: DPTT: Results of the field experiments.^a

day 25, center:					
time		3180	4200	6600	10800
$C_r(0, t)$	CFC-12	2.2E-4	1.6E-4	7.7E-5	5.1E-5
$C_r(0, t)$	CFC-114	4.1E-4	2.6E-4	1.3E-4	6.9E-5
$C_r(0, t)$	CFC-11	6.8E-4	4.0E-4	2.1E-4	1.1E-4
day 25, 950 cm:					
time		3180	4500	6600	10800
$C_r(0, t)$	CFC-12	4.5E-4	2.5E-4	1.5E-4	7.3E-5
$C_r(0, t)$	CFC-114	5.9E-4	3.3E-4	1.9E-4	8.8E-5
$C_r(0, t)$	CFC-11	5.7E-4	2.7E-4	1.3E-4	5.6E-5
day 102, center:					
time		3240	4620	7380	11940
$C_r(0, t)$	CFC-12	2.3E-4	1.2E-4	8.5E-5	4.9E-5
$C_r(0, t)$	CFC-114	3.4E-4	1.8E-4	1.2E-4	7.0E-5
$C_r(0, t)$	CFC-11	5.7E-4	3.1E-4	1.5E-4	7.8E-5
day 102, 73 cm:					
time		4020	7500		
$C_r(0, t)$	CFC-12	5.2E-4	1.4E-4		
$C_r(0, t)$	CFC-114	7.3E-4	1.9E-4		
$C_r(0, t)$	CFC-11	6.8E-4	2.1E-4		
day 102, 235 cm:					
time		2640	6600	10500	
$C_r(0, t)$	CFC-12	3.6E-4	1.1E-4	4.6E-5	
$C_r(0, t)$	CFC-114	4.8E-4	1.5E-4	6.1E-5	
$C_r(0, t)$	CFC-11	6.2E-4	1.4E-4	5.8E-5	
day 102, 950 cm:					
time		2400	6000		
$C_r(0, t)$	CFC-12	3.7E-4	9.5E-5		
$C_r(0, t)$	CFC-114	5.0E-4	1.2E-4		
$C_r(0, t)$	CFC-11	4.6E-4	9.8E-5		

^a $C_r(0, t)$ is dimensionless. The dimension of time t is [s].
The injected volume V_{in} was 5 [cm³].

Table B.5: DPTT: Lysimeter, results injection point.^a

day 8, L1:					
time	2400	3180	4500	6720	11100
$C_r(0, t)$ SF ₆	2.7E-4	1.7E-4	9.9E-5	5.2E-5	2.4E-5
$C_r(0, t)$ CFC-12	3.8E-4	2.6E-4	1.6E-4	8.4E-5	4.2E-5
$C_r(0, t)$ CFC-11	9.6E-4	6.7E-4	3.3E-4	1.9E-4	1.0E-4
day 14, L2:					
time	2400	3180	4500	6600	10800
$C_r(0, t)$ SF ₆	2.6E-4	1.9E-4	9.4E-5	5.0E-5	2.4E-5
$C_r(0, t)$ CFC-12	2.7E-4	2.1E-4	1.0E-4	5.9E-5	2.9E-5
$C_r(0, t)$ CFC-11	3.1E-4	2.6E-4	1.1E-4	6.3E-5	3.1E-5
day 19, L3:					
time	2400	3180	4500	7200	10800
$C_r(0, t)$ SF ₆	3.5E-4	2.4E-4	1.3E-4	6.2E-5	3.2E-5
$C_r(0, t)$ CFC-12	4.6E-4	3.3E-4	1.9E-4	9.7E-5	4.8E-5
$C_r(0, t)$ CFC-11	1.1E-3	7.4E-4	4.2E-4	2.2E-4	1.2E-4

^a $C_r(0, t)$ is dimensionless. The dimension of time t is [s].

The injected volume V_{in} was 5 [cm³].

Table B.6: DPTT: Lysimeter, results diffusive breakthrough curves.^a

day 8, L1:								
time	1200	2400	3600	4800	6000	7200	8400	9600
$C_r(r, t)$ SF ₆	7.4E-6	2.9E-5	3.3E-5	3.0E-5	2.5E-5	2.2E-5	2.0E-5	1.7E-5
$C_r(r, t)$ CFC-12	9.8E-7	1.1E-5	1.8E-5	2.5E-5	2.6E-5	2.5E-5	2.5E-5	2.2E-5
$C_r(r, t)$ CFC-11	5.1E-7	0	1.7E-7	5.7E-7	4.7E-7	3.9E-7	6.2E-7	1.1E-6
time	10800	12000	13200	14400	15600	16800	18000	19200
$C_r(r, t)$ SF ₆	1.5E-5	1.4E-5	1.3E-5	1.2E-5	1.0E-5	9.6E-6	9.9E-6	8.2E-6
$C_r(r, t)$ CFC-12	2.0E-5	1.8E-5	1.8E-5	1.6E-5	1.6E-5	1.4E-5	1.3E-5	1.3E-5
$C_r(r, t)$ CFC-11	1.9E-6	2.8E-6	2.7E-6	3.8E-6	4.4E-7	4.0E-6	4.9E-6	5.3E-6
time	20400	21600	22800	24000	25200	26400	27600	
$C_r(r, t)$ SF ₆	7.8E-6	8.3E-6	8.0E-6	7.6E-6	7.0E-6	7.9E-6	7.4E-6	
$C_r(r, t)$ CFC-12	1.2E-5	1.2E-5	1.5E-5	1.2E-5	1.1E-5	1.1E-5	1.0E-5	
$C_r(r, t)$ CFC-11	6.0E-6	6.0E-6	6.5E-6	6.3E-6	6.6E-6	6.6E-7	6.7E-6	
day 14, L2:								
time	1200	2400	3600	4800	6000	7200	8400	9600
$C_r(r, t)$ SF ₆	5.1E-6	2.5E-5	3.0E-5	2.8E-5	2.6E-5	2.4E-5	1.9E-5	1.7E-5
$C_r(r, t)$ CFC-12	2.1E-6	1.8E-5	2.3E-5	2.8E-5	2.6E-5	2.7E-5	2.3E-5	2.1E-5
$C_r(r, t)$ CFC-11	0	6.1E-7	6.1E-7	5.2E-6	7.2E-6	9.4E-6	9.5E-6	1.0E-5
time	10800	12000	13200	14400	15600	16800	18000	19200
$C_r(r, t)$ SF ₆	1.5E-5	1.4E-5	1.3E-5	1.3E-5	1.1E-5	1.0E-5	9.3E-6	8.4E-6
$C_r(r, t)$ CFC-12	1.9E-5	1.7E-5	1.6E-5	1.6E-5	1.5E-5	1.3E-5	1.2E-5	1.2E-5
$C_r(r, t)$ CFC-11	1.0E-5	1.0E-5	1.0E-5	1.0E-5	1.0E-5	9.1E-6	9.3E-6	9.0E-6
time	20400	21600	22800	24000	25200	26400	27600	
$C_r(r, t)$ SF ₆	8.7E-6	8.4E-6	8.4E-6	7.7E-6	7.8E-6	7.5E-6	7.6E-6	
$C_r(r, t)$ CFC-12	1.1E-5	1.1E-5	1.1E-5	1.1E-5	9.7E-6	9.7E-6	9.8E-6	
$C_r(r, t)$ CFC-11	8.9E-6	8.0E-6	8.0E-6	7.9E-6	7.1E-6	7.2E-7	7.7E-6	
day 19, L3:								
time	1200	2400	3600	4800	6000	7200	8400	9600
$C_r(r, t)$ SF ₆	6.4E-6	2.8E-5	3.2E-5		2.7E-5	2.4E-5	2.1E-5	1.8E-5
$C_r(r, t)$ CFC-12	1.9E-6	1.9E-5	2.7E-5		3.5E-5	2.4E-5	2.3E-5	2.1E-5
$C_r(r, t)$ CFC-11	0	2.3E-7	3.1E-6		8.6E-6	9.5E-6	1.1E-5	1.2E-5
time	10800	12000	13200	14400	15600	16800	18000	19200
$C_r(r, t)$ SF ₆	1.6E-5	1.5E-5	1.4E-5	1.2E-5	1.2E-5	1.0E-5	9.9E-6	9.4E-6
$C_r(r, t)$ CFC-12	1.9E-5	1.9E-5	1.4E-5	1.3E-5	1.4E-5	1.3E-5	1.2E-5	1.1E-5
$C_r(r, t)$ CFC-11	1.1E-5	1.1E-5	1.1E-5	1.1E-5	1.1E-5	1.0E-5	1.0E-6	9.7E-6
time	20400	21600	22800	24000	25200	26400	27600	
$C_r(r, t)$ SF ₆	8.9E-6	9.0E-6	7.8E-6	7.1E-6	7.0E-6	7.4E-6	6.9E-6	
$C_r(r, t)$ CFC-12	1.0E-5	1.0E-5	8.9E-5	7.6E-5	8.5E-6	9.6E-6	8.4E-6	
$C_r(r, t)$ CFC-11	9.2E-6	9.5E-6	8.4E-6	7.6E-6	8.0E-6	8.3E-7	7.6E-6	

^a $C_r(r, t)$ is dimensionless. The dimension of time t is [s]. The injected volume V_{in} was 5 [cm³].

Curriculum Vitae

Surname	Werner
Given name	David
Date and place of birth	27.11.73, Schaffhausen, Switzerland
Citizen of	Merishausen, Switzerland
School education	1980-1988 Primarschule, Sekundarschule in Beringen
	1988-1993 Kantonsschule in Schaffhausen
Higher education	1993-1998 Studies in Umweltnaturwissenschaften at ETH Zürich
Occupation	1998-1999 Employee of Umwelt and Consulting Wälti, Rafz
Doctoral studies	1999-2002 EPF Lausanne